University of Stuttgart

Institute for Theoretical Physics III

Master Thesis:

Symmetry Protected Topological Phases for Interacting Bosons

16th October 2019

Candidate:	Felix Roser
Supervisor:	Prof. Dr. H. P. Büchler
Secondary Corrector:	Prof. Dr. E. Lutz

Declaration

I declare that I have developed and written the enclosed master thesis completely by myself and have not used sources or means without declaration in the text. Any thoughts from others or literal quotations are clearly marked. The master thesis was not used in the same or in a similar version to achieve an academic grading or is being published elsewhere. Lastly, I assure that the electronic copy of this master thesis is identical in content with the enclosed version.

Stuttgart, 16th October 2019 Felix Roser

Introduction

Condensed matter physics is a broad field which deals with many-particle systems in which interaction strengths generally dominate over kinetic energies. One of the most significant phenomena observed in condensed matter systems are phase transitions. They are found in everyday life situations as the transition from frozen to liquid water (or vice versa), but there are also many other classical and quantum mechanical systems which can realize phase transitions (e.g. transitions into superconducting phases).[1] This posed the question if there is a unified theory for all phase transitions. In the 1930s, Landau developed a theory which is nowadays called *Landau theory of spontaneous symmetry breaking* (1937, [1]). It states that each phase of a system is characterized by a different specific symmetry. Phase transitions occur when the symmetry is spontaneously broken.

The Landau theory proved to be a very good and successful description of condensed matter systems, but with the discovery of the *integer quantum Hall effect* in 1980 by Klitzing *et al.* [2], a new era of condensed matter physics began. Integer quantum Hall systems show phase transitions at zero temperature, but the different phases have the same symmetry. This cannot be explained by the Landau theory any more. Instead, it motivated a new theory for the description of special phases in condensed matter based on the branch of mathematics called *topology*. In a nutshell, hidden topological invariants were found in the band structures of these systems which allow for the existence of different phases. The *fractional quantum Hall effect*, which was discovered in 1982 by Tsui *et al.* [3], was the first occurrence of an interacting system with different phases which share the same symmetry. Here, a band structure cannot be defined any more, but an intrinsic topological order allows for the existence of different phases with the same symmetry [4, 5, 6]. The work on topological phases goes still on today and is pursued by many researchers around the world.

Topological phases can be found in fermionic and bosonic systems, but only in two or more dimensions. In this thesis, we discuss special one-dimensional systems (mainly the so-called *Su–Schrieffer–Heeger* (SSH) *chain* and some variations) which are characterized by a symmetry.[2] As a symmetry is essentially an additional constraint for a system, these one-dimensional systems can realize phase transitions which are neither described by the Landau theory nor by intrinsic topological order. These phases are *symmetry protected topological* (SPT) *phases* and the topic of this thesis.

In recent experiments conducted by de Léséleuc *et al.* [7], two symmetry protected topological phases were realized in a bosonic SSH chain. This achievement motivates two questions: The first one is related to the work by Wen *et al.* in 2013 [8] which predicts the existence of a maximum of *four* phases in bosonic systems with the same protecting symmetry as in [7]. Can these four phases be realized by SSH chains? Moreover, in 2010 Kitaev *et al.* [9] showed that the classification of fermionic symmetry protected phases in Majorana chains breaks down to $\mathbb{Z}_8$ if interactions are allowed. What is the connection between the four bosonic phases and these eight phases in fermionic systems?

[1] A phase is the set of all states of a system which can be connected without a phase transition.
[2] A symmetry is a transformation which does not change the appearance of the system.

Thus, the goal of this work can be divided into two main parts: Firstly we focus on the work by Kitaev and reproduce the breakdown of phases in fermionic SSH chains. In the second part of this thesis, we discuss bosonic symmetry protected topological phases in SSH chains. Following the general approach by Wen, we will use different symmetry constraints to realize various phases in specific systems. By doing this, we also want to gain a deeper understanding of the connection between fermionic and bosonic topological phases.

Outline

This thesis consists of five main chapters structured in the following way:

- In Chapter 1, we give an introduction to the systems of consideration and in the classification of fermionic symmetry protected topological phases. We will discuss fermionic symmetries and give some insights on the winding number, which is the topological invariant used for the classification of phases.

- In Chapter 2, we introduce the SSH chain and show how different phases can be realized in this specific system. Furthermore, we will elaborate how stacked SSH chains without interactions can be used to realize an arbitrary amount of phases. In analogy to the work of Kitaev [9], we then show how in these stacked chains the number of phases breaks down to $\mathbb{Z}_4$ if we allow interactions.

- In Chapter 3, we make the transition from fermionic to bosonic systems. This requires us to introduce a new classification for phases as the fermionic classification cannot be applied here. We give some insights on matrix-product states and cohomology theory and use the bosonic SSH chain as an illustrative example.

- In Chapter 4, we will show how different symmetry representations for the same symmetry group allow for the existence of different phases. This enables us to show that stacked SSH chains with special symmetry constraints can be used to realize four and even 16 different phases in a single system. These phenomena were predicted by Wen *et al.* in 2013 [8].

- In Chapter 5, we compare the fermionic and the bosonic phases. To do so, we introduce a new formalism for the classification of bosonic phases based on stabilizer codes.

In Chapter 6, we give a short conclusion on the results of this thesis and briefly discuss some ideas for future work.

Zusammenfassung

Die Physik der kondensierten Materie ist ein weites Feld, das sich mit Vielteilchensystemen beschäftigt, in denen Wechselwirkungen über kinetische Energien dominieren. Zu den wichtigsten Phänomenen, die in solchen Systemen beobachtet werden, gehören Phasenübergänge. Wir beobachten sie im Alltag beispielsweise beim Übergang von gefrorenem zu flüssigem Wasser, aber Phasenübergänge treten auch in anderen klassischen und quantenmechanischen Systemen auf (beispielsweise beim Übergang in supraleitende Phasen).[3] So stellte sich die Frage, ob es eine einheitliche Theorie gibt, die alle Phasenübergänge beschreibt. In den 1930er Jahren entwickelte Landau eine Theorie, die wir heute *Landaus Theorie der spontanen Symmetriebrechung* nennen (1937, [1]). Sie besagt, dass verschiedene Phasen eines Systems durch eine unterschiedliche Symmetrien charakterisiert werden. Phasenübergänge treten auf, wenn eine solche Symmetrie spontan gebrochen wird.

Die Landau-Theorie setzte sich als eine besonders gute und allgemein gültige Beschreibung von Systemen kondensierter Materie durch. Mit der Entdeckung des *integralen Quanten-Hall-Effekts* durch Kitzing *et al.* [2] im Jahr 1980 begann jedoch eine neue Ära der Physik der kondensierten Materie. Hierbei treten mehrere Phasen auf, welche die gleiche Symmetrie teilen. Solche Systeme können nicht mehr durch die Landau-Theorie beschrieben werden. So wurde die Entwicklung einer neuen Theorie motiviert, die auf dem mathematischen Gebiet der *Topologie* basiert. Kurz gesagt wurden topologische Invarianten in der Bandstruktur dieser Systeme gefunden, die die Existenz verschiedener Phasen mit gleicher Symmetrie erlauben. Der *fraktionale Quanten-Hall-Effekt*, der im Jahr 1982 von Tsui *et al.* [3] entdeckt wurde, markiert das erste wechselwirkende System mit verschiedenen Phasen, die die gleiche Symmetrie teilen. An dieser Stelle kann keine Bandstruktur mehr definiert werden, aber eine intrinsische topologische Ordnung erlaubt die Existenz verschiedener Phasen mit der gleichen Symmetrie [4, 5, 6]. Bis heute sind topologische Phasen ein sehr aktives Forschungsgebiet auf der ganzen Welt.

Topologische Phasen können in fermionischen und bosonischen Systemen gefunden werden. Sie existieren jedoch nur in zwei oder mehr Dimensionen. In dieser Arbeit werden wir spezielle eindimensionale Systeme betrachten (hauptsächlich die sogenannte *Su–Schrieffer–Heeger-Kette* (SSH-Kette) und einige Abwandlungen davon), die durch eine zusätzliche Symmetrie charakterisiert sind.[4] Da eine Symmetrie prinzipiell eine zusätzliche Einschränkung des Systems darstellt, können in diesen eindimensionalen Systemen Phasenübergänge realisiert werden, die weder durch die Landau-Theorie noch durch intrinsische topologische Ordnung beschrieben werden können. Diese Phasen sind *symmetriegeschützte topologische* (SPT) *Phasen*. Sie sind das Thema dieser Arbeit.

In neuen Experimenten von Léséleuc *et al.* [7] wurden zwei symmetriegeschützte topologische Phasen in einer SSH-Kette realisiert. Dieses Ergebnis führt nun zu zwei Fragen: Die erste Frage hängt mit der Arbeit von Wen *et al.* aus dem Jahr 2013 [8] zusammen. Danach können in Systemen mit der gleichen Symmetrie wie in [7] maximal *vier* Phasen

[3] Eine Phase ist die Menge aller Zustände eines Systems, die ohne einen Phasenübergang miteinander verbunden werden können.

[4] Eine Symmetrie ist eine Transformation, die das Erscheinungsbild des Systems nicht verändert.

existieren. Können diese vier Phasen durch SSH-Ketten realisiert werden? Des weiteren zeigte Kitaev *et al.* im Jahr 2010 [9], dass die Klassifikation von fermionischen symmetriegeschützten topologischen Phasen in Majorana Ketten zu $\mathbb{Z}_8$ zusammenbricht, sobald Wechselwirkungen erlaubt werden. Wie hängen diese acht fermionischen Phasen mit den vier bosonischen Phasen zusammen?

Das Ziel dieser Arbeit setzt sich aus zwei Hauptbestandteilen zusammen: Zunächst betrachten wir die Arbeit von Kitaev und reproduzieren den Zusammenbruch der Phasen in fermionischen SSH-Ketten. Im zweiten Teil dieser Arbeit diskutieren wir bosonische symmetriegeschützte topologische Phasen in SSH-Ketten. Wir folgen der allgemeinen Herangehensweise von Wen und nutzen verschiedene Symmetriebeschränkungen, um unterschiedliche Phasen in bestimmten Systemen zu realisieren. So erhalten wir ein tieferes Verständnis über den Zusammenhang zwischen fermionischen und bosonischen topologischen Phasen.

Übersicht

Diese Arbeit besteht aus fünf Hauptkapiteln, die folgendermaßen strukturiert sind:

- In Kapitel 1 geben wir eine Einführung zu den betrachteten Systemen und zur Klassifikation von fermionischen symmetriegeschützten topologischen Phasen. Wir diskutieren fermionische Symmetrien und betrachten die Windungszahl. Sie stellt die topologische Invariante dar, mithilfe derer die Phasen klassifiziert werden.

- In Kapitel 2 führen wir die SSH-Kette ein und zeigen, wie in diesem System verschiedene Phasen realisiert werden können. Außerdem werden wir erarbeiten, wie geschichtete SSH-Ketten ohne Wechselwirkungen genutzt werden können, um eine beliebige Anzahl an Phasen zu realisieren. In Analogie zur Arbeit von Kitaev [9] zeigen wir, wie in diesen geschichteten Ketten die Zahl der Phasen auf $\mathbb{Z}_4$ zusammenbricht, falls wir Wechselwirkungen erlauben.

- In Kapitel 3 vollziehen wir den Übergang von fermionischen zu bosonischen Systemen. Da hier die Klassifikation der fermionischen Phasen nicht mehr angewendet werden kann, müssen wir eine neue Klassifikation einführen. Wir geben Einblicke zu Matrix-Produkt Zuständen und zur Kohomologietheorie und nutzen die bosonische SSH-Kette als ein konkretes und illustratives Beispiel.

- In Kapitel 4 werden wir zeigen, wie verschiedene Symmetriedarstellungen der selben Symmetriegruppe die Existenz verschiedener Phasen erlauben. So können wir zeigen, dass geschichtete SSH-Ketten mit bestimmten Symmetriebeschränkungen genutzt werden können, um vier oder sogar 16 Phasen in einem einzigen System zu realisieren. Diese Phänomene wurden im Jahr 2013 von Wen *et al.* [8] vorhergesagt.

- In Kapitel 5 vergleichen wir die fermionischen und bosonischen Phasen miteinander. Dafür führen wir einen neuen Formalismus für die Klassifikation bosonischer Phasen ein, welcher auf Stabilizer Codes basiert.

In Kapitel 6 fassen wir die Ergebnisse dieser Arbeit kurz zusammen und diskutieren einige Ideen für zukünftige Arbeiten.

Contents

1. Classification of Fermionic Phases

In this chapter, we will introduce a classification of symmetry protected topological (SPT) phases in fermionic one-dimensional systems without interactions.

1.1. Fermionic Chains

Before we actually work on the definition and the classification of symmetry protected topological phases of fermions, we want to characterize the systems we consider.

In general we work with one-dimensional chains as shown in Figure 1.1. Those chains consist of L identical unit cells which are coupled to each other in some way. While the chain is considered to be long $L \to \infty$, which we will refer to as the thermodynamic limit, all couplings and interactions within the chain have to act on a short range. This means that the coupling lengths always stay finite and do not scale with L.

Every unit cell has some internal degrees of freedom and therefore an inner dimension d. The second quantized Hamiltonian of an open chain like this can be written as

$$\hat{H} = \sum_{i=1}^{L} \hat{H}_i^{\text{int}} + \sum_{i=1}^{L-1} \hat{H}_i^{\text{c}} \tag{1.1}$$

with an internal Hamiltonian $\hat{H}_i^{\text{int}}$ describing the individual unit cell i and a coupling Hamiltonian H_i^{c} which describes the couplings between the neighbouring cells i and $i+1$. Such a Hamiltonian, which fulfils our requirement that the system only features short-range interactions, is referred to as a *local Hamiltonian*. It might seem unclear why only neighbouring unit cells should couple to each other. If that is not the case, since we only allow short-range couplings we can always choose bigger unit cells until all interactions are occuring between neighbouring cells. As we can see in Figure 1.1, any open chain consists of two edge regions and a bulk between them. While the bulk region is completely periodic, the edges break the translational symmetry. In Equation (1.1) this shows up as there is one more internal term than there are coupling terms. While this will later lead to some very interesting effects which occur on the edges of

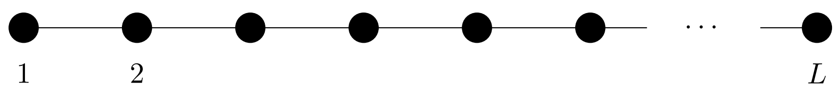

Figure 1.1.: We consider a long chain consisting of L identical unit cells. Every unit cell has a d-dimensional Hilbert space and we do not allow long-range interactions of any kind.

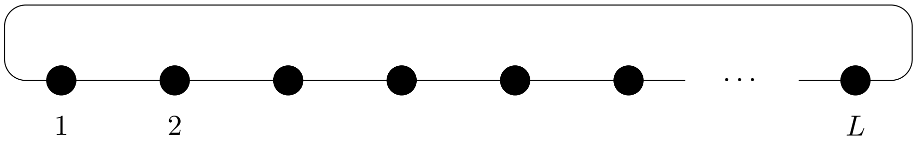

Figure 1.2.: An open chain is obtained by cutting a closed periodical ring of unit cells open between two cells.

the chains, we will start out with closed chains as shown in Figure 1.2. These rings are now completely translational invariant with only a bulk and no edges. Here we get a Hamiltonian of the form

$$\hat{H} = \sum_{i=1}^{L} \left(\hat{H}_i^{\text{int}} + \hat{H}_i^{\text{c}} \right). \tag{1.2}$$

Again the coupling Hamiltonian $\hat{H}_i^c$ couples between the neighbouring sites i and $i+1$ and we use the cyclic index $L+1=1$. By simply cutting one coupling open we can later transform a closed chain into an open chain.

We require for our Hamiltonians, that they are gapped.[1] This property will make more sense when we come to the definition of topological phases in these systems.

1.1.1. Fermionic Chains in the Momentum Space

At this point we want to make a little intermezzo and talk about the partial diagonalization of the Hamiltonian by a Fourier transformation. As we know, a translational invariant system with periodic boundary conditions and no interactions has a diagonal second quantized Hamiltonian in the momentum space. Our system also is translational invariant and we do not allow interactions. Therefore a Fourier transformation can actually make some calculations much easier.

First of all we have the second quantized Hamiltonian

$$\hat{H} = \sum_{ij} H_{ij} \hat{c}_i^\dagger \hat{c}_j \tag{1.3}$$

which is built from the first quantized Hamiltonian H. The operators $\hat{c}^\dagger$ and $\hat{c}$ denote the fermionic ladder operators. We will generally distinguish between second and first quantized operators by marking all second quantized operators with a circumflex. Here H is a $(d \cdot L) \times (d \cdot L)$ matrix. Our goal is to make this matrix smaller by using the translational invariance of our chains and the periodic boundary conditions.

Before we actually perform the transition into momentum space, we create a double index $(i\alpha)$ and $(j\beta)$ with $i, j \in \{1, \cdots, L\}$ and $\alpha, \beta \in \{1, \cdots, d\}$. This enables us to separate the index of the unit-cells and the inner index enumerating the degrees of

[1] A Hamiltonian is gapped if the ground state of the corresponding system is separated from the first exited state by a finite energy gap.

freedom of each unit cell. Now we have the Hamiltonian

$$\sum_{ij\alpha\beta} H_{(i\alpha),(j\beta)} \hat{c}^{\dagger}_{(i\alpha)} \hat{c}_{(j\beta)}. \tag{1.4}$$

The translational invariance tells us that

$$H_{(i\alpha),(j\beta)} = H_{(0\alpha),((j-i)\beta)}. \tag{1.5}$$

As we chose our unit cells such that only neighbouring cells interact, all terms with $|i-j| \geq 2$ vanish. The Fourier transformation acts only on the outer indices which enumerate the unit cells and is performed by

$$\hat{c}^{\dagger}_{k\alpha} = \frac{1}{\sqrt{L}} \sum_{j=1}^{L} e^{\mathrm{i}kj} \hat{c}^{\dagger}_{j\alpha} \tag{1.6a}$$

$$\hat{c}_{k\alpha} = \frac{1}{\sqrt{L}} \sum_{j=1}^{L} e^{-\mathrm{i}kj} \hat{c}_{j\alpha} \tag{1.6b}$$

with the momentum index

$$k = \frac{2\pi \mathrm{i}}{L} \tag{1.7}$$

for $i \in \{1, \cdots, L\}$. The inverse Fourier transformation can similarly be calculated by

$$\hat{c}^{\dagger}_{j\alpha} = \frac{1}{\sqrt{L}} \sum_{k} e^{-\mathrm{i}kj} \hat{c}^{\dagger}_{k\alpha} \tag{1.8a}$$

$$\hat{c}_{j\alpha} = \frac{1}{\sqrt{L}} \sum_{k} e^{\mathrm{i}kj} \hat{c}_{k\alpha}. \tag{1.8b}$$

Inserting the Fourier transformed ladder operators into Equation (1.4) gives us

$$\begin{aligned}
\hat{H} =& \frac{1}{L} \sum_{ij\alpha\beta kk'} H_{i\alpha,j\beta} e^{-\mathrm{i}(ki-k'j)} \hat{c}^{\dagger}_{k\alpha} \hat{c}_{k'\beta} && \text{(1.9a)}\\
=& \frac{1}{L} \sum_{ij\alpha\beta kk'} [\delta_{i,j-1} H_{0\alpha,1\beta} + \delta_{i,j} H_{0\alpha,0\beta} \\
& +\delta_{i,j+1} H_{1\alpha,0\beta}]\, e^{-\mathrm{i}(ki-k'j)} \hat{c}^{\dagger}_{k\alpha} \hat{c}_{k'\beta} && \text{(1.9b)}\\
=& \frac{1}{L} \sum_{i\alpha\beta kk'} \Big[e^{-\mathrm{i}(ki-k'(i+1))} H_{0\alpha,1\beta}\ e^{-\mathrm{i}(ki-k'i)} H_{0\alpha,0\beta} \\
& + e^{-\mathrm{i}(ki-k'(i-1))} H_{1\alpha,0\beta} \Big] \hat{c}^{\dagger}_{k\alpha} \hat{c}_{k'\beta} && \text{(1.9c)}\\
=& \frac{1}{L} \sum_{i\alpha\beta kk'} \Big[e^{\mathrm{i}k'} H_{0\alpha,1\beta} + H_{0\alpha,0\beta} + e^{-\mathrm{i}k} H_{1\alpha,0\beta} \Big] e^{-\mathrm{i}i(k-k')} \hat{c}^{\dagger}_{k\alpha} \hat{c}_{k'\beta} && \text{(1.9d)}\\
=& \sum_{\alpha\beta kk'} \Big[e^{\mathrm{i}k'} H_{0\alpha,1\beta} + H_{0\alpha,0\beta} + e^{-\mathrm{i}k'} H_{1\alpha,0\beta} \Big] \delta_{k,k'} \hat{c}^{\dagger}_{k\alpha} \hat{c}_{k'\beta} && \text{(1.9e)}
\end{aligned}$$

$$=\sum_{\alpha\beta k}\underbrace{\left[e^{\mathrm{i}k}H_{0\alpha,1\beta}+H_{0\alpha,0\beta}+e^{-\mathrm{i}k}H_{1\alpha,0\beta}\right]}_{(H(k))_{\alpha\beta}}\hat{c}^{\dagger}_{k\alpha}\hat{c}_{k\beta}. \tag{1.9f}$$

In this calculation we found a way to express the first quantized Hamiltonian as a k-dependent $d \times d$ matrix

$$(H(k))_{\alpha\beta}=\left[e^{\mathrm{i}k}H_{0\alpha,1\beta}+H_{0\alpha,0\beta}+e^{-\mathrm{i}k}H_{1\alpha,0\beta}\right]. \tag{1.10}$$

We will use this later in numerous calculations.

1.2. Symmetries

The systems we consider are special in yet another way. They all carry one or more symmetries. In the following we will discuss the details on the actions of symmetries in fermionic chains.

Let us consider a mathematical symmetry group G which contains a finite or infinite number of elements g and an operation

$$g_3 = g_1 \cdot g_2 \tag{1.11}$$

on these elements. The definition of groups requires g_3 to be also an element of the group G. Besides that, the operation $\cdot$ is commutative[2]. Every group G has an identity element 1 which fulfils

$$g = 1 \cdot g = g \cdot 1 \tag{1.12}$$

and for every element g there exists an inverse element g^{-1} such that

$$1 = g \cdot g^{-1} = g^{-1} \cdot g. \tag{1.13}$$

The elements of the symmetry group G are completely abstract. To describe a physical symmetry for a quantum mechanical system, we need to find a good representation of the group G. This means to find concrete objects $\hat{U}_g$ for all elements g which inherit the group structure

$$\hat{U}_{g_3} = \hat{U}_{g_1 \cdot g_2} = \hat{U}_{g_1}\hat{U}_{g_2}. \tag{1.14}$$

This is called a linear representation. The elements $\hat{U}_g$ act on the Hilbert space of our physical system. They are always unitary. In general, a quantum mechanical system is now symmetric under the symmetry group G if its second quantized Hamiltonian fulfils

$$\hat{U}_g\hat{H} = \hat{H}\hat{U}_g \tag{1.15}$$

for all elements g.

In the following we will describe how different symmetries act on fermionic systems [10].

[2] This is always the case for the symmetries in this thesis. In general, symmetry groups do not have to be commutative (Abelian). For example rotations in three dimensions are not commutative.

1.2.1. Unitarily Realized Symmetries

In this chapter we will only consider systems of non-interacting fermions. Therefore the second quantized Hamiltonian can be written as

$$\hat{H} = \sum_{i,j} \hat{c}_i^\dagger H_{i,j} \hat{c}_j \tag{1.16}$$

in terms of the first quantized Hamiltonian H and the fermionic ladder operators $\hat{c}$ and $\hat{c}^\dagger$.

Even though a system is only symmetric under some symmetry representation $\hat{U}_g$ if the condition

$$\hat{U}_g \hat{H} \hat{U}_g^{-1} = \hat{H} \tag{1.17}$$

holds, symmetries can act differently on the first quantized Hamiltonian H. We write U_g for the representation of the symmetry in the first quantized formalism.

A system is symmetric under a *unitarily realized symmetry* if there is a unitary representation U_g for every $g \in G$ acting on the single-particle Hilbert space such that the first quantized Hamiltonian fulfils

$$U_g H U_g^\dagger = H. \tag{1.18}$$

Here we can write a dagger because the representations U_g are simply unitary matrices ($U_g^{-1} = U_g^\dagger$).

The matrices U_g are related to the second quantized operators $\hat{U}_g$ via

$$\hat{U}_g \hat{c}_i \hat{U}_g^{-1} = \sum_j U_{g,ij}^\dagger \hat{c}_j \tag{1.19a}$$

$$\hat{U}_g \hat{c}_i^\dagger \hat{U}_g^{-1} = \sum_j \hat{c}_j^\dagger U_{g,ji}. \tag{1.19b}$$

This actually is, how the action of the symmetry is defined.

We can easily show that these relations make sense if we plug them into Equation (1.17). We start by using Equation (1.16) which leads to

$$\hat{U}_g \underbrace{\sum_{ij} \hat{c}_i^\dagger H_{ij} \hat{c}_j}_{=\hat{H}} \hat{U}_g^{-1} = \sum_{ij} \hat{c}_i^\dagger H_{ij} \hat{c}_j. \tag{1.20}$$

We can now insert $\mathbb{1} = \hat{U}_g^{-1} \hat{U}_g$ into the equation and get

$$\sum_{ij} \hat{U}_g \hat{c}_i^\dagger \hat{U}_g^{-1} H_{ij} \hat{U}_g \hat{c}_j \hat{U}_g^{-1} = \sum_{ij} \hat{c}_i^\dagger H_{ij} \hat{c}_j. \tag{1.21}$$

Keep in mind that H_{ij} are just the complex elements of the matrix H so they commute with $\hat{U}$. Now we can insert Equation (1.19a) and Equation (1.19b) and rearrange the terms to get

$$\sum_{ij} \hat{c}_i^\dagger \left(U_g H U_g^\dagger \right)_{ij} \hat{c}_j = \sum_{ij} \hat{c}_i^\dagger H_{ij} \hat{c}_j. \tag{1.22}$$

This equation only holds if $U_g H U_g^\dagger = H$, which is exactly Equation (1.18).

1.2.2. Anti-Unitarily Realized Symmetries

Not all symmetries fulfil Equation (1.18). There are actually three other possibilities for the realization of symmetries in fermionic systems. They are called anti-unitarily realized symmetries[3] which means that they contain a unitary operation and a complex conjugation. All fermionic symmetries that appear in this thesis are of this kind. We will shortly define all three classes of anti-unitarily realized symmetries and name them after their most popular physical representation.

All following classes of physical symmetries are technically representations of the $\mathbb{Z}_2$ symmetry group. This group contains only two elements which we call 1 (the trivial element) and g (the non-trivial element). It fulfils $g \cdot g = 1$. One typical geometric representation of this group can be a rotation of a two-dimensional object by $180\,^\circ$. The group element g corresponds to a rotation of the object, while the element 1 corresponds to no rotation. Rotating an object twice means applying the representation of $g \cdot g$. Also we know that a full rotation by $360\,^\circ$ leads to the same result as no rotation at all which is represented by $g \cdot g = 1$. This means that rotations by $180\,^\circ$ inherit the structure of the $\mathbb{Z}_2$ group.

The same holds for the anti-unitarily realized symmetries which we discuss here. That means that we will only consider the non-trivial element of $\mathbb{Z}_2$. The trivial element is always represented by the unity $\mathbb{1}$.

Time-Reversal Symmetry

Let $\hat{T}$ be the representation of the non-trivial element $g \neq 1$ of time-reversal symmetry in the second quantized formalism. As always it fulfils

$$\hat{T}\hat{H}\hat{T}^{-1} = \hat{H}. \tag{1.23}$$

Furthermore the action of the symmetry is defined by the relations

$$\hat{T}\hat{c}_i\hat{T}^{-1} = \sum_j U^\dagger_{T,ij}\hat{c}_j \tag{1.24a}$$

$$\hat{T}\hat{c}_i^\dagger\hat{T}^{-1} = \sum_j \hat{c}_j^\dagger U_{T,ji} \tag{1.24b}$$

$$\hat{T}\mathrm{i}\hat{T}^{-1} = -\mathrm{i} \tag{1.24c}$$

with some unitary matrix U_T. While the first two equations are similar as for a unitarily realized symmetry, the third condition makes this realization anti-unitary. It leads to the fact that we can no longer expect U_T to be the first quantized operator corresponding to $\hat{T}$ which we call T. Instead we find

$$T = U_T \circ K \tag{1.25}$$

[3] In this context we call a symmetry anti-unitary if at some point a complex conjugation appears. The operators of the symmetry realization may still be unitary (see also [10]).

where K denotes the complex conjugation. The first quantized Hamiltonian is symmetric under T

$$THT^{-1} = H \tag{1.26}$$

but not under the unitary matrix U_T. Instead we find

$$U_T H^* U_T^\dagger = H. \tag{1.27}$$

It can be shown [10], that two different kinds of time-reversal symmetries are possible. In fact, the operator T can square to

$$T^2 = \pm \mathbb{1}. \tag{1.28}$$

How do these conditions relate to an actual time-reversal? If $\hat{T}$ is supposed to reverse the time t, it has to act on the second quantized time-evolution operator $\hat{U}(t)$ in the following way:

$$\hat{T}\,\hat{U}(t) = \hat{U}(-t)\;\hat{T}. \tag{1.29}$$

In the first quantized picture this means that

$$Te^{iHt}T^{-1} = e^{-iHt} \tag{1.30}$$

has to hold. If the Hamiltonian would now fulfil $H = H^*$, we could simply implement the time-reversal by a complex conjugation $T = K$. As this is not the case in general, we need a unitary U_T such that Equation (1.27) holds. Then we define $T = U_T \circ K$ and this operator actually implements time-reversal.

Charge-Conjugation Symmetry

Let $\hat{C}$ be the second quantized operator of charge-conjugation symmetry. This class of symmetries is defined by the conditions

$$\hat{C}\hat{c}_i\hat{C}^{-1} = \sum_j \left(U^*_{C,ij}\right)^\dagger \hat{c}_j^\dagger \tag{1.31a}$$

$$\hat{C}\hat{c}_i^\dagger\hat{C}^{-1} = \sum_j \hat{c}_j U^*_{C,ji} \tag{1.31b}$$

$$\hat{C}\mathrm{i}\hat{C}^{-1} = \mathrm{i}. \tag{1.31c}$$

While the first two equations again implement the action of the symmetry on the fermionic Fock space, the third condition makes $\hat{C}$ an anti-unitary operator. As we can see, the operator of the charge-conjugation symmetry transposes creation operators to annihilation operators and vice versa. This is how an actual charge-conjugation can be implemented. While as always a system is symmetric under the symmetry $\hat{C}$ if

$$\hat{C}\hat{H}\hat{C}^{-1} = \hat{H} \tag{1.32}$$

holds, the unitary matrices U_C fulfil

$$U_C H^* U_C^\dagger = -H. \tag{1.33}$$

In the first quantized picture the operator $\hat{C}$ takes the form

$$C = U_C \circ K. \tag{1.34}$$

Similarly to Equation (1.26) this gives us

$$CHC^{-1} = -H \tag{1.35}$$

but with a minus sign.

As for the time-reversal symmetry we find the two possibilities

$$C^2 = \pm\mathbb{1}. \tag{1.36}$$

Sublattice Symmetry

The sublattice symmetry (or chiral symmetry) is the most important one for this thesis. It is a combination of time-reversal and charge-conjugation symmetry:

$$\hat{S} = \hat{T} \cdot \hat{C}. \tag{1.37}$$

It acts on the fermion Fock space via

$$\hat{S}\hat{c}_i\hat{S}^{-1} = \sum_j \left(U^*_{S,ij}\right)^\dagger \hat{c}^\dagger_j \tag{1.38a}$$

$$\hat{S}\hat{c}^\dagger_i\hat{S}^{-1} = \sum_j \hat{c}_j U^*_{S,ji} \tag{1.38b}$$

and is anti-unitary

$$\hat{S}\mathrm{i}\hat{S}^{-1} = -\mathrm{i}. \tag{1.38c}$$

U_S is an anti-unitary matrix which is related to the representations of time-reversal and charge-conjugation symmetry on the single-particle Hilbert space by

$$U_S = U_T U^*_C. \tag{1.39}$$

Bringing the operator $\hat{S}$ in the first quantized picture is simply done by converting the operators $\hat{T}$ and $\hat{C}$:

$$S = T \cdot C = (U_T \circ K) \cdot (U_C \circ K) = U_T U^*_C. \tag{1.40}$$

This is exactly the matrix U_S which we know from Equation (1.39).

Since we know how the time-reversal and the charge-conjugation symmetries act on the first quantized Hamiltonian, we also know that

$$SHS^{-1} = -H \tag{1.41}$$

holds.

In contrast to the time-reversal and the charge-conjugation symmetry, for sublattice symmetries we always find

$$S^2 = \mathbb{1}. \tag{1.42}$$

Name	T^2	C^2	S^2
A	0	0	0
AIII	0	0	1
AI	+1	0	0
AII	−1	0	0
D	0	+1	0
C	0	−1	0
BDI	+1	+1	1
CII	−1	−1	1
DIII	−1	+1	1
CI	+1	−1	1

Table 1.1.: List of all different possible combinations of anti-unitarily realized symmetries. Zeros correspond to the symmetry being broken in the system.

1.2.3. Ten-Fold Way

If a system does not fulfil any unitarily realized symmetry, it can still be symmetric under combinations of the three different anti-unitarily realized symmetries[4]. In Table 1.1, all those possible combinations are listed. This classification is called the ten-fold way [10].

There are $3 \cdot 3 = 9$ possibilities to fulfil or break time-reversal and charge-conjugation symmetry. If the system is symmetric under time-reversal *and* charge-conjugation symmetry, we get a sublattice symmetry for free since according to Equation (1.37) it is a combination of the other two symmetries. Still a system can break time-reversal and charge-conjugation symmetry but still fulfil a sublattice symmetry. This gives us one additional symmetry class called AIII. In this thesis we will take a closer look on specific systems which fulfil an AIII-symmetry.

1.3. Symmetry Protected Topological Phases

Let us go back to the closed chain systems sketched in Figure 1.2. Our system has a gapped Hamiltonian $\hat{H}$. In general, we assume that the system is in the (non-degenerate) ground state. Now let the local Hamiltonian $\hat{H}(\lambda)$ be a smooth function dependent of a parameter $\lambda \in [0, 1]$. Two ground states of the Hamiltonians $\hat{H}(0)$ and $\hat{H}(1)$ are said to be in the same *topological phase* if and only if there exists a smooth gapped path $\hat{H}(\lambda)$ between both Hamiltonians. If there is no way to find a path connecting both Hamiltonians without closing the band gap at some λ, the two ground states belong to two different phases. Figure 1.3 shows a sketch of a parameter space of some Hamiltonian $\hat{H}$ with different phases.

Now we are able to find systems with different topological phases. If we want to realize even more phases, we can do so by forbidding some additional paths $\hat{H}(\lambda)$. We do this by choosing some symmetry representation $\hat{S}$ of a group G and requiring $\hat{S}\hat{H}(\lambda) = \hat{H}(\lambda)\,\hat{S}$

[4]Including the different signs of T^2 and C^2

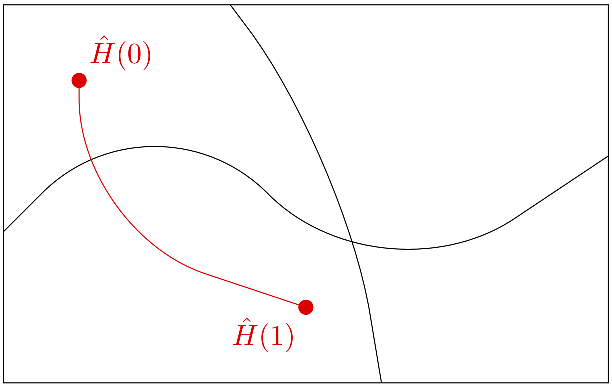

Figure 1.3.: Sketch of the parameter space of the Hamiltonian for some arbitrary system. Black lines seperate the different topological phases. Any Hamiltonian located on a black line has no band gap. In this picture we see that there is no continuos path from $\hat{H}(0)$ to $\hat{H}(1)$ without a phase transition. On the other hand, if two Hamiltonians belong to the same phase, there still exist some paths which close the gap at some point.

for all values of λ along a given path. Obviously this restriction forbids some of the paths connecting two Hamiltonians in the same phase. If a symmetry bans all gapped paths between two Hamiltonians, they belong to two different new phases which are protected by the symmetry. These phases are called *symmetry protected topological phases.*

1.3.1. Topological Invariant

Topology is a branch of mathematics in which geometric objects are investigated and compared to each other. It turns out that there exist some topological invariants for some shapes which cannot be changed by continuously deforming the object. The most common example is the comparison of a sphere and a torus (doughnut). The obvious difference is that a torus has one hole and a sphere has none. There is no way to continuously transform a torus into a sphere without closing the hole at some point. On the other hand, a torus can be transformed into any other shape which has exactly one hole. The number of holes can therefore not be changed and is called a topological invariant.

This observation is very similar to our phases. A system cannot be brought into another phase with a continuous path $\hat{H}(\lambda)$ without closing the band gap. This is why we speak of topological phases. The obvious question is: Is there also a topological invariant for symmetry protected topological phases?

1.3.2. Consequences of the Sublattice Symmetry

In fact, we find that there exists a number which differs between different phases and can in principal be calculated for any given system with Hamiltonian $\hat{H}$. In this thesis we want to take a closer look at the topological invariant ν (also called the winding number in this case), given the fact that the Hamiltonian is symmetric under a sublattice symmetry

$$\hat{S}\hat{H} = \hat{H}\hat{S}. \tag{1.43}$$

Before we go into the definition of the winding number, we have a look at the properties of the actual systems we consider. Those properties will prove to be very useful later on. As we showed in Subsection 1.1.1, the first quantized Hamiltonian can be expressed as a $d \times d$ matrix which depends on the momentum $H(k)$. Remember that d is the number of internal degrees of freedom of the identical unit cells.

Furthermore, the action of the symmetry S on the first quantized Hamiltonian is according to Equation (1.41)

$$SHS^{-1} = -H. \tag{1.44}$$

Now assume that the Hamiltonian has an eigenstate $|\psi_n\rangle$ with eigenvalue ϵ_n, such that $H|\psi_n\rangle = \epsilon_n |\psi_n\rangle$. Then we can calculate that the state $S|\psi_n\rangle$ is also an eigenstate of the Hamiltonian, but with eigenvalue $-\epsilon_n$:

$$HS|\psi_n\rangle = -SH|\psi_n\rangle = -S\epsilon_n|\psi_n\rangle = -\epsilon_n S|\psi_n\rangle. \tag{1.45}$$

What does this mean for the many-particle ground state? We have the same amount of positive and negative eigenenergies and the spectrum is symmetric around $\epsilon = 0$. It is easy to show that this property also holds in the second quantized case. Therefore in the ground-state, all states with negative energy are occupied by fermions while all states with positive energies are unoccupied. In principle there can also be some zero-energy states. In this case, the ground state would have a degeneracy. Still we want our Hamiltonian to be gapped. This means that in the thermodynamic limit ($L \to \infty$) a finite energy is needed to excite the system. If there was a state with zero energy, this could be filled without using any energy. Therefore we do not allow energy eigenvalues $\epsilon = 0$ for our Hamiltonian $\hat{H}$, because according to our definition it would not be a gapped Hamiltonian any more.

The first quantized Hamiltonian can be brought into the diagonalized form

$$H = \begin{pmatrix} \epsilon_1 & & & & \\ & -\epsilon_1 & & & \\ & & \epsilon_2 & & \\ & & & -\epsilon_2 & \\ & & & & \ddots \end{pmatrix}. \tag{1.46}$$

In this basis, the operator of the sublattice symmetry takes the form

$$S = \begin{pmatrix} 0 & -1 & & & \\ -1 & 0 & & & \\ & & 0 & -1 & \\ & & -1 & 0 & \\ & & & & \ddots \end{pmatrix}. \tag{1.47}$$

Here, S contains a finite number of two dimensional blocks with the eigenvalues 1 and -1 each. It can easily be shown that this fulfils Equation (1.43). Another useful basis is the eigenbasis of S such that

$$S = \begin{pmatrix} \mathbb{1} & 0 \\ 0 & -\mathbb{1} \end{pmatrix}. \tag{1.48}$$

In this basis it can be shown that the Hamiltonian takes the form

$$H = \begin{pmatrix} 0 & h^\dagger \\ h & 0 \end{pmatrix} \tag{1.49}$$

with the block matrix h.

1.3.3. Definitions of the Winding Number

We perform a Fourier transformation on the chain of fermions as discussed above. This basically diagonalizes the Hamiltonian on the unit cell level, while leaving out the internal degrees of freedom of each cell. This means that each momentum eigenstate $|k_i\rangle$ has some internal index $i \in \{1, \cdots, d\}$ corresponding to the d degrees of freedom in the unit cells. As the spectrum is symmetric for systems with a sublattice symmetry, for each momentum k only the lower half of the states $|k_i\rangle$ is occupied. Therefore we assume that we diagonalized the Hamiltonian $H(k)$ on the internal indices i and we ordered the eigenstates such that the eigenenergies ϵ_i for $i \in \{1, \cdots, d/2\}$ are negative. The upper half $i \in \{d/2 + 1, \cdots, d\}$ corresponds to the unoccupied states with positive energy.

The winding number can be defined by [11, 12]

$$\nu = \int_{-\pi}^{\pi} \mathrm{d}k \sum_{i=1}^{d/2} \langle k_i \,|\, \mathrm{i}\partial_k \,|\, k_i \rangle \,. \tag{1.50}$$

The sum indicates that we perform the integral for all occupied states. Calculating this integral gives us a whole number which we call the winding number of the system. Each symmetry protected topological phase corresponds to one winding number and changing the phase (while closing the band gap) means changing the winding number. The winding number is a topological invariant of the system.

Throughout the literature we find even more definitions of the winding number. For example in [13] we find

$$\nu = \int_{-\pi}^{\pi} \frac{\mathrm{d}k}{2\pi\mathrm{i}} \operatorname{Tr}\left(h^{-1}\partial_k h\right) \tag{1.51}$$

with the matrix h defined in Equation (1.49) as well as

$$\nu = \int_{-\pi}^{\pi} \frac{\mathrm{d}k}{2\pi\mathrm{i}} \partial_k \log(\det(h)) \tag{1.52}$$

and

$$\nu = \int_{-\pi}^{\pi} \frac{\mathrm{d}k}{2\pi} \partial_k \arg(\det(h)) \,. \tag{1.53}$$

Furthermore, we find the formula

$$\nu = \mathrm{Tr}\left(\int_{-\pi}^{\pi} \frac{\mathrm{d}k}{4\pi\mathrm{i}} S g^{-1} \partial_k g\right) \tag{1.54}$$

with the inverse matrix $g = H^{-1}$ of the Hamiltonian.

In some cases the Hamiltonian can be written in terms of the vector of Pauli matrices

$$\boldsymbol{\sigma} = \begin{pmatrix} \sigma^x \\ \sigma^y \\ \sigma^z \end{pmatrix} \tag{1.55a}$$

$$\sigma^x = \begin{pmatrix} 0 & 1 \\ 1 & 0 \end{pmatrix} \tag{1.55b}$$

$$\sigma^y = \begin{pmatrix} 0 & -\mathrm{i} \\ \mathrm{i} & 0 \end{pmatrix} \tag{1.55c}$$

$$\sigma^z = \begin{pmatrix} 1 & 0 \\ 0 & -1 \end{pmatrix} \tag{1.55d}$$

as

$$H = \boldsymbol{d} \cdot \boldsymbol{\sigma} \tag{1.56}$$

with some vector $\boldsymbol{d}$. In this case the winding number can be calculated by [14]

$$\nu = \frac{1}{2\pi} \int_{-\pi}^{\pi} \left(\hat{\boldsymbol{d}}(k) \times \frac{\mathrm{d}}{\mathrm{d}k} \hat{\boldsymbol{d}}(k)\right)_z \mathrm{d}k. \tag{1.57}$$

Now we somehow ended up with six different definitions of the winding number. As none of them is very intuitive, we will discuss them in the following and prove that they are all equivalent to each other.

1.3.4. Equivalence of Winding Numbers

We want to show that the definitions of the winding numbers in Subsection 1.3.3 are indeed equivalent.[5] Figure 1.4 is meant to give an overview on the following calculations. We enumerated the definitions to bring some structure into the proof. We will only show the equivalences $2 \Leftrightarrow 5$, $1 \Leftrightarrow 2$, $1 \Leftrightarrow 3$ and $3 \Leftrightarrow 4$. As shown in Figure 1.4, this will then prove, that all winding numbers are essentially the same.

Equivalence of 1 and 3 The trace $\mathrm{Tr}\left[h^{-1}\partial_k h\right]$ is invariant under any basis transformation. Therefore we can diagonalize h and h^{-1} which obviously requires the same basis for both matrices. Now the matrices only have the diagonal elements $h_{ii} = \lambda_i$ which are the eigenvalues of h. We can then calculate the trace:

[5] We will exclude Equation (1.50) from these considerations.

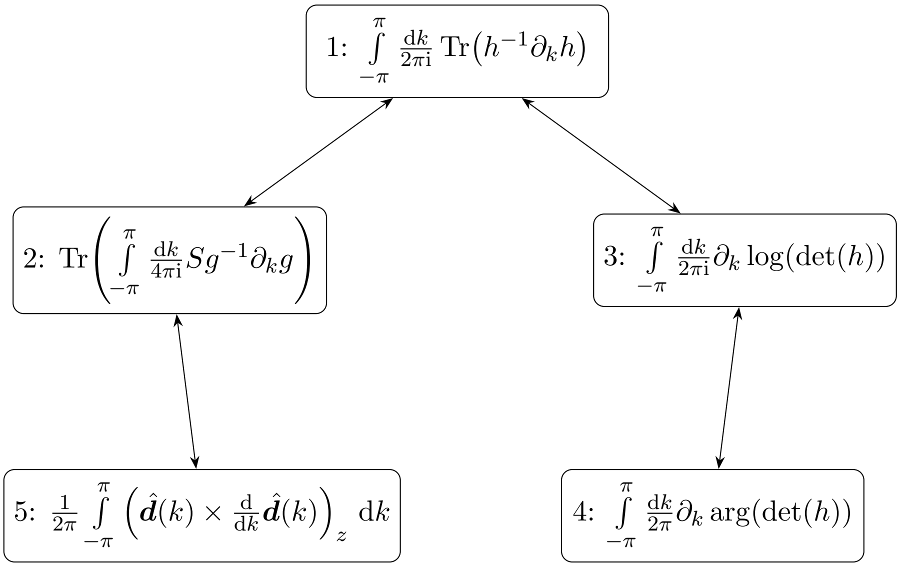

Figure 1.4.: Overview of the different winding numbers we defined in Subsection 1.3.3. In Subsection 1.3.4 we prove that all of those winding numbers are equivalent to each other. We do this by showing the equivalences indicated by the arrows in this image.

$$
\begin{aligned}
\operatorname{Tr}\left[h^{-1}\partial_k h\right] &= \sum_i \lambda_i^{-1}\partial_k \lambda_i && (1.58a)\\
&= \frac{\partial_k \prod_i \lambda_i}{\prod_i \lambda_i} && (1.58b)\\
&= \partial_k \left[\log\left(\prod_i \lambda_i\right)\right] && (1.58c)\\
&= \partial_k \left[\log(\det(h))\right]. && (1.58d)
\end{aligned}
$$

This proves that Equation (1.51) and Equation (1.52) are equivalent.

Equivalence of 3 and 4 The following equation holds for all logarithms with complex arguments:

$$\log(z) = \log(|z|) + \mathrm{i}\arg(z)\,. \tag{1.59}$$

If we now look at Equation (1.52) and insert this relation, we find

$$\int_{-\pi}^{\pi} \frac{\mathrm{d}k}{2\pi\mathrm{i}} \partial_k \log(\det(h)) = \int_{-\pi}^{\pi} \frac{\mathrm{d}k}{2\pi\mathrm{i}} \partial_k \left[\log(|\det(h)|) + \mathrm{i}\arg(\det(h))\right] \tag{1.60}$$

$$= \frac{1}{2\pi\mathrm{i}} \underbrace{\log(|\det(h)|)\big|_{-\pi}^{\pi}}_{=0} + \frac{1}{2\pi\mathrm{i}} \int_{-\pi}^{\pi} \mathrm{d}k\, \mathrm{i}\partial_k \arg(\det(h)) \tag{1.61}$$

$$= \int_{-\pi}^{\pi} \frac{\mathrm{d}k}{2\pi} \partial_k \arg(\det(h)) \,. \tag{1.62}$$

This works because in contrast to $\arg(\det(h))$, the absolute value $|\det(h)|$ is a single-valued function. This proves the equivalence of Equation (1.52) and Equation (1.53).

Equivalence of 1 and 2 Again we start off with

$$\nu = \mathrm{Tr}\left(\int_{-\pi}^{\pi} \frac{\mathrm{d}k}{4\pi \mathrm{i}} S g^{-1} \partial_k g \right) \tag{1.63}$$

and as our basis we choose the eigenbasis of S such that

$$S = \begin{pmatrix} \mathbb{1} & 0 \\ 0 & -\mathbb{1} \end{pmatrix} \tag{1.64}$$

and

$$H = \begin{pmatrix} 0 & h^\dagger \\ h & 0 \end{pmatrix} . \tag{1.65}$$

Then the inverse Hamiltonian is given by

$$H^{-1} = \begin{pmatrix} 0 & h^{-1} \\ \left(h^\dagger\right)^{-1} & 0 \end{pmatrix} . \tag{1.66}$$

Now we can calculate the trace in Equation (1.63):

$$\begin{aligned}
\mathrm{Tr}\big[S g^{-1} \partial_k g\big] &= \mathrm{Tr}\big[S H \partial_k H^{-1}\big] && (1.67a)\\
&= \mathrm{Tr}\left[\begin{pmatrix} \mathbb{1} & 0 \\ 0 & -\mathbb{1} \end{pmatrix} \begin{pmatrix} 0 & h^\dagger \\ h & 0 \end{pmatrix} \partial_k \begin{pmatrix} 0 & h^{-1} \\ \left(h^\dagger\right)^{-1} & 0 \end{pmatrix} \right] && (1.67b)\\
&= \mathrm{Tr}\left[\begin{pmatrix} h^\dagger \partial_k \left(h^\dagger\right)^{-1} & 0 \\ 0 & -h \partial_k h^{-1} \end{pmatrix} \right] && (1.67c)\\
&= \mathrm{Tr}\left[h^\dagger \partial_k \left(h^\dagger\right)^{-1} - h \partial_k h^{-1} \right] && (1.67d)\\
&= -\,\mathrm{Tr}\big[h \partial_k h^{-1} - \mathrm{h.c.}\big] && (1.67e)\\
&= \mathrm{Tr}\big[-h \partial_k h^{-1}\big] - \mathrm{c.c.}. && (1.67f)
\end{aligned}$$

We can insert the hermitean conjugate because the trace is invariant under cyclic permutations. It is obvious that

$$0 = \partial_k \mathbb{1} = \partial_k \left(h h^{-1}\right) = h \partial_k h^{-1} + h^{-1} \partial_k h \tag{1.68}$$

which gives us

$$\mathrm{Tr}\big[Sg^{-1}\partial_k g\big] = \mathrm{Tr}\big[h^{-1}\partial_k h\big] - \text{c.c.} \tag{1.69}$$
$$= 2\mathrm{i}\,\mathrm{Im}\big(\mathrm{Tr}\big[h^{-1}\partial_k h\big]\big)\,. \tag{1.70}$$

We are not allowed simply to ignore the Im yet, but we can work around that if we take the integral of this expression:

$$\int\limits_{-\pi}^{\pi} \mathrm{d}k\ \mathrm{Tr}\big[Sg^{-1}\partial_k g\big] = 2\mathrm{i}\int\limits_{-\pi}^{\pi} \mathrm{d}k\ \mathrm{Im}\big(\mathrm{Tr}\big[h^{-1}\partial_k h\big]\big)\,. \tag{1.71}$$

Following the same calculation as in Equation (1.60), we find that the real part of $\mathrm{Tr}\big[h^{-1}\partial_k h\big]$ vanishes in the integral, so we can add it to the equation. We do this by simply dropping the Im. This gives us

$$\int\limits_{-\pi}^{\pi} \mathrm{d}k\ \mathrm{Tr}\big[Sg^{-1}\partial_k g\big] = \int\limits_{-\pi}^{\pi} 2\,\mathrm{Tr}\big[h^{-1}\partial_k h\big]\ \mathrm{d}k \tag{1.72}$$

and therefore proves that

$$\mathrm{Tr}\left(\int\limits_{-\pi}^{\pi} \frac{\mathrm{d}k}{4\pi\mathrm{i}} Sg^{-1}\partial_k g\right) = \int_{-\pi}^{\pi} \frac{\mathrm{d}k}{2\pi\mathrm{i}}\,\mathrm{Tr}\big(h^{-1}\partial_k h\big)\,. \tag{1.73}$$

This means that both definitions of the winding number are actually the same.

Equivalence of 2 and 5 First of all, it is clear that we can only write the k-dependent Hamiltonian as $H = \boldsymbol{d}\cdot\boldsymbol{\sigma}$ if the unit-cells of our system are two-level systems and $H(k)$ is therefore a 2×2 matrix. This way $\boldsymbol{d}$ is a simple tree-dimensional vector with complex elements d_x, d_y and d_z. Then it is always possible to write $H = \boldsymbol{d}\cdot\boldsymbol{\sigma}$, because the Pauli matrices and $\mathbb{1}$ form a basis of all complex 2×2 matrices. Still the Hamiltonian has a symmetric spectrum, which does not allow a contribution of the matrix $\mathbb{1}$. Therefore the matrices σ^x, σ^y and σ^z form a sufficient basis for H.

We start by choosing the eigenvectors of S as our basis, such that $S = \sigma^z$ and $d_z = 0$. In Equation (1.54) we insert the Hamiltonian:

$$\mathrm{Tr}\left[\int_{-\pi}^{\pi} \frac{\mathrm{d}k}{4\pi\mathrm{i}} Sg^{-1}\partial_k g\right] = \mathrm{Tr}\left[\int_{-\pi}^{\pi} \frac{\mathrm{d}k}{4\pi\mathrm{i}} SH\partial_k H^{-1}\right] \tag{1.74}$$
$$= \mathrm{Tr}\left[\int_{-\pi}^{\pi} \frac{\mathrm{d}k}{4\pi\mathrm{i}} \sigma^z\left(\sigma^x d_x + \sigma^y d_y\right)\partial_k\left(\sigma^x d_x + \sigma^y d_y\right)^{-1}\right]. \tag{1.75}$$

We then invert the right part which leads to

$$= \mathrm{Tr}\left[\int_{-\pi}^{\pi} \frac{\mathrm{d}k}{4\pi\mathrm{i}} \sigma^z\left(\sigma^x d_x + \sigma^y d_y\right)\partial_k\left(\sigma^x \frac{d_x}{d_x^2 + d_y^2} + \sigma^y \frac{d_y}{d_x^2 + d_y^2}\right)\right]. \tag{1.76}$$

Now we can apply the derivation using the product rule. This leads to some lengthy calculations. Some of the terms appearing can directly be ignored because the product of the Pauli matrices vanishes:

$$
\begin{aligned}
&= \operatorname{Tr} \int_{-\pi}^{\pi} \frac{\mathrm{d}k}{4\pi \mathrm{i}} \sigma^z \left(\sigma^x d_x + \sigma^y d_y\right) \\
&\quad \cdot \left[\sigma^x \left(\frac{1}{d_x^2 + d_y^2} \partial_k d_x - d_x \frac{1}{\left(d_x^2 + d_y^2\right)^2} \left(2 d_x \partial_k d_x + 2 d_y \partial_k d_y\right)\right)\right. \\
&\quad \left. + \sigma^y \left(\frac{1}{d_x^2 + d_y^2} \partial_k d_y - d_y \frac{1}{\left(d_x^2 + d_y^2\right)^2} \left(2 d_x \partial_k d_x + 2 d_y \partial_k d_y\right)\right)\right] &\quad (1.77a)\\
&= \operatorname{Tr} \int_{-\pi}^{\pi} \frac{\mathrm{d}k}{4\pi \mathrm{i}} \left[\sigma^z \sigma^x d_x \sigma^y \frac{1}{d_x^2 + d_y^2} \partial_k d_y\right. \\
&\quad - \sigma^z \sigma^x d_x \sigma^y d_y \frac{1}{\left(d_x^2 + d_y^2\right)^2} \left(2 d_x \partial_k d_x + 2 d_y \partial_k d_y\right) \\
&\quad + \sigma^z \sigma^y d_y \sigma^x \frac{1}{d_x^2 + d_y^2} \partial_k d_x \\
&\quad \left. - \sigma^z \sigma^y d_y \sigma^x d_x \frac{1}{\left(d_x^2 + d_y^2\right)^2} \left(2 d_x \partial_k d_x + 2 d_y \partial_k d_y\right)\right] &\quad (1.77b)\\
&= \operatorname{Tr} \int_{-\pi}^{\pi} \frac{\mathrm{d}k}{4\pi \mathrm{i}} \left[\mathrm{i}\mathbb{1} \left(\frac{d_x}{d_x^2 + d_y^2} \partial_k d_y - \frac{d_x d_y}{d_x^2 + d_y^2} \left(2 d_x \partial_k d_x + 2 d_y \partial_k d_y\right)\right)\right. \\
&\quad \left. - \mathrm{i}\mathbb{1} \left(\frac{d_y}{d_x^2 + d_y^2} \partial_k d_x - \frac{d_x d_y}{d_x^2 + d_y^2} \left(2 d_x \partial_k d_x + 2 d_y \partial_k d_y\right)\right)\right] &\quad (1.77c)\\
&= \operatorname{Tr} \int_{-\pi}^{\pi} \frac{\mathrm{d}k}{4\pi} \mathbb{1} \frac{d_x \partial_k d_y - d_y \partial_k d_x}{d_x^2 + d_y^2} &\quad (1.77d)\\
&= \int_{-\pi}^{\pi} \frac{\mathrm{d}k}{2\pi} \frac{d_x \partial_k d_y - d_y \partial_k d_x}{d_x^2 + d_y^2} &\quad (1.77e)\\
&= \frac{1}{2\pi} \left(\hat{\boldsymbol{d}}(k) \times \frac{\mathrm{d}}{\mathrm{d}k} \hat{\boldsymbol{d}}(k)\right)_z \mathrm{d}k. &\quad (1.77f)
\end{aligned}
$$

This proves the equivalence of Equation (1.54) and Equation (1.57).[6]

Interpretation of 5 Why is this topological invariant called a winding number? We want to interpret this in more detail using Equation (1.57). As we elaborated now, the vector $\boldsymbol{d}(k)$ is confined in the x-y-plane. As we go from $k = -\pi$ to π, it follows a closed smooth path on this plane. Equation (1.57) then counts how many times this closed curve is winded around the origin of the coordinate system. Therefore it makes sense to call ν a winding number.

In principle there are two ways of changing the winding number. Of course we could add a z-component $d_z \neq 0$ to the vector $\boldsymbol{d}(k)$ and when we deform the curve, we lift

[6] The vector $\hat{\boldsymbol{d}}$ denotes the unit vector $\hat{\boldsymbol{d}} = \boldsymbol{d}/|\boldsymbol{d}|$.

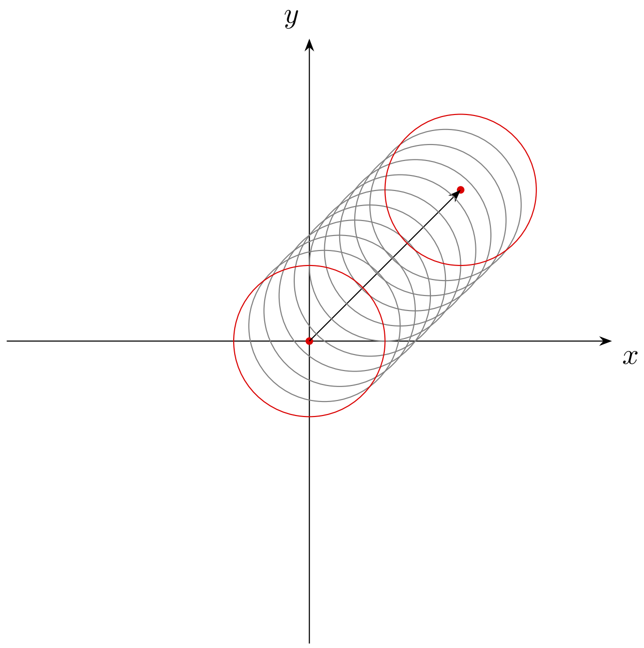

Figure 1.5.: In this sketch we show the curve painted by the vector $\boldsymbol{d}(k)$ for $k \in [-\pi, \pi]$. It can for example be a simple circle around the origin which gives us a winding number of $\nu = \pm 1$, depending on the direction of rotation. We can change the winding number for example by moving the curve, such that it does not include the origin any more, which gives us $\nu = 0$. When we do this in a smooth way, we cannot avoid it to cross the origin at some point. This closes the band gap. The same happens for every kind of smooth deformation of the path.

it over the origin. This is in principle possible but it violates the sublattice symmetry constraint given by Equation (1.44). Another way to change the winding number is to deform or to move it within the x-y-plane. In Figure 1.5, a sketch of a circular curve is shown which is translated such that it does not include the origin in the end. As we can see, there is no smooth deformation or translation of the curve that changes the winding number without there being a point, where for one momentum k_0 we find $\boldsymbol{d}(k_0) = \boldsymbol{0}$. This is where the path crosses the origin. If the vector $\boldsymbol{d}$ vanishes, the Hamiltonian H vanishes. This means that if we want to change the winding number without breaking the symmetry, we have to close the band gap.

Although the vector $\boldsymbol{d}(k)$ is a quite abstract and unintuitive object, we see that the winding number is indeed a good topological invariant which characterizes our symmetry protected topological phases perfectly. It can only be changed by breaking the symmetry or by closing the band gap of the system. These are exactly the same requirements for changing the phase.

Interpretation of 4 As $\boldsymbol{d}(k)$ is a relatively abstract vector and as it can only be defined in systems which have a 2×2 Hamiltonian $H(k)$, we also take a look at Equation (1.53). This gives us a less figurative but maybe more honest interpretation. If we define

$$\nu = \int_{-\pi}^{\pi} \frac{\mathrm{d}k}{2\pi} \partial_k \arg(\det(h)) \,, \tag{1.78}$$

we can bring the matrix h in a diagonal form. Every eigenvalue

$$\lambda_i = r_i e^{\mathrm{i}\phi_i} \tag{1.79}$$

of $h(k)$ is a complex number which draws a closed path on the complex plane for $k \in [-\pi, \pi]$. This means that we can define a winding number for every eigenvalue around the centre of the complex plane. We find that these winding numbers are embedded in the topological invariant:

$$\nu = \int_{-\pi}^{\pi} \frac{\mathrm{d}k}{2\pi} \partial_k \arg\left(\prod_i \lambda_i\right) \tag{1.80}$$

$$= \int_{-\pi}^{\pi} \frac{\mathrm{d}k}{2\pi} \partial_k \left[\sum_i \phi_i\right] \tag{1.81}$$

$$= \frac{1}{2\pi} \sum_i \phi_i \bigg|_{-\pi}^{\pi} . \tag{1.82}$$

Now we see that the topological invariant ν is nothing but the sum of all winding numbers for all eigenvalues of h in the complex plane.

Still, if we want to change the winding number, we have to change the winding number of at least one $\lambda_i(k)$ which means that at some point it has to cross the origin of the complex plane. At this point, the Hamiltonian has a zero eigenvalue and again the gap is closed.

1.4. Edge Modes

Till now, our classification of symmetry protected topological phases was purely mathematical and based on the winding number. Now we want to find some actual physical differences between states that belong to different phases. In general this is not trivial. In this thesis we will work with states in different phases which are related to each other by a shifted of half a unit cell. In these cases, the phases only exist because of our definition of a unit cell. Finding differences between the phases besides the abstract winding number is therefore not a trivial task.

If we consider our closed chain in Figure 1.2, we see that the eigenmodes of the systems typically are delocalized. This is due to the translational symmetry of the system and the fact that we can partially diagonalize the system via a Fourier transformation.

In the remainder of this section we will cut our chain open as shown in Figure 1.1. In one dimension, this means that we end up with two edges at the left and the right end of the system. As shown in [15], depending on the phase of the system, this gives rise to so-called *edge modes*. Those correspond to single-particle wave functions which only live near the edge and have a finite penetration depth into the bulk of the system. Throughout this thesis we will work with examples of these edge modes.

The energies of these edge modes are usually inside the band gap of the system. Therefore they are also called *in-gap modes*. This allows us to experimentally observe the phase of the system: Some (trivial) phases do not support in-gap modes and some (non-trivial) phases do. Looking for excitations within the band gap will therefore give us some information about the actual phase of the system. Similarly to the phase, also the topological edge modes of the system are protected by the symmetry and therefore robust with respect to symmetry-preserving perturbations.

This connection between the topological state of the bulk and the existence of edge modes for open boundary conditions is referred to as *bulk-boundary correspondence*.

1.4.1. Towards Quantum Computation

We have now given an overview on the topic of symmetry protected topological phases in one-dimensional fermionic systems. Before proceed with the specific systems considered in this thesis, we want to make a brief intermezzo and explain why these special systems are interesting from a more applied point of view.

In quantum computation one relies on quantum bits (qubits) which are analogous to the bits of a classical computer. They are supposed to be simple, degenerate two-level systems with states $|\uparrow\rangle$ and $|\downarrow\rangle$ which are analogous to the binary 1 and 0 of classical computers. The main challenge of building a working quantum computer is to find two-level systems which are suited to be used for this application. They should be as stable, unperturbed and scalable as possible while not requiring elaborate cooling devices. Because of the existence of edge states, symmetry protected topological phases may provide a workaround for some of these problems.

If we knew what a perturbation on a system looks like, we could simply take it into account when we build our quantum computer. This is obviously not possible, but perturbations are not completely unpredictable either. In many cases, we know for example that perturbations are only short-range correlated and weak. Also a perturbation might obey one or more symmetry constraints. For example, a perturbation might conserve the particle number in a system or not change the parity of the particle number in superconductors. Thus, there may be additional perturbation terms in the Hamiltonian which are short-range correlated, weak and conserve certain symmetries. If we find a system with a symmetry protected topological phase which only features perturbations commuting with the symmetry, these perturbations will not be able to change the phase of the system and lift the degeneracy of the ground states. Therefore we say that the phase is *protected by the symmetry* and we do not need to know what our perturbations look like.

How does this help us to find good qubits? Consider a long open, chain in a topological phase with degenerate edge modes. The energies of these edge-modes are also protected by the symmetry constraint. In this thesis, for example, we work with the so called SSH chain which features one fermionic edge mode with energy $\epsilon = 0$ on each end of the chain. The energy of the system does not depend on the occupancy of these modes, so we find $2 \cdot 2 = 4$ degenerate ground-states and we are able to store information on the edges of the system. These systems could, in principle, be used as qubits, because they feature a ground state degeneracy which is protected by a symmetry constraint.[7] As long as all perturbations obey the symmetry constraint (and the chains are long enough), we do not need to come up with clever ideas to suppress those perturbations: They simply decouple from the qubit.

[7] We want to make clear, that the SSH chain is not a good candidate for these applications because the symmetry constraints we use do not appear like this in reality (small magnetic fields on the edge could immediately lift the ground state degeneracy). On the other hand, Majorana chains [16] (which also feature symmetry protected topological phases) feature more realistic symmetries which are actually conserved.

2. Fermionic Phases in the SSH Chain

The Su–Schrieffer–Heeger (SSH) model was first introduced in 1979 [17]. It was meant to help us understand solitons in long polyacetylene molecules. In this thesis, we will use the SSH model for a different purpose.

2.1. Introduction to the SSH Chain

The SSH chain falls in the class of systems which we introduced in Figure 1.1. A sketch of it is shown in Figure 2.1. Each unit cell contains two sites which can be occupied by one fermion each. They are coupled by hopping terms of strength J_1. The unit cells are also coupled via hopping terms of magnitude J_2. The chain features two sublattices A and B which either include all upper or all lower lattice sites. All couplings in the system connect the two sublattices. This is the symmetry constraint of this system which we call an AIII sublattice symmetry. There are no couplings which connect a site of sublattice A (B) to another site of A (B).

Of course we can close the SSH chain such that it becomes a ring with periodic boundary conditions. We simply add a hopping term of magnitude J_2 to connect the very first site of the chain to the last site. This will be necessary to calculate winding numbers in this system.

2.1.1. Hamiltonian of the SSH Chain

We will enumerate the $2L$ sites of the SSH chain by simply counting them starting with the left site in the first unit cell. This way, all odd numbers correspond to the sites in sublattice B, while sites in sublattice A have even indices. Each particle can occupy one of the states $|i\rangle$ with $i \in \{1, \cdots, 2L\}$, meaning that it occupies the site i. In this basis,

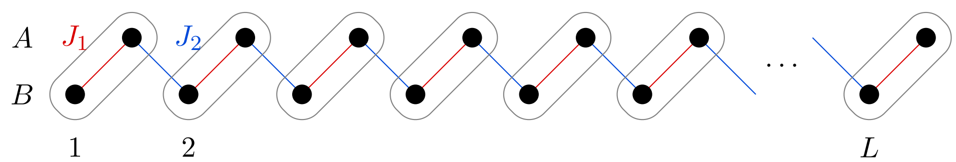

Figure 2.1.: Sketch of an SSH chain. The system features unit cells with two sites each. The sites are coupled by fermionic hopping terms of magnitude J_1 and J_2. The SSH chain also conserves a sublattice symmetry of type AIII (see Table 1.1).

the first quantized Hamiltonian that describes the SSH chain [14] is

$$H = J_1 \sum_{i=1}^{L} \left(|2i\rangle \langle 2i-1| + \text{h.c.} \right) + J_2 \sum_{i=1}^{L-1} \left(|2i+1\rangle \langle 2i| + \text{h.c.} \right), \tag{2.1}$$

or written in matrix form

$$H = \begin{pmatrix} 0 & J_1 & & & & & 0 \\ J_1 & 0 & J_2 & & & & \\ & J_2 & 0 & J_1 & & & \\ & & J_1 & 0 & & & \\ & & & & \ddots & & \\ & & & & & 0 & J_1 \\ 0 & & & & & J_1 & 0 \end{pmatrix}. \tag{2.2}$$

Here we assumed that $J_1, J_2 \in \mathbb{R}$. In principle these numbers can also be complex but then they have to be included into the brackets of Equation (2.1) such that the Hamiltonian matrix stays hermitean.[1] Then Equation (2.2) reads

$$H = \begin{pmatrix} 0 & J_1 & & & & & 0 \\ J_1^* & 0 & J_2 & & & & \\ & J_2^* & 0 & J_1 & & & \\ & & J_1^* & 0 & & & \\ & & & & \ddots & & \\ & & & & & 0 & J_1 \\ 0 & & & & & J_1^* & 0 \end{pmatrix}. \tag{2.3}$$

According to Equation (1.3), the second quantized Hamiltonian is

$$\hat{H} = \sum_{i=1}^{2L} J_1 \hat{c}_{2i-1}^\dagger \hat{c}_{2i} + \sum_{i=1}^{L-1} J_2 \hat{c}_{2i}^\dagger \hat{c}_{2i+1} + \text{h.c.}. \tag{2.4}$$

What does the band structure of the SSH chain look like? We cannot simply diagonalize the Hamiltonian matrix in Equation (2.2), especially when the system length L gets very large. Therefore we close the chain to a ring which modifies the Hamiltonian slightly:

$$H = \begin{pmatrix} 0 & J_1 & & & & 0 & J_2 \\ J_1 & 0 & J_2 & & & 0 & 0 \\ & J_2 & 0 & J_1 & & & \\ & & J_1 & 0 & & & \\ & & & & \ddots & & \\ 0 & 0 & & & & 0 & J_1 \\ J_2 & 0 & & & & J_1 & 0 \end{pmatrix}. \tag{2.5}$$

[1]Most of the calculations of this thesis either allow complex coupling constants, or can be slightly modified to allow them. Nevertheless, we will usually assume that J and J' are real numbers.

Now we can perform a Fourier transformation on the unit cells and according to Equation (1.10) obtain

$$H(k) = \begin{pmatrix} 0 & J_1 + e^{-ik} J_2 \\ J_1 + e^{ik} J_2 & 0 \end{pmatrix}. \tag{2.6}$$

This 2×2 matrix can now easily be diagonalized. We find the energy bands

$$E_{\pm}(k) = \pm\sqrt{J_1^2 + J_2^2 + 2J_1 J_2 \cos(k)}. \tag{2.7}$$

It is obvious that if either J_1 or J_2 are zero, both bands are flat. If they are both not zero, we get curved bands. The band gap can easily be calculated by

$$\Delta E = |J_1 - J_2|\,. \tag{2.8}$$

This immediately shows us that the gap is closed if $J_1 = J_2$. We will later see that this is indeed the point at which a phase transition occurs.

2.1.2. Symmetry of the SSH Chain

As we already mentioned, the SSH chain contains a sublattice symmetry of type AIII. In the second quantization, the generator of this symmetry group is represented by

$$\hat{S} = \left[\prod_{i=1}^{L} \left(\hat{c}_{2i-1}^{\dagger} - \hat{c}_{2i-1}\right)\left(\hat{c}_{2i}^{\dagger} + \hat{c}_{2i}\right)\right] \circ K. \tag{2.9}$$

At this point it is important to remember the anti-commutation relations of the fermionic ladder operators:

$$\left\{\hat{c}_i^{\dagger}, \hat{c}_j^{\dagger}\right\} = 0 \tag{2.10a}$$

$$\left\{\hat{c}_i, \hat{c}_j\right\} = 0 \tag{2.10b}$$

$$\left\{\hat{c}_i, \hat{c}_j^{\dagger}\right\} = \delta_{i,j}. \tag{2.10c}$$

We can work out a few useful relations. First of all, the symmetry operator does not squares to one[2]:

$$\hat{S}^2 = \left(\left[\prod_{i=1}^{L} \left(\hat{c}_{2i-1}^{\dagger} - \hat{c}_{2i-1}\right)\left(\hat{c}_{2i}^{\dagger} + \hat{c}_{2i}\right)\right] \circ K\right)^2 \tag{2.11a}$$

$$= \prod_{i=1}^{L} \left(\hat{c}_{2i-1}^{\dagger} - \hat{c}_{2i-1}\right)^2 \cdot \left(\hat{c}_{2i}^{\dagger} + \hat{c}_{2i}\right)^2 \tag{2.11b}$$

$$= \prod_{i=1}^{L} -\mathbb{1} \cdot \mathbb{1} \tag{2.11c}$$

[2]To do this calculation, one has to keep an eye on the fermionic commutation relations.

$$= (-1)^L \mathbb{1}. \tag{2.11d}$$

We still can find a inverse operator to $\hat{S}$:

$$\hat{S}^{-1} = \left[\prod_{i=L}^{1} \left(\hat{c}_{2i} + \hat{c}_{2i}^\dagger\right)\left(\hat{c}_{2i-1} - \hat{c}_{2i-1}^\dagger\right)\right] \circ K. \tag{2.12}$$

It is easy to show that this gives $\hat{S}\hat{S}^{-1} = \mathbb{1}$.

We can now check that the symmetry $\hat{S}$ actually commutes with the Hamiltonian $\hat{H}$. To do so, we use the relations

$$\hat{S}\hat{c}_{2i-1}^\dagger\hat{S}^{-1} = \hat{c}_{2i-1} \tag{2.13a}$$
$$\hat{S}\hat{c}_{2i-1}\hat{S}^{-1} = \hat{c}_{2i-1}^\dagger \tag{2.13b}$$
$$\hat{S}\hat{c}_{2i}^\dagger\hat{S}^{-1} = -\hat{c}_{2i} \tag{2.13c}$$
$$\hat{S}\hat{c}_{2i}\hat{S}^{-1} = -\hat{c}_{2i}^\dagger \tag{2.13d}$$

to find

$$\hat{S}\hat{c}_{2i-1}^\dagger\hat{c}_{2i}\hat{S}^{-1} = \hat{S}\hat{c}_{2i-1}^\dagger\hat{S}^{-1}\hat{S}\hat{c}_{2i}\hat{S}^{-1} = -\hat{c}_{2i-1}\hat{c}_{2i}^\dagger = \hat{c}_{2i}^\dagger\hat{c}_{2i-1}. \tag{2.14}$$

This is the hermitean conjugate of $\hat{c}_{2i-1}^\dagger\hat{c}_{2i}$. If we now take a look at Equation (2.4), we can directly see that $\hat{S}\hat{H}\hat{S}^{-1} = \hat{H}$.

In the first quantization, we can also work out the unitary matrix S which generates the sublattice symmetry. It has to fulfil

$$SH(k)\,S^{-1} = -H(k)\,. \tag{2.15}$$

Here we use the momentum-dependent first quantized Hamiltonian $H(k)$ from Equation (2.6). Furthermore, S is supposed to be a unitary matrix. It is straightforward to see that the matrix

$$S = \sigma^z = \begin{pmatrix} 1 & 0 \\ 0 & -1 \end{pmatrix} \tag{2.16}$$

fulfils these requirements.

As we mentioned before, the symmetry does not only describe some characteristics of the Hamiltonian. It is also a constraint for the whole system even with perturbations. Therefore we are well advised to try to understand what the constraint of the sublattice symmetry really is.

Consider two even numbers e_1 and e_2 as well as two odd numbers o_1 and o_2. What is the action of the symmetry S on hopping terms between sites e_1 and e_2 (o_1 and o_2)? We can find that these hopping terms get a minus sign by the symmetry:

$$\hat{S}\left(\hat{c}_{e_1}^\dagger\hat{c}_{e_2} + \hat{c}_{e_2}^\dagger\hat{c}_{e_1}\right)\mathrm{S}^{-1} = -\left(\hat{c}_{e_1}^\dagger\hat{c}_{e_2} + \hat{c}_{e_2}^\dagger\hat{c}_{e_1}\right) \tag{2.17a}$$
$$\hat{S}\left(\hat{c}_{o_1}^\dagger\hat{c}_{o_2} + \hat{c}_{o_2}^\dagger\hat{c}_{o_1}\right)\mathrm{S}^{-1} = -\left(\hat{c}_{o_1}^\dagger\hat{c}_{o_2} + \hat{c}_{o_2}^\dagger\hat{c}_{o_1}\right). \tag{2.17b}$$

If on the other hand we take an even number e and an odd number o, we will always find

$$\hat{S}\left(\hat{c}_e^\dagger \hat{c}_o + \hat{c}_o^\dagger \hat{c}_e\right) \mathrm{S}^{-1} = \left(\hat{c}_e^\dagger \hat{c}_o + \hat{c}_o^\dagger \hat{c}_e\right). \tag{2.18}$$

This means that our Hamiltonian can only contain hopping terms between even and odd numbered sites. If we add a hopping term which couples two even (odd) sites, the Hamiltonian will break the sublattice symmetry. This includes the counting of particles on a single site ($\hat{n}_i = \hat{c}_i^\dagger \hat{c}_i$). On the other hand, in Figure 2.1 we saw that even and odd sites correspond to the different sublattices of the SSH chain. The sublattice symmetry forces our system to suppress all fermion tunnelling processes within a single sublattice.

Also keep in mind that the Hamiltonian is supposed to be local which requires the hopping distance $|e - o|$ to be finite in the thermodynamic limit.

The choice of S is not unique. Obviously, we can change the global phase of S without any physical consequences, but we also could have chosen

$$\hat{S}' = \left[\prod_{i=1}^{L} \left(\hat{c}_{2i-1}^\dagger + \hat{c}_{2i-1}\right)\left(\hat{c}_{2i}^\dagger - \hat{c}_{2i}\right)\right] \circ K. \tag{2.19}$$

This would yield the same physical restrictions for our SSH chain.

2.1.3. Winding Number of the SSH Chain

We want to calculate the winding number of the SSH chain and find different phases. To do so, we use Equation (1.53). This choice is completely arbitrary and any other formula in Figure 1.4 would give the same result.

From Equation (1.49) and Equation (2.6) we know that

$$h(k) = J_1 + J_2 e^{ik}. \tag{2.20}$$

The winding number is now calculated by

$$\begin{aligned}
\nu &= \int_{-\pi}^{\pi} \frac{\mathrm{d}k}{2\pi} \partial_k \arg(\det(h)) && (2.21\text{a})\\
&= \int_{-\pi}^{\pi} \frac{\mathrm{d}k}{2\pi} \partial_k \arg\left(\det\left(J_1 + J_2 e^{ik}\right)\right) && (2.21\text{b})\\
&= \int_{-\pi}^{\pi} \frac{\mathrm{d}k}{2\pi} \partial_k \arg\left(J_1 + J_2 e^{ik}\right) && (2.21\text{c})\\
&= \frac{1}{2\pi} \arg\left(J_1 + J_2 e^{ik}\right)\Big|_{-\pi}^{\pi}. && (2.21\text{d})
\end{aligned}$$

The function $J_1 + J_2 e^{ik}$ draws a perfect circle with radius J_2 and midpoint J_1 into the complex plane. In the formula above we count how often this circle goes around the origin of the plane.

Obviously there are only two possibilities. If $|J_1| > |J_2|$, the offset of the circle is bigger than its radius such that it does not include the origin. In this case we get the

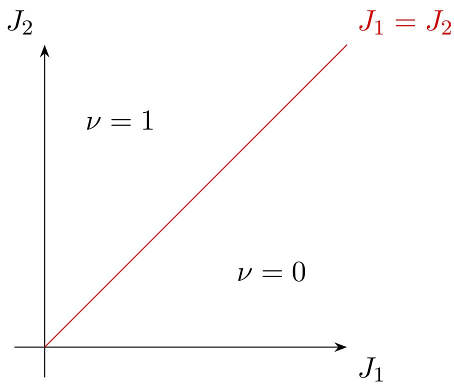

Figure 2.2.: This is the phase diagram of the SSH-chain for real and positive values of J_1 and J_2.

winding number $\nu = 0$. We call the corresponding phase the *trivial phase*. Instead, if $|J_1| < |J_2|$, the radius of the circle is so big compared to its offset that it includes the origin. Due to the positive sign in the exponential function e^{+ik} we get a positive sign for the winding number $\nu = +1$. This means that there is another *non-trivial phase*, which we also call the *topological phase*. We also see that with this system we cannot realize more than these two phases. In this thesis we will discuss different ways to stack multiple SSH chains on top of each other to realize more than just one non-trivial phase.

Above, we left out the special case $|J_1| = |J_2|$. At this point the edge of the circle in the complex plane exactly goes through the origin. This means that there is a value k_0 for which $J_1 + J_2 e^{ik_0} = 0$. We cannot calculate the argument any more because $\arg(0)$ is not defined. This means that for $|J_1| = |J_2|$ the winding number is no longer defined and the classification of the symmetry protected topological phases in our breaks down. This is where a phase transition takes place. As we already saw above, this is the same point at which the band gap is closed. Figure 2.2 shows the phase diagram of the SSH chain.

In this calculation the symmetry constraint on the SSH chain seems to be left out of consideration. This is actually not true. We know that only because of the sublattice symmetry, we can even write the Hamiltonian as two off-diagonal block matrices (see Equation (1.49)). This is where we already took into account that the sublattice symmetry always stays conserved.

What distinguishes the different phases from each other? Consider our SSH chain with periodic boundaries and for example $J_1 > J_2$. This chain is in the trivial phase. If we now exchange J_1 and J_2, obviously we end up in the topological phase but the actual physical system looks exactly the same as before. We can either exchange the coupling constants or we can shift the whole periodic system by half a unit cell – the result is the same. This shows us that in the SSH chain, our phases depend strongly on the definition of the unit cells. If we shift the unit cells by one site, the topological phase becomes trivial and vice versa. It is important to understand that our symmetry

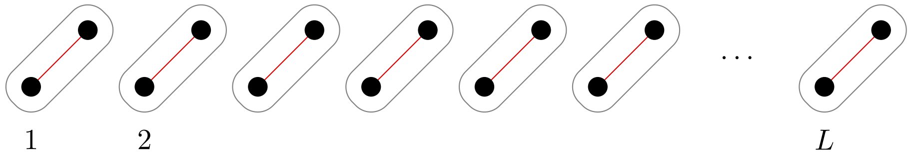

Figure 2.3.: Trivial phase of the SSH chain in the dimerized limit. The chain consists of L identical seperate subsystems with a 4-dimensional Hilbert space each.

protected topological phases are basically a choice. When we cut our SSH chain such that it becomes a long string with two ends, we will see some physical differences between the phases. This is simply due to the fact that we always cut in between two unit cells. In this case the choice is made while cutting the system open.

2.1.4. Fully Dimerized SSH Chain

Throughout this thesis we will mostly focus on two special cases of the open SSH chain. We will only look at the fully dimerized limits which means, that one of the coupling constants J_1 and J_2 vanishes. We will see that these systems are not only much easier to work with but they are also very helpful from a didactical point of view.

Obviously, there is no point in looking at a SSH chain without any couplings ($J_1 = J_2 = 0$). Therefore we start with the trivial phase and $J_1 \neq 0$ while $J_2 = 0$. As we can see in Figure 2.3, the system breaks down to L identical subsystems with Hamiltonian

$$\hat{H}_{\text{sub}} = J_1 \left(\hat{c}_1^\dagger \hat{c}_2 + \text{h.c.} \right). \tag{2.22}$$

This Hamiltonian acts on a four-dimensional Hilbert space with basis $|0,0\rangle$, $|1,0\rangle$, $|0,1\rangle$ and $|1,1\rangle$, corresponding to the respective sites being occupied (1) or not (0). We find a unique ground state

$$|\psi\rangle = \frac{1}{\sqrt{2}} \left(|1,0\rangle + |0,1\rangle \right) \tag{2.23}$$

for each unit cell. This is in case $J_1 < 0$. If $J_1 > 0$, we have to write a minus sign instead of the plus for the superposition. It has the energy $\epsilon = -|J_1|$. This means that in the ground state each unit cell is half-filled.

The ground state of the system is given by

$$|\Omega\rangle = \prod_{i=1}^{L} \left(\frac{\hat{c}_{2i}^\dagger + \hat{c}_{2i-1}^\dagger}{\sqrt{2}} \right) |0\rangle\,, \tag{2.24}$$

with the vacuum $|0\rangle$. This is simply the product state of the dimers in Equation (2.23).

Now we can take a look at the much more interesting case which is the dimerized limit of the topological phase. As we can see in Figure 2.4, the unit cells are now connected to each other. Still the bulk of the system can be divided in perfectly separated dimers which are exactly the same as in the trivial phase. Only the edges differ from the case

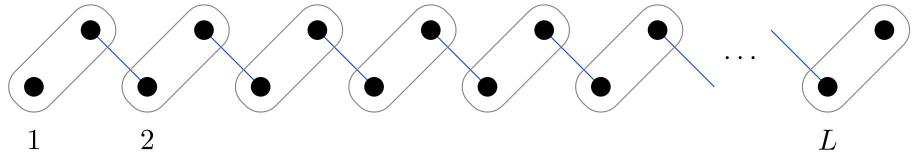

Figure 2.4.: Topological phase of the SSH chain in the dimerized limit. The bulk of the system looks exactly as in the trivial case (see Figure 2.3) but the edges of the system are single separated sites. This leads to the existance of edge states and a 4-fold degeneracy of the ground state.

above because each edge features a single site. A single unconnected site can be filled or not – since it does not even appear in the Hamiltonian, the energy stays the same. For each edge there are the two possibilities $|0\rangle$ and $|1\rangle$ for the ground state, which gives us a four-fold degeneracy.

The four ground states of the topological phase of the SSH chain in the dimerized limit are given by

$$|l, r\rangle = \left(\hat{c}_1^\dagger\right)^l \left(\hat{c}_L^\dagger\right)^r \prod_{i=1}^{L-1} \left(\frac{\hat{c}_{2i}^\dagger + \hat{c}_{2i+1}^\dagger}{\sqrt{2}}\right) |0\rangle\,, \tag{2.25}$$

with the occupation numbers $l, r \in \{0, 1\}$ of the furthermost left and right site.

If we go back into the first quantized formalism, we find the two edge modes which are the single-particle states located at the edges of the system. These states have the energy $\epsilon = 0$ and are therefore in-gap modes.

If we are not in the perfectly dimerized case and allow a $J_2 \neq 0$, we will see that the edge modes are not located at the outermost site any more [14]. Still we can computationally calculate the wave functions of these states and see that their amplitude vanishes exponentially in the system. This means that they penetrate the system only on a finite length which is negligible for $L \to \infty$. Therefore, it is still feasible to call these states edge modes. Only when $J_1 = J_2$, the edge modes break down. This is when the phase transition occurs.

2.1.5. Conservation of the Particle Number

The number of fermions on a site can be obtained by the operator $\hat{n}_i = \hat{c}_i^\dagger \hat{c}_i$. Accordingly, the particle number of the whole SSH chain is expressed via the operator

$$\hat{N} = \sum_{i=1}^{2L} \hat{n}_i. \tag{2.26}$$

The Hamiltonian of the SSH chain features only hopping terms. Therefore the particle number in the chain is a conserved quantity. This constraint can be expressed as a symmetry. In contrast to the anti-unitary symmetries above which correspond to a $\mathbb{Z}_2$ symmetry group, the particle number conservation symmetry is represented by

$$\hat{R}_\phi = e^{\mathrm{i}\phi\hat{N}}. \tag{2.27}$$

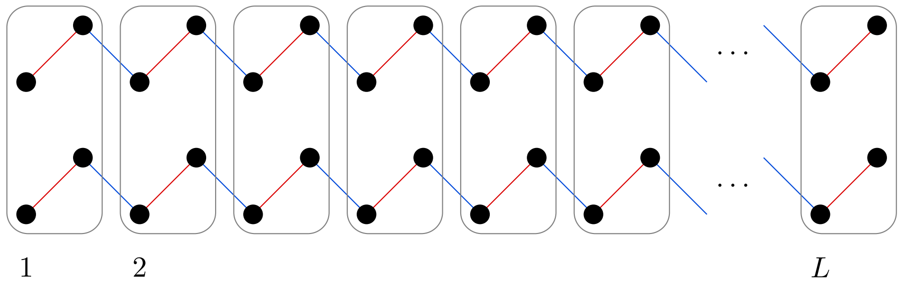

Figure 2.5.: If we stack SSH chains on top of each other, we can realize more than two symmetry protected topological phases in a single system.

Here we have $0 \leq \phi < 2\pi$ and a continuous symmetry. The corresponding symmetry group is called $U(1)$.

A Hamiltonian conserves the particle number if and only if for all ϕ, the Hamiltonian commutes with the operator $\hat{R}_\phi$:

$$\hat{R}_\phi \hat{H} \hat{R}_\phi^{-1} = \hat{H}. \tag{2.28}$$

It can be shown that this is true for the SSH chain.

2.2. Stacked SSH Chains

From now on we will only look at SSH chains in the fully dimerized limit. How many symmetry protected topological phases can we realize using one-dimensional fermionic SSH chains?

We already showed that a single SSH chain can only realize two different phases. Therefore we will try to stack more than one chain on top of each other as shown in Figure 2.5. This is still a one dimensional system but now we have new degrees of freedom (four different hopping amplitudes), so we might be able to realize more than two phases.

Let us start with two SSH chains. There are multiple ways to realize a sublattice symmetry on this system but we will choose the simplest one:

$$\hat{S} = \left[\prod_{i=1}^{L} \left(\hat{c}_{2i-3}^\dagger - \hat{c}_{2i-3} \right) \left(\hat{c}_{2i-2}^\dagger - \hat{c}_{2i-2} \right) \left(\hat{c}_{2i-1}^\dagger + \hat{c}_{2i-1} \right) \left(\hat{c}_{2i}^\dagger + \hat{c}_{2i} \right) \right] \circ K. \tag{2.29}$$

Here we enumerate the sites as shown in Figure 2.6. Now the sites 1 and 2 of each unit cell belong to the same sublattice, while sites 3 and 4 belong to the other one. This symmetry can be easily expanded to n stacked chains.

How can we calculate the winding number of a system with n stacked SSH chains? As the chains are completely separated, the Hamiltonian H can be brought in a block

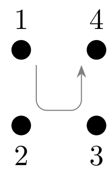

Figure 2.6.: When we stack two SSH chains on top of each other, we enumerate them counterclockwise in each unit cell starting from the top left site.

matrix form. This also holds for h:

$$h = \begin{pmatrix} h_1 & & & 0 \\ & h_2 & & \\ & & \ddots & \\ 0 & & & h_n \end{pmatrix}. \tag{2.30}$$

It can easily be shown that

$$\det(h) = \prod_{i=1}^{n} \det(h_i)\,. \tag{2.31}$$

Using Equation (1.52), we can calculate the winding number:

$$\nu = \int_{-\pi}^{\pi} \frac{\mathrm{d}k}{2\pi \mathrm{i}} \partial_k \log(\det(h)) \tag{2.32a}$$

$$= \int_{-\pi}^{\pi} \frac{\mathrm{d}k}{2\pi \mathrm{i}} \partial_k \log\left(\prod_{i=1}^{n} \det(h_i)\right) \tag{2.32b}$$

$$= \int_{-\pi}^{\pi} \frac{\mathrm{d}k}{2\pi \mathrm{i}} \partial_k \sum_{i=1}^{n} \log(\det(h_i)) \tag{2.32c}$$

$$= \sum_{i=1}^{n} \int_{-\pi}^{\pi} \frac{\mathrm{d}k}{2\pi \mathrm{i}} \partial_k \log(\det(h_i)) \tag{2.32d}$$

$$= \sum_{i=1}^{n} \nu_i. \tag{2.32e}$$

This shows us that in these systems the winding number is actually additive as long as the chains are not coupled to each other.

2.2.1. Stacking Two Chains

There are four different ways to combine two chains in the trivial or topological phase. We start with the case of both chains being in the trivial state (see Figure 2.7). The combined system is obviously still in its trivial phase with winding number $\nu = 0$. This is not only the intuitive result, but can also quickly been proven using the fact that the winding number is additive.

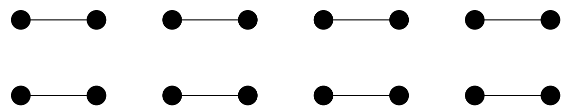

Figure 2.7.: Two SSH chains in the fully dimerized limit are stacked on top of each other. They are both in the trivial phase. The combined system is also in the trivial phase with winding number $\nu = 0$.

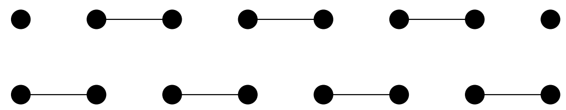

Figure 2.8.: If we put a SSH chain in the topological state on top of a chain in the trivial state, we end up with a combined system which has the winding number $\nu = 1$.

We can also stack one trivial and one topological chain on top of each other. This gives us a system in a topological phase with winding number $\nu = 1$. In fact there are two ways to do this. We can either have the topological chain on top as shown in Figure 2.8, or below the trivial chain (see Figure 2.9). From the winding number we know that those two systems belong to the same symmetry protected topological phase. This means that there has to exist a way of converting the system shown in Figure 2.8 into the system in Figure 2.9. In fact we can find a smooth path which connects both Hamiltonians without closing the gap. In the following we will discuss this path.

If we want to go from Figure 2.8 to Figure 2.9, it is immediately clear that we will need to introduce some couplings between the two chains. Switching the state in the chains separately would necessarily result in a phase transition in each of them. The challenge is to find a smooth path which not only performs the transition, but also makes it easy to prove that the band gap is never closed.

The idea is to choose the path such that the system always stays divided in small identical segments. Then to compute the band structure of the whole system we would only need to calculate the bands on one segment. Our path is illustrated in Figure 2.10. We start off with the Hamiltonian

$$\hat{H}_0 = \sum_{i=1}^{L-1} \left[\hat{c}^\dagger_{4i} \hat{c}_{4_i+1} + \text{h.c.} \right] + \sum_{i=1}^{L} \left[\hat{c}^\dagger_{4i-2} \hat{c}_{4_i-1} + \text{h.c.} \right]. \tag{2.33}$$

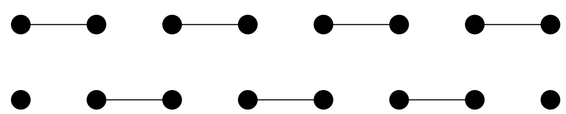

Figure 2.9.: In analogy to Figure 2.8, we can also have the upper SSH chain in the trivial state while the lower one is in the topological state. This system has the winding number $\nu = 1$ as well.

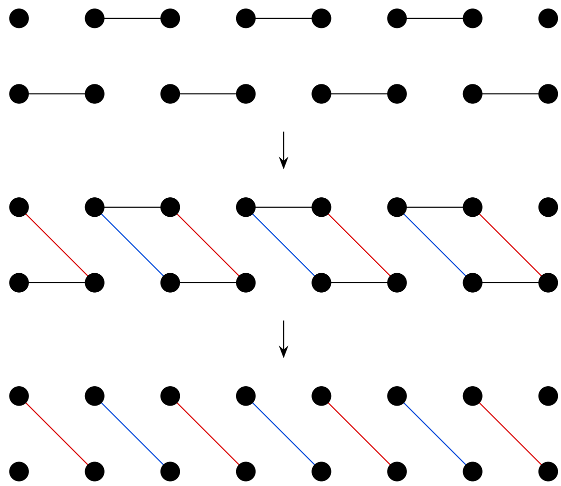

Figure 2.10.: Illustration of the path that can be used to convert the system shown in Figure 2.8 into the system shown in Figure 2.9. Diffferent colors correspond to the different signs of the hopping terms in V. Throughout the whole path, the system stays cut up into small segments of three (on the left edge) or four sites each. These segments can easily be computed to show that the total Hamiltonian stays gapped. The image only shows the first half of the procedure. The second half is completely identical but the upper and lower chain are swapped.

Then we switch on some coupling terms between the chains of the form

$$\hat{V} = \hat{c}_1^\dagger \hat{c}_3 - \hat{c}_4^\dagger \hat{c}_6 + \hat{c}_5^\dagger \hat{c}_7 - \hat{c}_8^\dagger \hat{c}_{10} + \cdots + \hat{c}_{4L-3}^\dagger \hat{c}_{4L-1} + \text{h.c.}. \tag{2.34}$$

We do this in a linear way by using the path

$$\hat{H}(\lambda \in [0,1]) = (1-\lambda)\,\hat{H}_0 + \lambda \hat{V}, \tag{2.35}$$

which will end in the lower system illustrated in Figure 2.10. It can easily be shown that $\hat{V}$ only connects sites from different sublattices and therefore commutes with the symmetry operator $\hat{S}$.

Obviously, the Hamiltonian $\hat{H}(0)$ is gapped. This is also true for $\hat{H}(1)$ since this system only consists of dimers (remember that we do not count the edge modes). Every other point on the path $\hat{H}(\lambda)$ can be constructed of the two elements shown in Figure 2.11. The Hilbert spaces of these building blocks are 16-dimensional and on the edge of the system 8-dimensional. Here we ignore the single site on the right edge of the system because this is trivial to solve ($\hat{H} = 0$).

It is computationally easy to prove that in neither of those two elements the gap is closed (see Appendix A). The ring of four sites does always have a unique ground state. At the other hand, the three-site-system has a degenerate ground state for all $\lambda \in [0,1]$. This is consistent with the fact that there is an edge mode which cannot be removed without a phase transition.

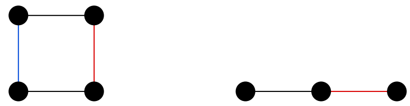

Figure 2.11.: These are the building elements for any Hamiltonian along the path sketched in Figure 2.10. The left element is what constructs the bulk of the system while the right smaller element is on the left edge. Their Hilbert spaces are 16- and 8-dimensional.

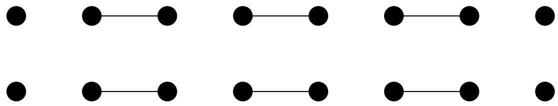

Figure 2.12.: If we stack two SSH chains in the topological state on top of each other, we find a new phase with winding number $\nu = 2$. This means that two SSH chains can be used to realize up to three symmetry protected topological phases. We can also stack even more chains on top of each other while every additional SSH chain results in one additional phase. The phases of stacked SSH chains form a $\mathbb{Z}$ group structure.

Now we know that the path $\hat{H}(\lambda)$ is gapped. This means, we are already half way there for the complete transition to Figure 2.9. All we still have to do is to perform the same path backwards again but with the trivial Hamiltonian at the upper chain and the topological Hamiltonian at the lower chain. It is easy to see that this completes the desired path. As this second half of the transition is performed in the same way as the first one (only mirrored in time and space), we already know that it is gapped.

Using two stacked SSH chains, we found completely different states which according to the winding number belonged to the same symmetry protected topological phase. Now we actually found a smooth gapped path to connect the two states and show that they can be transformed into each other without a phase transition.

Last but not least, we can also stack two topological SSH chains on top of each other. This gives us the system shown in Figure 2.12. The winding number is now $\nu = 2$ which means that we found a new symmetry protected topological phase.

2.2.2. Stacking More than Two Chains

In the discussions above, a pattern starts to form. It is quite obvious, that if we stack n SSH chains on top of each other, we can realize $n + 1$ symmetry protected topological phases with the winding numbers $\nu \in \{0, 1, \cdots, n\}$. Adding a topological chain to the system increases the winding number by 1. This shows us, that the topological phases form a $\mathbb{Z}$ group structure and we can in principle realize as many phases as we want to.

2.3. Interactions – Breakdown of Topological Phases

We did now classify symmetry protected topological phases for non-interacting one-dimensional fermionic systems. Furthermore we elaborated that the fermionic SSH chain is a system which can realize two different phases. Stacking $n > 0$ SSH-chains on top of each other allows us to realize $n+1$ different phases, which makes the number of possible phases infinitely high. The winding number is in $\mathbb{Z}$.

Now we want to expand our classification of symmetry protected topological phases to include interacting fermions. This is important because we want to have stable phases which are robust under perturbations as long as these perturbations fulfil a Symmetry constraint. Till now, we also required the perturbations to be expressed as single-particle operators. If we allow them to be interactions between particles, this will make our approach more general.

Interactions also come with some new problems. The winding number ν is only defined for non-interacting systems. Therefore we cannot use it for the classification of the phases as we did before. This does not mean that the phases are not defined any more. The winding number is a purely mathematical construct which basically inherited the physical properties of symmetry protected topological phases. The physical definition of a phase does still work: Two states are in the same symmetry protected topological phase, if and only if there exists a smooth, gapped path which connects their Hamiltonians. Throughout the whole path, the system has to fulfil the requirements of the symmetry constraint.

Now we can already see that the number of phases that can be realized in a system can either stay the same or decrease if we allow interactions. This is simply because we allow new paths for our Hamiltonian which could connect two originally separated phases.[3]

How does the number of phases change if we allow interactions? This was already elaborated in 2010 by Fidkowsky and Kitaev in [9]. They worked with stacked Majorana chains which originally have a topological invariant in $\mathbb{Z}$ (similarly to the invariant for stacked SSH chains). With interactions, it can be proven that the space $\mathbb{Z}$ of the topological invariant breaks down to $\mathbb{Z}_8$ ([9]). This means that there only exist at most eight different symmetry protected topological phases in systems of stacked Majorana chains. These can be realized with seven chains. Adding an eighth chain will not increase the number of phases.

In this thesis, we will not go into the details of the Majorana chain. Instead, we will combine two Majorana chains (in a specific way) such that they form a SSH chain. This will allow us to show that the number of phases that are realizable with stacked SSH chains is decreased, too.

[3]This is true for the systems considered in this thesis. In principle there can also exist a phase which depends on interactions to even exist. This means that the number of particles can also increase if all Hamiltonians on a phase feature interactions.

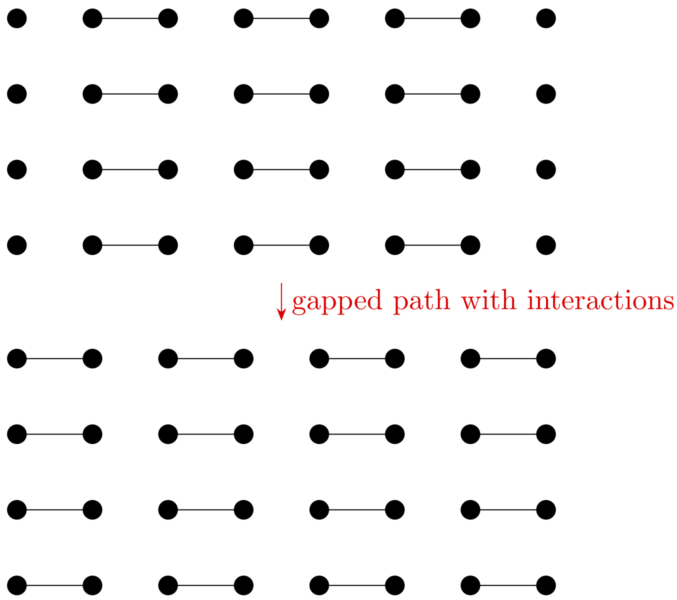

Figure 2.13.: We can find a specific path to connect four topological SSH chains to four trivial chains. This is a proof for the breakdown of the $\mathbb{Z}$ topological invariant to $\mathbb{Z}_4$ in systems of stacked SSH chains.

2.3.1. Connection of Four Topological SSH Chains to the Trivial Phase

As in [9] the classification of Majorana chains broke down to $\mathbb{Z}_8$ and we construct each SSH chain out of two Majorana chains, we intuitively expect the classification to break down to $\mathbb{Z}_4$. This would mean that there exists a gapped path to connect four SSH chains in the topological state to a system with four trivial SSH chains (since that is how the $\mathbb{Z}_4$ group structure works). This is sketched in Figure 2.13.

Working with this big system is in principle possible but very costly, since the dimension of each unit cell is $2^8 = 256$. To reduce the effort, we will not solve this system analytically but numerically. Furthermore we will choose our path such that it is always performed on separated cells of 8 sites (unit cells of the system in the trivial case). If all chains are in the topological phase, we will start with ignoring the edges of the system and instead look at the cells.

In Figure 2.14 we show an exemplary single cell with black lines indicating the hopping terms between the sites. The image also shows how we enumerate the sites. The ladder operators will be called $\hat{a}_i^{(\dagger)}$ and $\hat{b}_i^{(\dagger)}$ ($i \in \{1, \cdots, 4\}$), depending on the sublattice of the corresponding site.

Now we define a set of new operators (see Table 2.1). The operators acting on sublattice A are called $\hat{c}$, while the operators on sublattice B are labelled $\hat{c}'$. In the following we will call them Majorana operators. We will not go into the details of the Majorana chain (see Section C.1), but these operators were used to convert a system of eight Majorana chains into a system of four SSH chains.

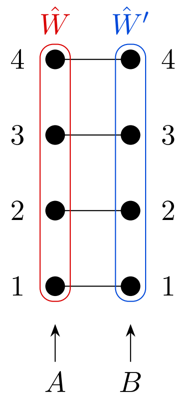

Figure 2.14.: The path leaves the cells of the system separated. The interactions $\hat{W}$ and $\hat{W}'$ will only couple the sites on a single column. To make the calculations as clear as possible, we call the ladder operators $\hat{a}_i^{(\dagger)}$ and $\hat{b}_i^{(\dagger)}$, depending on the sublattice they act on (A or B).

$\hat{c}_1 = \left(\hat{a}_1 + \hat{a}_1^\dagger\right)$	$\hat{c}'_1 = -\mathrm{i}\left(\hat{b}_1 - \hat{b}_1^\dagger\right)$
$\hat{c}_2 = \mathrm{i}\left(\hat{a}_1 - \hat{a}_1^\dagger\right)$	$\hat{c}'_1 = \left(\hat{b}_1 + \hat{b}_1^\dagger\right)$
$\hat{c}_3 = \left(\hat{a}_2 + \hat{a}_2^\dagger\right)$	$\hat{c}'_3 = -\mathrm{i}\left(\hat{b}_2 - \hat{b}_2^\dagger\right)$
$\hat{c}_4 = -\mathrm{i}\left(\hat{a}_2 - \hat{a}_2^\dagger\right)$	$\hat{c}'_4 = -\left(\hat{b}_2 + \hat{b}_2^\dagger\right)$
$\hat{c}_5 = \left(\hat{a}_3 + \hat{a}_3^\dagger\right)$	$\hat{c}'_5 = -\mathrm{i}\left(\hat{b}_3 - \hat{b}_3^\dagger\right)$
$\hat{c}_6 = \mathrm{i}\left(\hat{a}_3 - \hat{a}_3^\dagger\right)$	$\hat{c}'_6 = \left(\hat{b}_3 + \hat{b}_3^\dagger\right)$
$\hat{c}_7 = \left(\hat{a}_4 + \hat{a}_4^\dagger\right)$	$\hat{c}'_7 = -\mathrm{i}\left(\hat{b}_4 - \hat{b}_4^\dagger\right)$
$\hat{c}_8 = -\mathrm{i}\left(\hat{a}_4 - \hat{a}_4^\dagger\right)$	$\hat{c}'_8 = -\left(\hat{b}_4 + \hat{b}_4^\dagger\right)$

Table 2.1.: Set of operators to make calculations with four SSH chains and interactions easier. These operators are actually Majorana modes, which shows how SSH chains can be obtained from two Majorana chains.

What are the properties of the Majorana operators? First of all it is important to see that they build a complete basis of our Fock space, just as the fermionic ladder operators did. This is possible, because we can also form linear combinations of the Majorana operators and obtain the fermionic ladder operators. Furthermore the Majorana operators are self-adjoint

$$\hat{c}_i^\dagger = \hat{c}_i \tag{2.36a}$$
$$\left(\hat{c}'_i\right)^\dagger = \hat{c}'_i \tag{2.36b}$$

and square to one:

$$\hat{c}_i^2 = \mathbb{1} \tag{2.37a}$$
$$\left(\hat{c}'_i\right)^2 = \mathbb{1}. \tag{2.37b}$$

They also fulfil the fermionic commutation relations.

We will now express the Hamiltonian of the cell (Figure 2.14) of our system using the Majorana operators. Initially, the Hamiltonian is simply the sum of kinetic terms which are part of the SSH chains:

$$T = \sum_{i=1}^{4} \left[\hat{a}_i^\dagger \hat{b}_i + \hat{b}_i^\dagger \hat{a}_i\right]. \tag{2.38}$$

It can be shown that this is actually the same (up to a scaling factor) as

$$T = \sum_{i=1}^{8} i\hat{c}_i\hat{c}'_i. \tag{2.39}$$

The path of the Hamiltonian also includes an interaction term which is given by

$$\hat{W}_{\text{tot}} = \hat{W} + \hat{W}' \tag{2.40}$$

with

$$\begin{aligned}\hat{W} =&\hat{c}_1\hat{c}_2\hat{c}_3\hat{c}_4 + \hat{c}_5\hat{c}_6\hat{c}_7\hat{c}_8 + \hat{c}_1\hat{c}_2\hat{c}_5\hat{c}_6 + \hat{c}_3\hat{c}_4\hat{c}_7\hat{c}_8 - \hat{c}_2\hat{c}_3\hat{c}_6\hat{c}_7\\ &- \hat{c}_1\hat{c}_4\hat{c}_5\hat{c}_8 + \hat{c}_1\hat{c}_3\hat{c}_5\hat{c}_7 + \hat{c}_3\hat{c}_4\hat{c}_5\hat{c}_6 + \hat{c}_1\hat{c}_2\hat{c}_7\hat{c}_8 - \hat{c}_2\hat{c}_3\hat{c}_5\hat{c}_8\\ &- \hat{c}_1\hat{c}_4\hat{c}_6\hat{c}_7 + \hat{c}_2\hat{c}_4\hat{c}_6\hat{c}_8 - \hat{c}_1\hat{c}_3\hat{c}_6\hat{c}_8 - \hat{c}_2\hat{c}_4\hat{c}_5\hat{c}_7\end{aligned} \tag{2.41a}$$

$$\begin{aligned}\hat{W}' =&\hat{c}'_1\hat{c}'_2\hat{c}'_3\hat{c}'_4 + \hat{c}'_5\hat{c}'_6\hat{c}'_7\hat{c}'_8 + \hat{c}'_1\hat{c}'_2\hat{c}'_5\hat{c}'_6 + \hat{c}'_3\hat{c}'_4\hat{c}'_7\hat{c}'_8 - \hat{c}'_2\hat{c}'_3\hat{c}'_6\hat{c}'_7\\ &- \hat{c}'_1\hat{c}'_4\hat{c}'_5\hat{c}'_8 + \hat{c}'_1\hat{c}'_3\hat{c}'_5\hat{c}'_7 + \hat{c}'_3\hat{c}'_4\hat{c}'_5\hat{c}'_6 + \hat{c}'_1\hat{c}'_2\hat{c}'_7\hat{c}'_8 - \hat{c}'_2\hat{c}'_3\hat{c}'_5\hat{c}'_8\\ &- \hat{c}'_1\hat{c}'_4\hat{c}'_6\hat{c}'_7 + \hat{c}'_2\hat{c}'_4\hat{c}'_6\hat{c}'_8 - \hat{c}'_1\hat{c}'_3\hat{c}'_6\hat{c}'_8 - \hat{c}'_2\hat{c}'_4\hat{c}'_5\hat{c}'_7.\end{aligned} \tag{2.41b}$$

This is the same interaction that was used in [9]. In the following we will show that this $\hat{W}_{\text{tot}}$ conserves the particle number. We will only do this for $\hat{W}$. The calculation for $\hat{W}'$ is almost identical. We take Equation (2.41a) and divide it into two different parts. The first section includes the terms $\hat{c}_1\hat{c}_2\hat{c}_3\hat{c}_4$, $\hat{c}_5\hat{c}_6\hat{c}_7\hat{c}_8$, $\hat{c}_1\hat{c}_2\hat{c}_5\hat{c}_6$, $\hat{c}_3\hat{c}_4\hat{c}_7\hat{c}_8$, $\hat{c}_3\hat{c}_4\hat{c}_5\hat{c}_6$ and

$\hat{c}_1\hat{c}_2\hat{c}_7\hat{c}_8$. These terms all include pairs of Majorana operators which act on the same fermionic site, like

$$\hat{c}_1\hat{c}_2 = \left(\hat{a}_1 + \hat{a}_1^\dagger\right) \mathrm{i} \left(\hat{a}_1 - \hat{a}_1^\dagger\right) = \mathrm{i} \left[\underbrace{\hat{a}_1\hat{a}_1}_{=0} + \hat{a}_1^\dagger\hat{a}_1 - \hat{a}_1\hat{a}_1^\dagger - \underbrace{\hat{a}_1^\dagger\hat{a}_1^\dagger}_{=0}\right]. \tag{2.42}$$

We immediately see that there is no way for these pairs to violate the particle number conservation which also holds for the products of the pairs.

Now we move on to the other terms in Equation (2.41a) which include $-\hat{c}_2\hat{c}_3\hat{c}_6\hat{c}_7$, $-\hat{c}_1\hat{c}_4\hat{c}_5\hat{c}_8$, $\hat{c}_1\hat{c}_3\hat{c}_5\hat{c}_7$, $-\hat{c}_2\hat{c}_3\hat{c}_5\hat{c}_8$, $-\hat{c}_1\hat{c}_4\hat{c}_6\hat{c}_7$, $\hat{c}_2\hat{c}_4\hat{c}_6\hat{c}_8$, $-\hat{c}_1\hat{c}_3\hat{c}_6\hat{c}_8$ and $-\hat{c}_2\hat{c}_4\hat{c}_5\hat{c}_7$. We can actually rewrite these terms as

$$\begin{aligned} & - \hat{c}_2\hat{c}_3\hat{c}_6\hat{c}_7 - \hat{c}_1\hat{c}_4\hat{c}_5\hat{c}_8 + \hat{c}_1\hat{c}_3\hat{c}_5\hat{c}_7 - \hat{c}_2\hat{c}_3\hat{c}_5\hat{c}_8 \\ & - \hat{c}_1\hat{c}_4\hat{c}_6\hat{c}_7 + \hat{c}_2\hat{c}_4\hat{c}_6\hat{c}_8 - \hat{c}_1\hat{c}_3\hat{c}_6\hat{c}_8 - \hat{c}_2\hat{c}_4\hat{c}_5\hat{c}_7 \\ = & - \left(\hat{c}_2\hat{c}_3 + \hat{c}_1\hat{c}_4\right)\left(\hat{c}_6\hat{c}_7 + \hat{c}_5\hat{c}_8\right) - \left(\hat{c}_2\hat{c}_4 - \hat{c}_1\hat{c}_3\right)\left(\hat{c}_5\hat{c}_7 - \hat{c}_6\hat{c}_8\right) \end{aligned} \tag{2.43}$$

and now look at the separate factors individually. They can easily be calculated, for example:

$$\left(\hat{c}_2\hat{c}_3 + \hat{c}_1\hat{c}_4\right) = \mathrm{i}\left(\hat{a}_1 - \hat{a}_1^\dagger\right)\left(\hat{a}_2 + \hat{a}_2^\dagger\right) + \left(\hat{a}_1 + \hat{a}_1^\dagger\right)(-\mathrm{i})\left(\hat{a}_2 - \hat{a}_2^\dagger\right) \tag{2.44a}$$

$$= \mathrm{i}\left[\hat{a}_1\hat{a}_2 + \hat{a}_1\hat{a}_2^\dagger - \hat{a}_1^\dagger\hat{a}_2 - \hat{a}_1^\dagger\hat{a}_2^\dagger - \hat{a}_1\hat{a}_2 + \hat{a}_1\hat{a}_2^\dagger - \hat{a}_1^\dagger\hat{a}_2 + \hat{a}_1^\dagger\hat{a}_2^\dagger\right] \tag{2.44b}$$

$$= \mathrm{i}\left[\hat{a}_1\hat{a}_2^\dagger - \hat{a}_1^\dagger\hat{a}_2 + \hat{a}_1\hat{a}_2^\dagger - \hat{a}_1^\dagger\hat{a}_2\right]. \tag{2.44c}$$

All those terms are conserving the particle number. This also holds for $(\hat{c}_6\hat{c}_7 + \hat{c}_5\hat{c}_8)$, $(\hat{c}_2\hat{c}_4 - \hat{c}_1\hat{c}_3)$ and $(\hat{c}_5\hat{c}_7 - \hat{c}_6\hat{c}_8)$. Therefore also their products conserve the particle number.

Now we know that $\hat{W}$ does not change the number of fermions in our system. The same also holds for $\hat{W}'$ and therefore also for $\hat{W}_{\mathrm{tot}}$.

Besides the conservation of the particle number, the interaction $\hat{W}_{\mathrm{tot}}$ should also conserve the sublattice symmetry of the SSH chains. This symmetry (on a single cell) is given by

$$\hat{S} = \prod_{i=1}^{4}\left(\hat{a}_i + \hat{a}_i^\dagger\right)\left(\hat{b}_i - \hat{b}_i^\dagger\right) \circ K \tag{2.45}$$

$$= \prod_{i=1}^{4} \mathrm{i}\hat{c}_{2i-1}\hat{c}'_{2i-1} \circ K. \tag{2.46}$$

The sublattice symmetry can be expressed as a product of all Majorana operators with odd indices. All terms of $\hat{W}_{\mathrm{tot}}$ consist of two even and two odd Majorana operators. Therefore the interaction commutes with $\hat{S}$.

Now we have all we need to construct the path which connects four topological SSH chains with four trivial chains. It is given by

$$\hat{H}(\lambda \in [0,1]) = (1-\lambda)\,T + \lambda \hat{W}_{\mathrm{tot}}. \tag{2.47}$$

This path switches off the hopping terms in Figure 2.14 while switching on the interactions. At $\lambda = 1$, all kinetic terms vanish and the system consists of $2L$ columns of four sites each, which are connected via the interactions $\hat{W}$ or $\hat{W}'$. We can then perform the same path again backwards but switch on the kinetic term of the trivial SSH chains (instead of the topological term). This performs the transition shown in Figure 2.13.

To prove that this path is actually allowed, we still have to show that it is gapped. As the Hamiltonian $\hat{H}(\lambda)$ acts on a 256-dimensional Hilbert space, we simply diagonalize the Hamiltonian numerically. The result can be seen in Figure 2.15. At the left side of the plot, the kinetic term $\hat{T}$ is switched on and the interactions are switched off. The energy spectrum of the cell is symmetric because of the sublattice symmetry (see Equation (1.45)). This argument only holds for non-interacting systems. Therefore, at $\lambda = 1$ with the interactions $\hat{W}_{\text{tot}}$ switched on, the spectrum is no longer symmetric.

As we can see, the whole path is gapped because the lowest eigenenergy never intersects any other energies. The ground state is also unique. We already know that for $\lambda = 0$ and as the path is smooth, it has to hold for all $\lambda \in [0, 1]$.

We now have a way of switching off all kinetic terms of the systems while holding the gap open with interactions on all of the columns. We do the same on the edge of the topological system which gaps out the (unprotected) edge states. Then we can switch on the kinetic terms of four trivial SSH chains, basically performing the same path backwards with shifted cells. This connects the phase with winding number $\nu = 4$ to the trivial phase ($\nu = 0$) and shows us that the winding number receives the $\mathbb{Z}_4$ group structure. If we allow interactions, we can only realize four different phases using stacked SSH chains.

[4] This plot can also be seen in [9]. Only some of the lines look differently. We suspect that an error has been made which does not affect the physical conclusions of this paper.

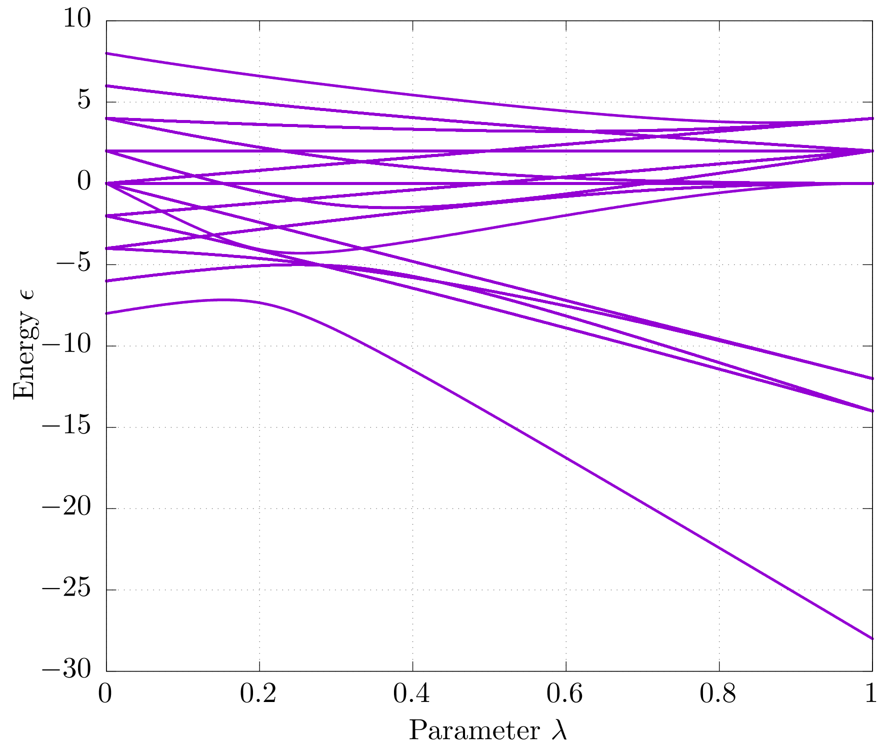

Figure 2.15.: Eigenenergies of the Hamiltonian $\hat{H}(\lambda)$ of one cell for $\lambda \in [0, 1]$. At $\lambda = 0$, the system consists of four separated SSH chains and the spectrum is symmetric. At $\lambda = 1$, the kinetic terms $\hat{T}$ of the SSH chains are switched off but the band gap is maintained by the interactions $\hat{W}_{\text{tot}}$. As we can see, throughout the whole path the lowest eigenenergy of the cell stays separated from all other energies. This means that the whole system stays gapped.[4]

3. Classification of Bosonic Phases

In Chapter 1, we classified symmetry protected topological phases in one-dimensional fermionic systems. In the following we want to do the same for systems of hard-core bosons (e.g. spins, see Subsection 3.1.1).

3.1. Jordan–Wigner Transformation

Consider a fermionic system with ladder operators $\hat{c}_i^\dagger$ and $\hat{c}_i$. It consists of L unit cells with d sites each[1]. If we want to perform simulations on such a system, we can do this by expressing the fermionic operators as matrices. These matrices must fulfil all requirements of the ladder operators, e.g. the commutation relations. Still there are multiple ways to do this. One of them is the so-called *Jordan–Wigner transformation* ρ_{JW}:

$$\rho_{\mathrm{JW}}(\hat{c}_j) = \prod_{i=1}^{j-1} \sigma_i^z \cdot \sigma_j^+ \tag{3.1a}$$

$$\rho_{\mathrm{JW}}\left(\hat{c}_j^\dagger\right) = \prod_{i=1}^{j-1} \sigma_i^z \cdot \sigma_j^- . \tag{3.1b}$$

A Pauli matrix σ_i acting on site i is an abbreviation of

$$\sigma_i = \underbrace{\mathbb{1} \otimes \mathbb{1} \otimes \cdots \otimes \mathbb{1}}_{i-1} \otimes \sigma \otimes \underbrace{\mathbb{1} \otimes \mathbb{1} \otimes \cdots \otimes \mathbb{1}}_{d \cdot L - i} \tag{3.2}$$

and the ladder operators are implemented by

$$\sigma^+ = \begin{pmatrix} 0 & 1 \\ 0 & 0 \end{pmatrix} \tag{3.3a}$$

$$\sigma^- = \begin{pmatrix} 0 & 0 \\ 1 & 0 \end{pmatrix} . \tag{3.3b}$$

The σ^z-matrices are necessary to implement the anticommutation relations of the fermions. The Jordan–Wigner transformation is not a local transformation. This is unavoidable as exchanging two fermions brings up a minus sign, no matter how large their distance is.

[1] In the previous chapters, d was the internal dimension of a unit cell. This is now 2^d.

3.1.1. Hard-Core Bosons

The Jordan–Wigner transformation does not only allow us to perform numerical simulations of fermionic systems. It can also make a transition from fermions to hard-core bosons. Consider a Hamiltonian which only features hopping terms between nearest neighbours ($\hat{c}_j^\dagger \hat{c}_{j+1} + \hat{c}_{j+1}^\dagger \hat{c}_j$). If we perform a Jordan–Wigner transformation on this term, we find

$$\begin{aligned}\rho_{\mathrm{JW}}\left(\hat{c}_j^\dagger \hat{c}_{j+1} + \hat{c}_{j+1}^\dagger \hat{c}_j\right) =& \rho_{\mathrm{JW}}\left(\hat{c}_j^\dagger\right)\rho_{\mathrm{JW}}(\hat{c}_{j+1}) + \rho_{\mathrm{JW}}\left(\hat{c}_{j+1}^\dagger\right)\rho_{\mathrm{JW}}(\hat{c}_j) && (3.4a)\\ =& \prod_{i=1}^{j-1}\sigma_i^z \cdot \sigma_j^- \cdot \prod_{i=1}^{j}\sigma_i^z \cdot \sigma_{j+1}^+ \\ &+ \prod_{i=1}^{j}\sigma_i^z \cdot \sigma_{j+1}^- \cdot \prod_{i=1}^{j-1}\sigma_i^z \cdot \sigma_j^+ && (3.4b)\\ =& \sigma_j^-\sigma_{j+1}^+ + \sigma_{j+1}^-\sigma_j^+. && (3.4c)\end{aligned}$$

As we can see, the σ^z-matrices cancel each other out and we are left with only σ^+- and σ^- matrices. Those fulfil bosonic commutation relations on different sites $i \neq j$:

$$\left[\sigma_i^+, \sigma_j^-\right] = 0 \tag{3.5a}$$

$$\left[\sigma_i^-, \sigma_j^-\right] = 0 \tag{3.5b}$$

$$\left[\sigma_i^+, \sigma_j^+\right] = 0. \tag{3.5c}$$

This means that we are working with matrices which represent bosonic ladder operators. On the same site this is not true:

$$\left\{\sigma_i^+, \sigma_i^-\right\} = 0. \tag{3.6}$$

On a single site the matrices seem to represent fermions. This is why we are not working with ordinary non-interacting bosons, but with hard-core bosons.

Hard-core bosons are a kind of interacting bosons. They have an infinitely high repulsion if two bosons are on the same site, but no interactions if they are located on different sites. This effectively means that a site can be occupied by maximally one boson. We implement this by using fermionic commutation relations on every site and bosonic commutation relations between different sites.

The most common example of hard-core bosons is a chain of spins. Each spin can point up or down which corresponds to one or no boson on the site. Spins are bosonic particles and if we exchange two of them we do not pick up a minus sign. Still, a spin can only be flipped once. Flipping it a second time will bring it back to the original state.

In this chapter, we want to classify symmetry protected topological phases for one-dimensional systems of hard-core bosons. As we can already see, we will not be able to modify the fermionic classification to suit a bosonic system because we now have interacting particles. Therefore we will need a completely new formalism.

3.1.2. Bosonic SSH Chain

We can apply the Jordan–Wigner transformation to the fermionic Hamiltonian of the SSH chain in Equation (2.4):

$$H_{\mathrm{B}} = \rho_{\mathrm{JW}}\left(\hat{H}_{\mathrm{F}}\right) = \rho_{\mathrm{JW}}\left(\sum_{i=1}^{2L} J_1 \hat{c}_{2i-1}^{\dagger}\hat{c}_{2i} + \sum_{i=1}^{L-1} J_2 \hat{c}_{2i}^{\dagger}\hat{c}_{2i+1} + \text{h.c.}\right) \tag{3.7a}$$

$$= \sum_{i=1}^{2L} J_1 \sigma_{2i-1}^{-}\sigma_{2i}^{+} + \sum_{i=1}^{L-1} J_2 \sigma_{2i}^{-}\sigma_{2i+1}^{+} + \text{h.c.}. \tag{3.7b}$$

This shows us that we can directly translate the fermionic SSH chain to an SSH chain of hard-core bosons which has the Hamiltonian

$$H_{\mathrm{B}} = \rho_{\mathrm{JW}}\left(\hat{H}_{\mathrm{F}}\right). \tag{3.8}$$

We can also apply the Jordan–Wigner transformation on the sublattice symmetry operator from Equation (2.9). This leads to

$$S_B = \rho_{\mathrm{JW}}\left(\hat{S}_{\mathrm{F}}\right) = \rho_{\mathrm{JW}}\left(\left[\prod_{i=1}^{L}\left(\hat{c}_{2i-1}^{\dagger} - \hat{c}_{2i-1}\right)\left(\hat{c}_{2i}^{\dagger} + \hat{c}_{2i}\right)\right] \circ K\right) \tag{3.9a}$$

$$= \left[\prod_{i=1}^{L}\left[\left(\prod_{j=1}^{2i-2}\sigma_j^z\right)\left(-\mathrm{i}\sigma_{2i-1}^{y}\right)\right]\left[\left(\prod_{k=1}^{2i-1}\sigma_k^z\right)\left(\sigma_{2i}^{x}\right)\right]\right] \circ K \tag{3.9b}$$

$$= \left[\prod_{i=1}^{L}\left(-\mathrm{i}\sigma_{2i-1}^{y}\right)\sigma_{2i-1}^{z}\left(\sigma_{2i}^{x}\right)\right] \circ K \tag{3.9c}$$

$$= \left[\prod_{i=1}^{2L}\sigma_i^x\right] \circ K. \tag{3.9d}$$

Now we can find one of the real differences between the fermionic and the bosonic SSH chain. The bosonic sublattice symmetry does not forbid hopping terms within in a single sublattice. For example, the term $\sigma_1^-\sigma_3^+ + \sigma_3^-\sigma_1^+ = \sigma_1^x\sigma_3^x + \sigma_3^y\sigma_1^y$ clearly commutes with S_{B}. This is due to the fact that fermionic hopping terms of non-neighbouring sites translate to bosonic interactions:

$$\rho_{\mathrm{JW}}\left(\hat{c}_1^{\dagger}\hat{c}_3 + \hat{c}_3^{\dagger}\hat{c}_1\right) = \sigma_1^-\sigma_2^z\sigma_3^+ + \sigma_3^-\sigma_2^z\sigma_1^+. \tag{3.10}$$

This interaction does indeed not commute with S_{B}.[2]

[2]Even though the sublattice symmetry implements a different restriction on the bosonic system compared to the fermionic SSH chain, we will still call it a sublattice symmetry in the following.

3.1.3. Jordan–Wigner String

We can now already guess that there are different ways to translate a one-dimensional fermionic system into a bosonic system. The Jordan–Wigner transformation strongly depends on the ordering of the fermionic sites which we call the *Jordan–Wigner string*. Depending on how we choose our Jordan–Wigner string in the fermionic system we can realize different systems of hard-core bosons. Even though some of them might be strongly interacting, while others might even feature only hopping terms, they all come from the same fermionic system and share the same band structure.

3.2. Matrix-Product States

To classify topological phases in non-interacting fermionic systems, we used the properties of the first quantized Hamiltonian in the momentum space. As we are now working with interacting bosons, our systems are no longer described accurately by first quantized Hamiltonians. Therefore, we will use the properties of the ground state $|\psi\rangle$ itself to classify bosonic symmetry protected topological phases.

To do this, we need an efficient way to express $|\psi\rangle$. We consider a chain of N spins with periodic boundary conditions while each spin has the dimension d.[3] Then we can generally write the state as

$$|\psi\rangle = \sum_{i_1,\cdots,i_N=1}^{d} c_{i_1,\cdots,i_N} |i_1,\cdots,i_N\rangle \tag{3.11}$$

with the complex numbers $c_{i_1,\cdots,i_N}$. The state $|i_1,\cdots,i_N\rangle = |i_1\rangle \otimes \cdots \otimes |i_N\rangle$ is simply the tensor product for all single spins. To describe a state, we need d^N coefficients c which gets computationally infeasible in the thermodynamic limit ($N \to \infty$).

We are only working with the ground states of local Hamiltonians. These states are usually only short range entangled. Therefore the states of consideration only take up a tiny part of the whole Hilbert space. It can be shown [18, 19, 20, 21, 22], that there is a more efficient way to describe these special states:

$$|\psi\rangle = \sum_{i_1,\cdots,i_N=1}^{d} \mathrm{Tr}\left[A^{[1]}_{i_1} A^{[2]}_{i_2} \cdots A^{[N]}_{i_N}\right] |i_1, i_2, \cdots, i_N\rangle \,. \tag{3.12}$$

Now we have N coefficients $A^{[j]}$ for the N spins with each an index $i_j \in \{1,\cdots,d\}$ enumerating the state of the corresponding spin which means that there are only $d \cdot N$ coefficients to store. This is a huge improvement. To make sure that we still can encode all the information, we let the coefficients $A^{[j]}$ be matrices. Then we call the state a *matrix-product state* (MPS)[4].

[3] For hard-core bosons, obviously $d = 2$. We can also combine multiple bosons to a unit cell which has a higher dimension.

[4] This is how a state can be expressed if it lives on a chain with periodic boundary conditions. If we

In general, these matrices are all different[5] and can also be very big. To make our life easier, we will restrict ourselves to our case. We only work with identical unit-cells. This makes the system completely periodic and allows us to choose the matrices $A^{[j]}$ identical:

$$|\psi\rangle = \sum_{i_1,\cdots,i_N=1}^{d} \mathrm{Tr}[A_{i_1}A_{i_2}\cdots A_{i_N}]\,|i_1,i_2,\cdots,i_N\rangle\,. \tag{3.13}$$

Then they are all quadratic $D \times D$-matrices.

Entanglements between the spins are implemented by the matrix multiplications. The further the entanglements in the chain reach, the bigger the matrices have to be. In principle, every state can be expressed as an MPS but this might require large matrices that can even scale with N. Still, if we only consider short-range correlated states, the matrix size D stays finite and we call it the *bond dimension*. This reduces the computational efforts massively compared to Equation (3.11).

3.2.1. Matrix-Product State Representation of the SSH Chain

To further illustrate the MPS representation, we provide an example which is strongly related to this thesis: the bosonic SSH chain in the dimerized limit. The Hamiltonian of the bosonic SSH chain is given by Equation (3.7b). We will expand it such that we close the chain to a ring.

We will start with the trivial case (see Figure 2.3). As we are working with hard-core bosons, it is easy to see that each unit cell has the same ground state as in the fermionic case. We choose the sign of the Hamiltonian such that the ground-state in a unit cell is given by

$$|\psi_i\rangle = \frac{1}{\sqrt{2}}\left(|\uparrow\rangle_{2i-1}|\downarrow\rangle_{2i} + |\downarrow\rangle_{2i-1}|\uparrow\rangle_{2i}\right). \tag{3.14}$$

Accordingly the total (not normalized) ground state is

$$|\psi\rangle = \bigotimes_{i=1}^{L}\left(|\uparrow\rangle_{2i-1}|\downarrow\rangle_{2i} + |\downarrow\rangle_{2i-1}|\uparrow\rangle_{2i}\right) \tag{3.15a}$$

$$= \sum_{\{i_j\}=1}^{d} \mathrm{Tr}[A_{i_1}\cdots A_{i_L}]\,|i_1,\cdots,i_L\rangle\,. \tag{3.15b}$$

We want to find the matrices A_i to bring the ground state in MPS form. Each virtual spin in this form corresponds to one unit cell in the SSH chain which means that $d = 4$ ($|\downarrow\downarrow\rangle$, $|\downarrow\uparrow\rangle$, $|\uparrow\downarrow\rangle$ and $|\uparrow\uparrow\rangle$). We can make this description more intuitive by splitting each unit cell index into a double index $i \to ij$ with $i, j \in \{\downarrow, \uparrow\}$ corresponding to the spins of each site in the unit cell. Then we find the matrices

$$A_{ij} = \sigma^x_{ij} \tag{3.16}$$

work with an open chain, we need to loose the trace and instead make the first and the last matrix left and right vectors. This way we still get a number as a coefficient. The trace implements the coupling of the first and the last spin.

[5] The matrices can also have different sizes, as long as they match for the matrix multiplications.

which represent the ground state as a matrix-product state. It can easily be shown that the state

$$\sum_{\{i_j\}=\downarrow}^{\uparrow} \mathrm{Tr}\big[A_{i_1 i_2} \cdots A_{i_{2L-1} i_{2L}}\big] \, |i_1 i_2, \cdots, i_{2L-1} i_{2L}\rangle \tag{3.17}$$

with these matrices is exactly the same as in Equation (3.15a). Furthermore, the matrices A_{ij} are just numbers which means that the bond dimension is $D = 1$. This is in accordance with the fact that the unit-cells of the ground state in the trivial SSH chain are not coupled to each other (see Figure 2.3) and therefore not entangled.

We can do the same for the ground-state of the topological SSH chain (see Figure 2.4). Then the ground state is given by

$$|\psi\rangle = \bigotimes_{i=1}^{L} \big(|\uparrow\rangle_{2i} \, |\downarrow\rangle_{2i+1} + |\downarrow\rangle_{2i} \, |\uparrow\rangle_{2i+1}\big) \tag{3.18}$$

which can also be transformed into an MPS. To do so, we use the matrices

$$A_{ij}^{\alpha\beta} = (A_{ij})_{\alpha\beta} = \delta_{i\alpha} \sigma^x_{j\beta} \tag{3.19}$$

which are actually 2×2-matrices. Again, it can easily be proven that the matrix-product state constructed by these matrices is exactly the ground state in Equation (3.18). The bond dimension $D = 2$ is due to the coupling of the unit cells to each other in the topological SSH chain. We call the matrix indices α and β *virtual indices* and will denote them by greek letters throughout this thesis.

3.3. Symmetry Protected Topological Phases

We want to find a classification for symmetry protected topological phases in one-dimensional systems of hard-core bosons (spins). We will base this on [23, 24, 25, 26]. All the following considerations are done with a closed chain[6] (with periodic boundary conditions, see Figure 1.2).

3.3.1. Cohomology Theory

Consider a symmetry group G and an element of this group $g \in G$. The action of the symmetry on the physical chain is given by the linear representation[7] $\rho(g)$ which acts locally on the unit cells by the linear representations $\pi(g)$:

$$\rho(g) = \underbrace{\pi(g) \otimes \pi(g) \otimes \cdots \otimes \pi(g)}_{L \text{ unit cells}} . \tag{3.20}$$

[6] We want to stress that we do not consider a closed fermionic chain which was transformed via the Jordan–Wigner transformation. This would result in a non-local term in the Hamiltonian. Instead we add a bosonic coupling between the first and the last unit cell.

[7] A representation ρ is called linear if it fulfils $\rho(g_1)\,\rho(g_2) = \rho(g_1 g_2)$.

The Hamiltonian is symmetric under $\rho(g)$ which means that these two operators commute:

$$[H, \rho(g)] = 0. \tag{3.21}$$

The system has a single non-degenerate ground state which is also an eigenstate of the symmetry operator:

$$\rho(g) |\psi\rangle = \alpha(g) |\psi\rangle . \tag{3.22}$$

Due to the unitarity of all symmetry representations, the factor $\alpha(g)$ is a global phase and satisfies the condition $|\alpha(g)| = 1$. It is itself a representation of the group G. The ground-state of the chain is symmetric under $\rho(g)$ up to a global phase $\alpha(g)$.

Now we express the ground state as an MPS according to Equation (3.13) with some matrices A_i for each of the identical unit cells. It can be shown [25, 26, 27], that these matrices transform under $\pi(g)$ as follows:

$$\sum_i [\pi(g)]_{ij} A_i = \gamma(g) V^{-1}(g) \cdot A_j \cdot V(g) . \tag{3.23}$$

The local representations $\pi(g)$ are expressed as matrices with the physical indices i and j. On the other hand, the dots $(\cdot)$ indicate a matrix product on the virtual indices of the matrix A_i. Equation (3.23) shows us that the action of the symmetry on the matrices of the MPS can be expressed as a basis transformation on the virtual indices performed by a unitary matrix $V(g)$ up to a phase $\gamma(g)$.

To fully understand this equation, we first need to make clear that it only holds under a specific condition. That is, that for a large enough n the set of the matrices $A_{i_1 i_2 \cdots i_n} = A_{i_1} A_{i_2} \cdots A_{i_n}$ for $i_j \in \{1, \cdots, d\}$ span the space of $D \times D$ matrices. This condition is called an *injectivity condition* ([25, 21]). Further insights on Equation (3.23) can be found in Appendix B.

The phase γ ($|\gamma(g)| = 1$) is a linear representation of the group G. On the other hand, the unitary matrices $V(g)$ form a projective representation of G which means that there exists a function $\chi(g_1, g_2)$ with $|\chi(g_1, g_2)| = 1$, such that

$$V(g_1) V(g_2) = \chi(g_1, g_2) V(g_1 g_2) \tag{3.24}$$

holds for all $g_1, g_2 \in G$ ([23]). We call χ a *cocycle*. It characterizes the projective representation V and thereby how the physical symmetry π acts on each unit cell. If it would fulfil $\chi(g_1 g_2) = 1$ for all $g_1, g_2 \in G$, the matrices V would form a linear representation. In this sense, every linear representation of a symmetry group is also a special projective representation.

The cocycles are obviously not completely arbitrary phases. They have to be implemented in such a way that the matrices $V(g)$ still inherit the group structure of G. Part of this structure is the associativity $(g_1 g_2)\, g_3 = g_1\, (g_2 g_3)$. This yields the so called *cocycle condition*:

$$\chi(g_1, g_2)\, \chi(g_1 g_2, g_3) = \chi(g_2, g_3)\, \chi(g_1, g_2 g_3) . \tag{3.25}$$

This condition will later be used to find valid cocycles for a given symmetry group G.

As we said, the cocycles χ characterize the action of the physical symmetry on the actual ground state of the bosonic chain. While this is in principle a true statement, we want to acknowledge that the choice of matrices $V(g)$ in Equation (3.23) is not unique. We can obviously find a new $\tilde{V}(g) = f(g)\, V(g)$ with a phase $f(g)$ ($|f(g)| = 1$) which still fulfils Equation (3.23). The two matrix functions V and $\tilde{V}$ correspond to an identical action of the symmetry on the state which means that also their cocycles χ and $\tilde{\chi}$ should correspond to each other. We can relate them in the following way:

$$\tilde{V}(g_1)\, \tilde{V}(g_2) = f(g_1)\, f(g_2)\, V(g_1)\, V(g_2) \tag{3.26a}$$
$$= f(g_1)\, f(g_2)\, \chi(g_1, g_2)\, V(g_1 g_2) \tag{3.26b}$$
$$= \frac{f(g_1)\, f(g_2)}{f(g_1 g_2)} \chi(g_1, g_2)\, \tilde{V}(g_1 g_2)\,. \tag{3.26c}$$

On the other hand, we know $\tilde{V}(g_1)\, \tilde{V}(g_2) = \tilde{\chi}(g_1, g_2)\, \tilde{V}(g_1 g_2)$. This gives us an equivalence relation for cocycles:

$$\tilde{\chi}(g_1, g_2) = \frac{f(g_1)\, f(g_2)}{f(g_1 g_2)} \chi(g_1, g_2)\,. \tag{3.27}$$

If two different cocycles can be connected by a phase f in this specific way, we know that they correspond to the same action of the symmetry on the ground state. Therefore we say that two cocycles belong to the same equivalence class $[\chi]$ if they can be connected by Equation (3.27).

This suggests that there might be different cocycle classes $[\chi]$. In fact, in some cases we find cocycles which are not equivalent, which leads to the existence of multiple classes. The set of all possible equivalence classes has an Abelian group structure. We call it the *second cohomology group* of G: $H^2(G, U(1))$. The classes $[\chi] \in H^2(G, U(1))$ are called *cohomology classes*.

Up to now, all the discussions above are made for unitary realized symmetries, meaning that the representations $\rho(g)$ are unitary. When we discussed the fermionic chains, we worked also with anti-unitary realized symmetries. We can also do this in the bosonic case by simply adding a complex conjugation to a representation $\rho(g)$. This requires us to adjust the cocycle condition slightly.

To do this, we introduce the function σ which tells us if an element g of G is represented by a unitary or an anti-unitary operator:

$$\sigma(g) = \begin{cases} +1 & g \text{ is represented by a unitary operator} \\ -1 & g \text{ is represented by an anti-unitary operator} \end{cases}. \tag{3.28}$$

Then the cocycle condition in Equation (3.25) can be adjusted to

$$\chi(g_1, g_2)\, \chi(g_1 g_2, g_3) = \chi^{\sigma(g_1)}(g_2, g_3)\, \chi(g_1, g_2 g_3)\,, \tag{3.29}$$

which we call the *twisted* cocycle condition. This twist also appears in the equivalence condition for the cocycles in Equation (3.27) which is adjusted to

$$\tilde{\chi}(g_1, g_2) = \frac{f(g_1)\, f^{\sigma(g_1)}(g_2)}{f(g_1 g_2)} \chi(g_1, g_2)\,. \tag{3.30}$$

3.3.2. Classification of Bosonic Phases

Let us consider a closed chain with Hamiltonian $H(\boldsymbol{\lambda})$ which depends on some parameters $\boldsymbol{\lambda}$. As long as this Hamiltonian fulfils our initial conditions (local, gapped, symmetric), it has a non-degenerate ground state. We can then express this ground state as an MPS and use this to derive the corresponding cocycle χ. Even though the parameters $\boldsymbol{\lambda}$ may have been continuous, the cocycles of different Hamiltonians are divided in discrete classes.

Just like in Section 1.3, we can consider two Hamiltonians $H(0)$ and $H(1)$ and a parameter $\lambda \in [0,1]$ connecting these two Hamiltonians smoothly: $H(\lambda)$. Now if the cocycles χ_0 and χ_1 belong to different cohomology classes, there must be a jump between the classes at some point on the path. This is where the phase transition happens.

3.3.3. Classification of the SSH Chain

To illustrate the previous statements we want to use the dimerized states of the SSH chain again. This shall serve as a concrete example. We will follow some calculations in [28].

As for the fermionic chain, we have a sublattice symmetry and a particle conservation symmetry. According to Equation (3.9d), the bosonic representation of the sublattice symmetry is given by

$$S_{\mathrm{B}} = \left[\prod_{i=1}^{2L} \sigma_i^x\right] \circ K. \tag{3.31}$$

The particle conservation symmetry is continuous. In the fermionic chain it takes the form of Equation (2.27). For bosonic systems we replace the particle number operator by

$$\rho_{\mathrm{JW}}(\hat{n}_i) = \frac{\mathbb{1} - \sigma_i^z}{2} \tag{3.32}$$

and end up with the continuous symmetry operators

$$R(\phi) = e^{\mathrm{i}\phi \sum_{i=1}^{2L} \frac{\mathbb{1}-\sigma_i^z}{2}}. \tag{3.33}$$

Now we have the physical representations $\rho(g)$ for the different abstract symmetry group elements g. These operators act on the whole SSH chain but in Equation (3.23) we are interested in the action of the symmetry on single unit cells k. The particle conservation for a single unit cell can be implemented by

$$r_k(\phi) = e^{i\phi} e^{-i\frac{\phi}{2}\left(\sigma_{2k-1}^z + \sigma_{2k}^z\right)}. \tag{3.34}$$

These operators add up to the global symmetry operators with Equation (3.20). When we do the same for the sublattice symmetry, we need to keep in mind that the complex conjugation is not technically a part of the symmetry group but a rule for the realization. Therefore it also has to be applied on each single unit cell. The anti-unitary sublattice symmetry is realized as

$$s_k = \sigma_{2k-1}^x \sigma_{2k}^x \circ K \tag{3.35}$$

on each unit cell. Furthermore we call the different abstract group elements corresponding to their representations S and R_ϕ. It is $\sigma(S) = -1$ because $\rho(S) = S_\mathrm{B}$ is an anti-unitary operator.

We start with the trivial phase of the SSH chain. The MPS for the ground state of this chain is given by the 1×1-matrices in Equation (3.16). If we plug them into Equation (3.23), we can find the representations V:

$$V_\mathrm{triv}(S) = 1 \tag{3.36a}$$
$$V_\mathrm{triv}(R_\phi) = 1 \tag{3.36b}$$
$$V_\mathrm{triv}(SR_\phi) = 1 \tag{3.36c}$$
$$V_\mathrm{triv}(R_\phi S) = 1. \tag{3.36d}$$

It can easily be checked that these trivial unitary matrices V solve Equation (3.23). Obviously, finding the cocycle for this representation is a trivial task:

$$\chi_\mathrm{triv}(g_1, g_2) = 1 \tag{3.37}$$

for all g_1 and g_2. Here we can already see why this phase of the SSH chain is called the trivial phase. It is because the symmetry acts trivially on the physical unit cells of the chain.

This is different in the topological phase. Here the matrices of the MPS have the bond dimension $D = 2$ and are given by Equation (3.19). As this is just an example, we will not go into the detailed calculations for this case. It can be shown that the matrices

$$V_\mathrm{top}(R_\phi) = e^{\mathrm{i}\phi\sigma^z} \tag{3.38a}$$
$$V_\mathrm{top}(S) = \sigma^x \circ K \tag{3.38b}$$

solve Equation (3.23). For $V_\mathrm{top}(R_\phi S)$ and $V_\mathrm{top}(SR_\phi)$ we can make a choice but we need to fulfil the cocycle condition. One possible way is to choose

$$V_\mathrm{top}(R_\phi S) = e^{-\mathrm{i}\frac{\phi}{2}(\mathbb{1}-\sigma^z)}\sigma^x \circ K \tag{3.39a}$$
$$V_\mathrm{top}(SR_\phi) = \sigma^x \circ K\, e^{-\mathrm{i}\frac{\phi}{2}(\mathbb{1}-\sigma^z)} \tag{3.39b}$$

which results in the following cocycle elements:

$$\chi_\mathrm{top}(S, S) = 1 \tag{3.40a}$$
$$\chi_\mathrm{top}(R_\phi, R_\theta) = 1 \tag{3.40b}$$
$$\chi_\mathrm{top}(R_\phi, S) = 1 \tag{3.40c}$$
$$\chi_\mathrm{top}(S, R_\phi) = e^{\mathrm{i}\phi}. \tag{3.40d}$$

It can be shown that this cocycle fulfils Equation (3.29).

Now we can compare the cocycles χ_triv and χ_top and use Equation (3.30) to check if they belong to the same cohomology class. To do this, we assume that they belong to the same class and try to find the function $f(g)$. If we assume $g_1 = R_\phi$ and $g_2 = R_\theta$ we find the condition[8]

$$1 = \frac{f(R_\phi)\, f(R_\theta)}{f(R_{\phi+\theta})}. \tag{3.41}$$

This can only be fulfilled for all ϕ and θ if we can write $f(R_\phi) = e^{\mathrm{i}k\phi}$ with some $k \in \mathbb{Z}$. The equation itself would also allow different values for k, but since $R_{\phi+2\pi} = R_\phi$, we need that same periodic behaviour for f. For $k \notin \mathbb{Z}$ we would find $f(R_{\phi+2\pi}) \neq f(R_\phi)$.

Now we can also look at the case $g_1 = S$, $g_2 = R_\phi$ which gives the condition

$$e^{i\phi} = \frac{f(S)}{f(R_\phi)\, f(SR_\phi)} \tag{3.42}$$

as well as the case $g_1 = R_\phi$, $g_2 = S$ which leads to

$$1 = \frac{f(R_\phi)\, f(S)}{f(SR_\phi)}. \tag{3.43}$$

We can easily combine these two equations and end up with

$$f(R_\phi) = e^{i\frac{\phi}{2}}. \tag{3.44}$$

This is a contradiction to the upper statement ($f(R_\phi) = e^{\mathrm{i}k\phi}$) and proves that the cohomology classes $[\chi_{\mathrm{triv}}]$ and $[\chi_{\mathrm{top}}]$ are actually not the same. This shows us that the two different dimerized limits of the bosonic SSH chain belong to two different phases.

3.3.4. Classifications for Specific Symmetries

In general, the maximum number of possible phases depends on the second cohomology group of the symmetry G. A specific system may not be able to realize all of them but we can calculate $H^2(G, U(1))$ for different symmetry groups independent of any real system. This was done in [8]. In Table 3.1, the cohomology groups for some selected symmetry groups are listed. The number of elements of a second cohomology group determines the maximum number of phases which can be realized in one dimension.

If a symmetry group is denoted with a T-exponent. This means that it is anti-unitarily realized. This notation can lead to some confusion because the representation is not a property of the symmetry group G itself. Still, this convention is easy to use and relatively clear.

Furthermore, we can also see that the second cohomology groups come with some intrinsic group structures. This is not to be ignored because we will later find these structures in the symmetry protected topological phases. For example, the SSH chain has a sublattice symmetry which corresponds to the group $\mathbb{Z}_2^T$ and a particle conservation symmetry which is a representation of the group $U(1)$. Therefore the combined symmetry group is $U(1) \times \mathbb{Z}_2^T$ which gives us the cohomology group $\mathbb{Z}_2^2$. This means

[8] The abstract elements of the particle conservation symmetry group $U(1)$ obviously inherit the algebraic structure of $U(1)$. This means that $R_\phi R_\theta = R_{\phi+\theta}$ and the elements are periodic ($R_{\phi+2\pi} = R_\phi$).

Symmetry group G	$H^2(G, U(1))$
$\mathbb{Z}_2^T$	$\mathbb{Z}_2$
$\mathbb{Z}_n$	$\mathbb{Z}_1$
$U(1)$	$\mathbb{Z}_1$
$U(1) \times \mathbb{Z}_2$	$\mathbb{Z}_1$
$U(1) \times \mathbb{Z}_2^T$	$\mathbb{Z}_2^2$
$\mathbb{Z}_2 \times \mathbb{Z}_2^T$	$\mathbb{Z}_2^2$
$D_2 \times \mathbb{Z}_2^T$	$\mathbb{Z}_2^4$

Table 3.1.: Second cohomology groups $H^2(G, U(1))$ for some different symmetry groups G. They show us how many symmetry protected topological phases are in principle possible for a given symmetry in one dimension. The last three groups will be especially important for this thesis. It is $D_2 = \mathbb{Z}_2 \times \mathbb{Z}_2$. All entries in this table can be found in [8]. Additional calculations on the easier symmetries in the upper half of the table can be found in [28]

that these symmetries can realize up to four phases. We found the same in the fermionic SSH chain. Still the group structure $\mathbb{Z}_2^2$ of the bosonic chain differs significantly from the fermionic structure $\mathbb{Z}_4$. We will discuss this deviation in more detail later.

3.4. Bulk-Boundary Correspondence

These discussions on the classification of symmetry protected topological phases are based on periodic bosonic chains. However, the actual systems we are interested in are usually open chains with edges. As we already discussed for fermionic systems in Section 1.4, interesting phenomena can appear on the edges of a chain in a topological phase. The same also happens in chains with hard-core bosons.

To understand this, we have another look at matrix-product states as in Equation (3.12). For an open chain, we have to modify this equation to

$$|\psi\rangle = \sum_{i_1,\cdots,i_N=1}^{d} A_{i_1}^{[1]} A_{i_2}^{[2]} \cdots A_{i_N}^{[N]} |i_1, i_2, \cdots, i_N\rangle \tag{3.45}$$

with a row vector $A_{i_1}^{[1]}$ and a column vector $A_{i_N}^{[N]}$. If we recall at Equation (3.23), we can immediately see how opening the chain affects the action of the symmetry: this condition does not hold any more at the edges ($A_{i_1}^{[1]}$ and $A_{i_L}^{[N]}$) of the system. Instead, on the edges, the physical symmetry operators form projective representations of the group G on the physical degrees of freedom. All projective representations are elements of one of the cohomology classes in $H^2(G, U(1))$. The symmetry actions on the system boundaries fall into the same class as the representations $V(g)$ (see Equation (3.23)) for the corresponding closed chain. This suggests that we can simply look at the edges of a chain instead of the bulk to identify the symmetry protected topological phases of the system [25]. This is sometimes referred to as *symmetry fractionalization* and relates to the *bulk-boundary correspondence*.

3.4.1. Bosonic In-Gap Modes

In Section 1.4, we already mentioned fermionic edge modes with in-gap energies. Using our bosonic classification, this becomes even clearer. Consider a system that is not in its trivial phase. This means that the symmetry representations $U(g)$ of the elements $g \in G$ on the edge of our system fall into a non-trivial cohomology class and are therefore truly projective. In general, non-trivial projective representations can only be realized in two or more dimensions [19].

Indeed, we have to remember that the symmetry representations $U(g)$ for all $g \in G$ still commute with the Hamiltonian H, but as the projective representation is non-trivial, they do not commute with each other in general. More precisely, there exist some elements $g_1, g_2 \in G$ such that

$$[U(g_1)\,, U(g_2)] \neq 0, \tag{3.46}$$

Commuting operators share a common eigenbasis. Since $[U(g_1)\,, H] = 0$, there exist two common eigenstates $|\psi_i\rangle$ of $U(g_1)$ and H which fulfil the conditions

$$H\,|\psi_1\rangle = \epsilon_1\,|\psi_1\rangle \tag{3.47a}$$

$$H\,|\psi_2\rangle = \epsilon_2\,|\psi_2\rangle \tag{3.47b}$$

$$\langle\psi_1\,|\,U(g_2)\,|\,\psi_2\rangle \neq 0. \tag{3.47c}$$

(It is always possible to find these eigenvectors.) Analogously it follows that there also exists a (different) common eigenbasis of $U(g_2)$ and H. This is only possible if $\epsilon_1 = \epsilon_2$.

Thus, if the phase of the system is not trivial, there exists a ground state degeneracy in the system. The number of degenerate ground states depends on the dimension of the smallest possible representation U, that belongs to the cohomology class that specifies the topological phase.[9]

[9] This refers to the ground state degeneracy which is protected by the symmetry of the system. In general, there can exist additional (spurious) degenerate states which can be gapped out by local perturbations without breaking the symmetry.

4. Bosonic Phases in the SSH Chain

We discussed the classification of bosonic symmetry protected topological phases in one dimension and elaborated that the phases are strongly connected to the second cohomology group $H^2(G, U(1))$ for the corresponding symmetry group G. In Table 3.1, the cohomology groups for different symmetry groups are listed. In this chapter, we actually want to realize the corresponding phases in SSH chains.

Coming from the fermionic SSH chain, the native symmetries of this system are the sublattice symmetry (which is a $\mathbb{Z}_2^T$ symmetry group representation) and the particle conservation symmetry (which is a representation of $U(1)$). While we can realize this $\mathbb{Z}_2^T \times U(1)$ symmetry, we are also able to find other symmetries in the SSH chain. These do not only lead to different physical results but may also be favourable from a didactical point of view.

4.1. Sublattice Symmetry and Parity Symmetry

If we have a look at Table 3.1, we will see that the groups $\mathbb{Z}_2^T \times \mathbb{Z}_2$ and $\mathbb{Z}_2^T \times U(1)$ actually yield the same cohomology group. While we can use the $U(1)$ group to implement particle conservation into our physical system, the $\mathbb{Z}_2$ group is simply a subgroup of $U(1)$ which can correspond to a parity conservation symmetry. This means that the total number of particles in the system is either odd or even and does not change. It is obvious that parity conservation is a necessity for particle number conservation. In other words, we can restrict the operator $R(\phi)$ in Equation (3.33) (which implements the particle conservation in a SSH chain) to the values $\phi = 0$ and $\phi = \pi$. The resulting two operators are a representation of $\mathbb{Z}_2$ and implement the parity conservation for our system.

Now we want to find the four cohomology classes which correspond to the group $\mathbb{Z}_2 \times \mathbb{Z}_2^T$. We call the non-trivial element of $\mathbb{Z}_2$ X and the non-trivial element of $\mathbb{Z}_2^T$ which is anti-unitarily realized Z. This way, our group G has the elements $\{1, X, Z, XZ\}$. We will now define four different cocycles and prove that they all belong to different cohomology classes. We will furthermore show that the classes inherit a $\mathbb{Z}_2^2$ group structure.

We define the cocycles

$$\chi_1(g_1, g_2) = 1 \tag{4.1a}$$

$$\chi_2(g_1, g_2) = \begin{cases} \omega(g_2) & \text{if } \sigma(g_1) = -1 \\ 1 & \text{else} \end{cases} \tag{4.1b}$$

$$\chi_3(g_1, g_2) = \begin{cases} \sigma(g_2) & \text{if } \sigma(g_1) = -1 \\ 1 & \text{else} \end{cases} \tag{4.1c}$$

$$\chi_4(g_1, g_2) = \chi_2(g_1, g_2) \cdot \chi_3(g_1, g_2) \tag{4.1d}$$

with the functions

$$\omega(g) = \begin{cases} -1 & \text{if } X \text{ in } g \\ 1 & \text{else} \end{cases} \tag{4.2a}$$

$$\sigma(g) = \begin{cases} -1 & \text{if } Z \text{ in } g \\ 1 & \text{else} \end{cases}. \tag{4.2b}$$

We still have to prove that these cocycles are valid but we can already see a $\mathbb{Z}_2^2$ structure in there. The idea is very simple. There are two non-trivial behaviours that can appear in representations of G:

- The representation of the element Z can square to one. This is implemented in χ_3.
- The representations of X and Z can anticommute. This is implemented in χ_2.

If both of these conditions are fulfilled, we simply multiply χ_2 and χ_3 and end up with χ_4. The cocycle χ_1 corresponds to the trivial case where none of these conditions are fulfilled.

Now we will use Equation (3.30) to show that none of these cocycles are equivalent. To do this, we have to make the six comparisons $\chi_1 \leftrightarrow \chi_2$, $\chi_1 \leftrightarrow \chi_3$, $\chi_2 \leftrightarrow \chi_3$, $\chi_4 \leftrightarrow \chi_1$, $\chi_2 \leftrightarrow \chi_4$ and $\chi_3 \leftrightarrow \chi_4$.

We start with the comparison of χ_1 nd χ_2. The idea is that we want to find different values for $g_1, g_2 \in G$ such that a contradiction appears after plugging them into Equation (3.30). If we choose $g_1 = g_2 = Z$, we find the equivalence condition

$$1 = \frac{f(Z)}{f(Z)\, f(1)} \cdot 1 \tag{4.3}$$

for the cocycles χ_1 and χ_2. This gives us $f(1) = 1$. If we now choose $g_1 = g_2 = XZ$, we will find the condition

$$1 = \frac{f(XZ)}{f(XZ)\, f(1)} \cdot (-1) \tag{4.4}$$

which gives $f(1) = -1$. Both statements cannot be true at the same time and therefore χ_1 and χ_2 belong to different cohomology classes ($[\chi_1] \neq [\chi_2]$).

Now we investigate the connection between χ_1 and χ_3. Choosing $g_1 = g_2 = 1$ gives us the condition

$$1 = \frac{f(1)\,f(1)}{f(1)} \cdot 1 \tag{4.5}$$

which requires $f(1) = 1$. At the same time, if we choose $g_1 = g_2 = Z$, we find

$$1 = \frac{f(Z)}{f(Z)\,f(1)} \cdot (-1) \tag{4.6}$$

and $f(1) = -1$. Again this is a contradiction and therefore $[\chi_1] \neq [\chi_3]$.

If we consider χ_2 and χ_3, we can choose $g_1 = Z$ and $g_2 = X$ which gives

$$-1 = \frac{f(Z)}{f(X)\,f(XZ)} \cdot 1. \tag{4.7}$$

Also, if we choose $g_1 = Z$ and $g_2 = XZ$ we find

$$-1 = \frac{f(Z)}{f(XZ)\,f(X)} \cdot (-1)\,. \tag{4.8}$$

Again, both statements cannot be true at the same time because that would require

$$\frac{f(Z)}{f(XZ)\,f(X)} = -\frac{f(Z)}{f(XZ)\,f(X)} \tag{4.9}$$

which is not possible for $|f(g)| = 1$. Therefore $[\chi_2] \neq [\chi_3]$.

The last non-trivial comparison has to be done for χ_4 and χ_1. We start with $g_1 = g_2 = 1$ and Equation (3.30) gives us

$$1 = \frac{f(1)\,f(1)}{f(1)} \cdot 1. \tag{4.10}$$

This requires $f(1) = 1$. We can also consider $g_1 = g_2 = Z$ which leads to the equivalence condition

$$-1 = \frac{f(Z)}{f(Z)\,f(1)} \cdot 1 \tag{4.11}$$

and $f(1) = -1$. Therefore $[\chi_4] \neq [\chi_1]$.

Because $\chi_4 = \chi_2 \cdot \chi_3$, the comparisions $\chi_2 \leftrightarrow \chi_4$ and $\chi_3 \leftrightarrow \chi_4$ are trivial. This shows us that we really found four different cocycles in four different cohomology classes which can be used to realize symmetry protected topological phases.

4.1.1. Realization in a Single SSH Chain

We now showed that if our symmetry in a physical system is a representation of the $\mathbb{Z}_2 \times \mathbb{Z}_2^T$ group, we can find a maximum of four phases. In a single SSH chain we can obviously only find the trivial phase and one additional one but depending on the symmetry representation the non-trivial phase may belong to different cohomology classes. We will use the symmetry group $\mathbb{Z}_2 \times \mathbb{Z}_2^T$ as an example to show how the different classes $[\chi_2]$ and $[\chi_4]$ can be realized in a single SSH chain. To do this, we will use Equation (3.23).

As in Subsection 3.2.1, we introduce the double index ij for each unit cell such that Equation (3.23) becomes

$$\sum_{i'j'} [\pi(g)]_{i'j',ij}\, A_{i'j'} = \gamma(g)\, V^{-1}(g) \cdot A_{ij} \cdot V(g)\,. \tag{4.12}$$

As the trivial case is not particularly interesting, we consider the bosonic SSH chain in the fully dimerized topological limit (see Figure 2.4). The MPS representation of this state is given by the matrix

$$A_{ij}^{\alpha\beta} = \delta_{i\alpha}\sigma^x_{j\beta}. \tag{4.13}$$

Now we can make a choice as we define the physical representation of our symmetry. For example we can choose the parity symmetry[1] $\pi(X) = \sigma_1^z\sigma_2^z$ and the sublattice symmetry $\pi(Z) = \sigma_1^x\sigma_2^x \circ K$.[2] Then we can insert these representations into Equation (3.23) and find the following relations:

$$\sum_{i'j'} \underbrace{\sigma^z_{i'i}\sigma^z_{j'j}}_{[\pi(X)]_{i'j',ij}} \cdot \underbrace{\delta_{i'\alpha}\sigma^x_{j'\beta}}_{A^{\alpha\beta}_{i'j'}} = \underbrace{1}_{\gamma(X)} \cdot [\sigma^z A_{ij}\sigma^z]_{\alpha\beta} \tag{4.14a}$$

$$\sum_{i'j'} \underbrace{\sigma^x_{i'i}\sigma^x_{j'j}}_{[\pi(Z)]_{i'j',ij}} \cdot \underbrace{\delta_{i'\alpha}\sigma^x_{j'\beta}}_{A^{\alpha\beta}_{i'j'}} = \underbrace{1}_{\gamma(Z)} \cdot [\sigma^x A_{ij}\sigma^x]_{\alpha\beta}\,. \tag{4.14b}$$

This gives us the projective representations $V(X) = \sigma^z$ and $V(Z) = \sigma^x \circ K$.[3]

To which cohomology class does this state belong? In fact, this is very easy to see. It is $V(Z)^2 = \mathbb{1}$ but $\{V(X)\,, V(Z)\} = 0$. Therefore the corresponding cocycle must be in the same class as χ_2 (in the class $[\chi_2]$).

We could have also chosen another symmetry representation, like for example $\pi(X) = \sigma_1^z\sigma_2^z$ and $\pi(Z) = \sigma_1^y\sigma_2^y \circ K$. Then the restrictions to our system are different and we allow other perturbations. Again, we can calculate the representations $V(X) = \sigma^z$ and $V(Z) = \sigma^y \circ K$. These are different from the ones before because now $V(Z)^2 = -\mathbb{1}$ and $\{V(X)\,, V(Z)\} = 0$. Therefore the system now belongs to the cohomology class $[\chi_4]$.

This shows us that we can realize different topological phases in a single SSH chain just by choosing different symmetry realizations. The same idea also applies for the other symmetry groups. We will later use this principle to realize more than two symmetry protected topological phases in stacked bosonic SSH chains.

[1] This is actually how the parity symmetry is physically implemented in real systems.
[2] This notation might be very confusing but is intentional.
[3] The complex conjugation has to be added here, such that the representation of Z is again anti-unitary.

4.2. Realizing 16 Phases

In Table 3.1, we can see that with a $D_2 \times \mathbb{Z}_2^T = \mathbb{Z}_2 \times \mathbb{Z}_2 \times \mathbb{Z}_2^T$ symmetry group it is even possible to realize 16 different cohomology classes with the group structure $\mathbb{Z}_2^4$. This is done in a very similar fashion as for the $\mathbb{Z}_2 \times \mathbb{Z}_2^T$ group.

We call the generators of the $\mathbb{Z}_2$ groups X and Y and the anti-unitary realized generator of $\mathbb{Z}_2^T$ is called Z. Now we can already see the analogy to the idea of the cocycles for the $\mathbb{Z}_2 \times \mathbb{Z}_2^T$ group. We can still have the same non-trivial elements in the representations of such a symmetry and just add two more possibilities:

- The representation of Z can square to -1. (Realized by χ_4.)
- The representations of X and Z can anticommute. (Realized by χ_2.)
- The representations of Y and Z can anticommute. (Realized by χ_3.)
- The representations of X and Y can anticommute. (Realized by χ_5.)

This gives us $2^4 = 16$ possibilities of fulfilling or not fulfilling these four conditions. Also this inherits the $\mathbb{Z}_2^4$ group structure. We can realize this with the following cocycles:

$$\chi_1(g_1, g_2) = 1 \tag{4.15a}$$

$$\chi_2(g_1, g_2) = \begin{cases} \omega(g_2) & \text{if } \sigma(g_1) = -1 \\ 1 & \text{else} \end{cases} \tag{4.15b}$$

$$\chi_3(g_1, g_2) = \begin{cases} \rho(g_2) & \text{if } \sigma(g_1) = -1 \\ 1 & \text{else} \end{cases} \tag{4.15c}$$

$$\chi_4(g_1, g_2) = \begin{cases} \sigma(g_2) & \text{if } \sigma(g_1) = -1 \\ 1 & \text{else} \end{cases} \tag{4.15d}$$

$$\chi_5(g_1, g_2) = \begin{cases} \rho(g_2) & \text{if } \omega(g_1) = -1 \\ 1 & \text{else} \end{cases} \tag{4.15e}$$

$$\chi_6(g_1, g_2) = \chi_2(g_1, g_2) \cdot \chi_3(g_1, g_2) \tag{4.15f}$$

$$\chi_7(g_1, g_2) = \chi_2(g_1, g_2) \cdot \chi_4(g_1, g_2) \tag{4.15g}$$

$$\chi_8(g_1, g_2) = \chi_2(g_1, g_2) \cdot \chi_5(g_1, g_2) \tag{4.15h}$$

$$\chi_9(g_1, g_2) = \chi_3(g_1, g_2) \cdot \chi_4(g_1, g_2) \tag{4.15i}$$

$$\chi_{10}(g_1, g_2) = \chi_3(g_1, g_2) \cdot \chi_5(g_1, g_2) \tag{4.15j}$$

$$\chi_{11}(g_1, g_2) = \chi_4(g_1, g_2) \cdot \chi_5(g_1, g_2) \tag{4.15k}$$

$$\chi_{12}(g_1, g_2) = \chi_2(g_1, g_2) \cdot \chi_3(g_1, g_2) \cdot \chi_4(g_1, g_2) \tag{4.15l}$$

$$\chi_{13}(g_1, g_2) = \chi_2(g_1, g_2) \cdot \chi_3(g_1, g_2) \cdot \chi_5(g_1, g_2) \tag{4.15m}$$

$$\chi_{14}(g_1, g_2) = \chi_2(g_1, g_2) \cdot \chi_4(g_1, g_2) \cdot \chi_5(g_1, g_2) \tag{4.15n}$$

$$\chi_{15}(g_1, g_2) = \chi_3(g_1, g_2) \cdot \chi_4(g_1, g_2) \cdot \chi_5(g_1, g_2) \tag{4.15o}$$

$$\chi_{16}(g_1, g_2) = \chi_2(g_1, g_2) \cdot \chi_3(g_1, g_2) \cdot \chi_4(g_1, g_2) \cdot \chi_5(g_1, g_2)\,. \tag{4.15p}$$

Cocycle Pair	First Choice (g_1, g_2)	Second Choice (g_1, g_2)
$\chi_1 \leftrightarrow \chi_5$	$(1, 1)$	(XYZ, XYZ)
$\chi_2 \leftrightarrow \chi_5$	$(1, 1)$	(XZ, XZ)
$\chi_3 \leftrightarrow \chi_5$	$(1, 1)$	(YZ, YZ)
$\chi_4 \leftrightarrow \chi_5$	$(1, 1)$	(Z, Z)
$\chi_2 \leftrightarrow \chi_3$	$(1, 1)$	(XZ, XZ)
$\chi_1 \leftrightarrow \chi_6$	$(1, 1)$	(XZ, XZ)
$\chi_1 \leftrightarrow \chi_7$	(Z, X)	(Z, XZ)
$\chi_1 \leftrightarrow \chi_8$	(XZ, Y)	(XZ, XYZ)
$\chi_1 \leftrightarrow \chi_9$	(Z, Y)	(Z, YZ)
$\chi_1 \leftrightarrow \chi_{10}$	(YZ, Y)	(YZ, Z)
$\chi_1 \leftrightarrow \chi_{11}$	$(1, 1)$	(Z, Z)
$\chi_1 \leftrightarrow \chi_{16}$	(X, Y)	(Y, X)

Table 4.1.: We use Equation (3.30) to prove that different pairs of cocycles are not equivalent. We do this by choosing two pairs of symmetry group elements, inserting them into the equation and finding a contradiction for the function $f(g)$.

Here we use the functions

$$\omega(g) = \begin{cases} -1 & \text{if } X \text{ in } g \\ 1 & \text{else} \end{cases} \tag{4.16a}$$

$$\rho(g) = \begin{cases} -1 & \text{if } Y \text{ in } g \\ 1 & \text{else} \end{cases} \tag{4.16b}$$

$$\sigma(g) = \begin{cases} -1 & \text{if } Z \text{ in } g \\ 1 & \text{else} \end{cases} . \tag{4.16c}$$

As in Section 4.1, we need to prove that all those cocycles belong to 16 different cohomology classes by using Equation (3.30). As these calculations get quite lengthy for 16 cocycles, we will only give short notices on how to show that each pairs are not equivalent.

First of all, the pairs $\chi_1 \leftrightarrow \chi_2$, $\chi_1 \leftrightarrow \chi_3$, $\chi_1 \leftrightarrow \chi_4$, $\chi_2 \leftrightarrow \chi_4$ and $\chi_3 \leftrightarrow \chi_4$ are exactly equivalent to the pairs in Section 4.1. We do not need to prove again that they all belong to different cohomology classes.

Now we need to compare these cocycles with χ_5 and also do the comparison $\chi_2 \leftrightarrow \chi_3$. Showing that these cocycles belong to different cohomology classes is done in the same way as in Section 4.1 via Equation (3.30). We simply assume two different pairs (g_1, g_2) and insert them into the equation with the corresponding cocycles and this gives us a contradiction. We will not show all those calculations here but we will write down the pairs of symmetry group elements (see Table 4.1) which can be used to find a contradiction. The explicit calculations are then very easy to be done.

Now we know that the cocycles χ_1 to χ_5 are all in five different cohomology classes. Furthermore we prove now that the cocycles χ_6 to χ_{11} also all belong to different classes (also compared to the cocycles χ_1 to χ_5). To do this, we need to show that the pairs $\chi_1 \leftrightarrow \chi_6$, $\chi_1 \leftrightarrow \chi_7$, $\chi_1 \leftrightarrow \chi_8$, $\chi_1 \leftrightarrow \chi_9$, $\chi_1 \leftrightarrow \chi_{10}$, $\chi_1 \leftrightarrow \chi_{11}$ as well as $\chi_1 \leftrightarrow \chi_{16}$ are not equivalent (see Table 4.1). Then all the remaining parts become trivial and we know that all cocycles χ_1 to χ_{11} and χ_{16} belong to different cohomology groups.[4]

To finish our calculations we still need to look at the cocycles χ_{12} to χ_{15}. Here it is also trivial to prove that these cocycles are not equivalent to each other and also not to the other cocycles. Again, this can be shown by inserting the cocycles in Equation (3.30) and multiplying both sides with cocycles until the resulting equivalence condition is one of those which we already proved.

4.3. Sublattice Symmetry and Particle Number Conservation

The symmetry group $U(1)\times\mathbb{Z}_2^T$ is the one which we originally considered for the fermionic SSH chain. From Table 3.1 we know that the second cohomology group of this symmetry is given by $\mathbb{Z}_2^2$, just as for the $\mathbb{Z}_2 \times \mathbb{Z}_2^T$ group. Now we want to find four cocycles which belong to the four cohomology classes.

Let R_ϕ for $0 \leq \phi < 2\pi$ be the elements of the group $U(1)$ and Z the generator of the anti-unitarily realized symmetry group $\mathbb{Z}_2^T$. We choose

$$\chi_1(g_1, g_2) = 1 \tag{4.17a}$$

$$\chi_2(g_1, g_2) = \begin{cases} \sigma(g_2) & \text{if } \sigma(g_1) = -1 \\ 1 & \text{else} \end{cases} \tag{4.17b}$$

$$\chi_3(g_1, g_2) = \begin{cases} e^{\mathrm{i}\phi_2} & \text{if } \sigma(g_1) = -1 \\ 1 & \text{else} \end{cases} \tag{4.17c}$$

$$\chi_4(g_1, g_2) = \chi_2(g_1, g_2) \cdot \chi_3(g_1, g_2) \tag{4.17d}$$

with

$$\sigma(g) = \begin{cases} -1 & \text{if } Z \text{ in } g \\ 1 & \text{else} \end{cases}. \tag{4.18}$$

These cocycles are actually not arbitrary guesses. Instead they are a continuous extension of the cocycles discussed in Section 4.1.

We will now once again use Equation (3.30) to show that these four cocycles belong to four different cohomology classes. We start with the comparison $\chi_1 \leftrightarrow \chi_2$. Here we first choose $g_1 = Z$ and $g_2 = 1$ which gives us the equivalence condition

$$1 = \frac{f(Z)}{f(1)\, f(Z)} \cdot 1 \tag{4.19}$$

[4]This is also due to the fact that for our cocycles the identity $\frac{1}{\chi} = \chi$ holds.

and therefore $f(1) = 1$. On the other hand, we can also choose $g_1 = g_2 = Z$ which gives us

$$-1 = \frac{f(Z)}{f(Z)\, f(1)} \cdot 1 \tag{4.20}$$

and $f(1) = -1$. This is a contradiction and therefore $[\chi_1] \neq [\chi_2]$.

Now we compare $\chi_1 \leftrightarrow \chi_3$. The choice $g_1 = 1$ and $g_2 = 1$ will obviously give us $f(1) = 1$. On the other hand, if we choose $g_1 = g_2 = ZR_\pi$, we get the equivalence condition

$$e^{i\pi} = \frac{f(ZR_\pi)}{f(ZR_\pi)\, f\left(\underbrace{ZR_\pi ZR_\pi}_{=1}\right)} \cdot 1 \tag{4.21}$$

which can easily be simplified to $f(1) = -1$. This shows $[\chi_1] \neq [\chi_3]$.

Furthermore we investigate the cocycles $\chi_2 \leftrightarrow \chi_3$. If we choose $g_1 = Z$ and $g_2 = R_\phi$, we find the condition

$$e^{i\phi} = \frac{f(Z)}{f(R_\phi)\, f(ZR_\phi)} \cdot 1. \tag{4.22}$$

On the other hand, for the choice $g_1 = Z$ and $G_2 = ZR_\phi$, we find

$$e^{i\phi} = \frac{f(Z)}{f(ZR_\phi)\, f(R_\phi)} \cdot (-1)\,. \tag{4.23}$$

Combining both equations leads us to the condition

$$\frac{f(Z)}{f(R_\phi)\, f(ZR_\phi)} = -\frac{f(Z)}{f(ZR_\phi)\, f(R_\phi)}. \tag{4.24}$$

This shows that $[\chi_2] \neq [\chi_3]$.

Now we still need to compare the cocycles $\chi_4 \leftrightarrow \chi_1$. If we choose $g_1 = Z$ and $g_2 = 1$ and insert them into Equation (3.30) we find the condition

$$1 = \frac{f(Z)}{f(1)\, f(Z)} \cdot 1 \tag{4.25}$$

and $f(1) = 1$. On the other hand (just as for the comparison $\chi_1 \leftrightarrow \chi_2$), we can choose $g_1 = g_2 = Z$ and find

$$-1 = \frac{f(Z)}{f(Z)\, f(1)} \cdot 1 \tag{4.26}$$

and $f(1) = -1$. This proves $[\chi_1] \neq [\chi_4]$

The only two comparisons left are $\chi_2 \leftrightarrow \chi_4$ and $\chi_3 \leftrightarrow \chi_4$. For these cocycles the identity $\chi_4 = \chi_2 \cdot \chi_3$ makes the comparisons trivial. This proves that all four cocycles belong to four different cohomology classes and it should indeed be possible to realize four symmetry protected topological phases with this symmetry group.

Again, the cohomology classes of these four cocycles inherit the $\mathbb{Z}_2^2$ group structure since $\left[\chi_i^2\right] = [\chi_1]$ for all $i \in \{1, \cdots, 4\}$ and $[\chi_2 \cdot \chi_3] = [\chi_4]$.[5]

[5] These equivalences can easily be proved by Equation (3.30).

4.4. Stacking Bosonic SSH Chains

We want to stack multiple separated SSH chains on top of each other. What is the combined phase of the chains if we know the individual cohomology classes which correspond to each chain?

To understand the underlying mechanism to this concept we consider two chains (not necessarily SSH chains) with ground states $|a\rangle$ and $|b\rangle$. Their combined ground state can be written as[6]

$$|\psi\rangle = |a\rangle \otimes |b\rangle = \sum_{\{i_k\}} \mathrm{Tr}[A_{i_1} \cdots A_{i_L}] \, |i_1 \cdots i_L\rangle \otimes \sum_{\{j_k\}} \mathrm{Tr}[B_{j_1} \cdots B_{j_L}] \, |j_1 \cdots j_L\rangle \,. \tag{4.27}$$

Using the identities $\mathrm{Tr}(A \otimes B) = \mathrm{Tr}(A) \cdot \mathrm{Tr}(B)$ and $AC \otimes BD = (A \otimes B)\,(C \otimes D)$, we can rewrite this to an MPS:

$$|\psi\rangle = \sum_{\{i_k, j_k\}} \mathrm{Tr}[A_{i_1} \cdots A_{i_L} \otimes B_{j_1} \cdots B_{j_L}] \, |i_1 j_1 \cdots i_L j_L\rangle \tag{4.28a}$$

$$= \sum_{\{i_k, j_k\}} \mathrm{Tr}\left[\underbrace{(A_{i_1} \otimes B_{j_1})}_{C_{i_1 j_1}} \cdots \underbrace{(A_{i_L} \otimes B_{j_L})}_{C_{i_L j_L}}\right] |i_1 j_1 \cdots i_L j_L\rangle \tag{4.28b}$$

$$= \sum_{\{i_k, j_k\}} \mathrm{Tr}[C_{i_1 j_1} \cdots C_{i_L j_L}] \, |i_1 j_1 \cdots i_L j_L\rangle \,. \tag{4.28c}$$

We can write the new matrices of the combined state as the Kronecker product $C_{ij} = A_i \otimes B_j$ of the original matrices of both chains.

For the following calculations all subsets a and b sort the operators and matrices to their SSH chain. Now we can have a look at Equation (3.23) which takes the form

$$\sum_i [\pi(g)]_{ii'} \, C_i = \gamma(g) \, V^{-1}(g) \cdot C_{i'} \cdot V(g) \,. \tag{4.29}$$

We can now rewrite this equation using $\pi(g) = \pi_a(g) \otimes \pi_b(g)$ and solve it by inserting $V(g) = V_a(g) \otimes V_b(g)$:

$$\sum_i [\pi(g)]_{i'i} \, (A_i \otimes B_i) \tag{4.30a}$$

$$= \gamma(g) \, V^{-1}(g) \cdot (A_{i'} \otimes B_{i'}) \cdot V(g) \tag{4.30b}$$

$$= \gamma(g) \left[V_a^{-1}(g) \otimes V_b^{-1}(g)\right] \cdot (A_{i'} \otimes B_{i'}) \cdot [V_a(g) \otimes V_b(g)] \tag{4.30c}$$

$$= \big(\gamma_a(g) \, V_a^{-1}(g) \cdot A_{i'} \cdot V_a(g)\big) \otimes \big(\gamma_b(g) \, V_b^{-1}(g) \cdot B_{i'} \cdot V_b(g)\big) \tag{4.30d}$$

Here we dropped the double index to make the calculation easier. We also inserted $\gamma(g) = \gamma_a(g) \cdot \gamma_b(g)$ and used the identity $(A \otimes B)^{-1} = A^{-1} \otimes B^{-1}$. This calculation shows us that combined systems of two chains a and b have the combined projective

[6] In the ground state there is no entanglement between the two chains.

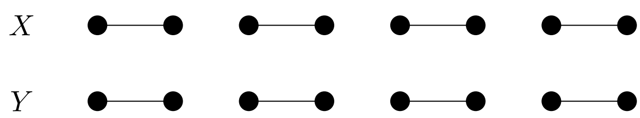

Figure 4.1.: Two bosonic SSH chains in the fully dimerized limit are stacked on top of each other. We choose the symmetry representation of the sublattice symmetry such that a σ^x matrix acts on each site in the upper chain and a σ^y matrix acts on each lower site.

representation $V(g) = V_a(g) \otimes V_b(g)$. It can easily be shown that the cocycle for $V(g)$ is given by $\chi(g_1, g_2) = \chi_a(g_1, g_2) \cdot \chi_b(g_1, g_2)$:

$$
\begin{aligned}
V(g_1) \cdot V(g_2) &= (V_a(g_1) \otimes V_b(g_1)) \cdot (V_a(g_2) \otimes V_b(g_2)) && \text{(4.31a)} \\
&= (V_a(g_1) \cdot V_a(g_2)) \otimes (V_b(g_1) \cdot V_b(g_2)) && \text{(4.31b)} \\
&= \chi_a(g_1, g_2)\, V_a(g_1 g_2) \otimes \chi_b(g_1, g_2)\, V_b(g_1 g_2) && \text{(4.31c)} \\
&= \underbrace{\chi_a(g_1, g_2)\, \chi_b(g_1, g_2)}_{\chi(g_1, g_2)} V(g_1 g_2)\,. && \text{(4.31d)}
\end{aligned}
$$

This is a very important finding. If we stack multiple chains with different cocycles on top of each other, the combined cocycle will be the product of all cocycles. This way, we can directly guess the phase of a system which consists of many chains. Keep in mind that this only works if the chains are completely separated.

4.4.1. Stacked Bosonic SSH Chains

Now we can apply this to the observations which we made in Subsection 4.1.1. Consider two bosonic SSH chains (see Figure 4.1). We use the $\mathbb{Z}_2 \times \mathbb{Z}_2^T$ symmetry group again. The parity symmetry acts as a σ^z matrix on each site of the whole combined system but we choose the sublattice symmetry representation such that σ^x matrices act on the upper chain and σ^y matrices act on the lower chain.

Now we can simply go through all four possible configurations of this system. If both chains are in the trivial phase, their cocycles are both trivial (see the equivalent Equation (4.1a)). The combined cocycle is the product of those two and is also trivial. The system is in the phase characterized by $[\chi_1]$. Now let us consider the upper chain in the topological phase. Then it has the cocycle χ_2 (see the equivalent Equation (4.1b)) while the lower chain is still in the trivial phase. The product of both cocycles is obviously still in the class $[\chi_2]$. If the upper SSH chain is in the trivial state and the lower chain is topological, the combined system is characterized by the class $[\chi_4]$. Combining both chains allows us now to realize the fourth phase which corresponds to $[\chi_3] = [\chi_2 \cdot \chi_4]$.

We want to point out two observations:

1. The mechanism used to create bosonic phases is very different from the way in which we stacked fermionic SSH chains to create up to four phases (see Section 2.2). We will discuss these differences in more detail later.

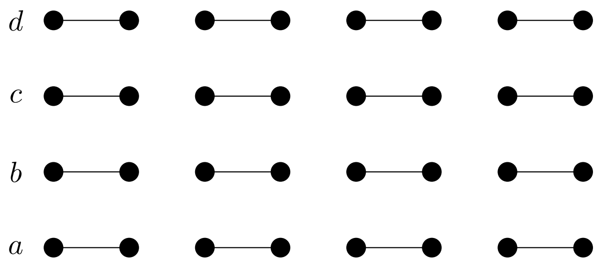

Figure 4.2.: Four bosonic SSH chains with the $D_2 \times \mathbb{Z}_2^T$ symmetry group can be used to realize up to 16 different phases. The concept is exactly identical to the realization of four phases with two bosonic SSH chains.

2. The physical symmetry realization is key to the realization of more than two phases. If we had chosen to realize the sublattice symmetry as σ^x matrices on all sites, we would have only been able to realize the phases $[\chi_1]$ and $[\chi_3]$.

We can now also consider the symmetry group $D_2 \times \mathbb{Z}_2^T$. This allows us in principle to realize 16 different symmetry protected topological phases. To do this, we can use four stacked SSH chains (see Figure 4.2) a to d and special realizations of the symmetry generators X, Y and Z. They are realized on each column of sites as

$$\xi(X) = \mathbb{1}_a \sigma_b^x \mathbb{1}_c \sigma_d^x \tag{4.32a}$$
$$\xi(Y) = \mathbb{1}_a \mathbb{1}_b \sigma_c^x \sigma_d^z \tag{4.32b}$$
$$\xi(Z) = \sigma_a^y \sigma_b^z \sigma_c^z \mathbb{1}_d \circ K. \tag{4.32c}$$

These matrices act on each site of their different chains. It is important to notice that the three realizations do not commute with each other but they commute on every full unit cell. By putting the different SSH chains into their topological state we can now realize 16 different combinations with 16 different phases. As the calculations are exactly the same as for the example above but longer, we will leave them out at this point.

5. Stabilizer Codes

Classifying bosonic symmetry protected topological phases as shown in Chapter 3 is a quite complex task and can take a lot of time. This is due to the fact that the ground states can become very complicated in some systems, especially if we add many interactions. On the other hand, in this thesis we only work with fully dimerized chains which in principle are very simple. In this chapter we present a method, which allows us to assign a specific system to a topological phase much faster. It will not require us to calculate the ground states, instead we only work with the Hamiltonian terms. We will first introduce a tool called *stabilizer codes* and later apply this tool to our problem.

5.1. Stabilizer Codes

The stabilizer formalism has been introduced in [29]. We base our following introduction loosely on [30].

Consider a spin system with N spins. All operations on this system can be performed by the group

$$G = \{\sigma_i^\alpha | i \in \{1, \cdots, N\}, \alpha \in \{0, x, y, z\}\} \tag{5.1}$$

which contains all Pauli matrices (including $\sigma^0 = \mathbb{1}$) on each site and also all possible combinations of products of these Pauli matrices.[1] Now we choose a set of elements of G which we call

$$g = \{g_1, g_2, \cdots, g_k \,|\, \forall\, i \in \{1, \cdots, k\} : g_i \in G\} \tag{5.2}$$

and we require the elements of g to fulfil the following two conditions:

- All elements of g commute: $[g_i, g_j] = 0$, $\forall\, i, j \in \{0, \cdots, k\}$.
- All elements of g square to one and $-\mathbb{1}$ is not an element of g: $g_i^2 = \mathbb{1}, \forall i \in \{0, \cdots, k\} \wedge -\mathbb{1} \notin g$.

Together with the multiplication of Pauli matrices, the set g can form a group

$$S = \langle g \rangle \subseteq G, \tag{5.3}$$

which we call the stabilizer group. This group includes all elements of g and all possible products of the elements of g.

[1] The group G of Pauli operators is not to be confused with symmetry groups, which we also sometimes call G.

Now we go back to our spin system which lives on the Hilbert space $\mathcal{H}$. The stabilizer group characterizes a *stabilized* subspace of $\mathcal{H}$ which we call

$$PS = \{|\psi\rangle \in \mathcal{H} \,|\, \forall g \in S : g\,|\psi\rangle = 1 \cdot |\psi\rangle\} \,. \tag{5.4}$$

This is the set of states on which all elements of S act as $\mathbb{1}$.

5.2. Classification of Phases Using Stabilizers

Consider an open system of N spins in its ground state. The Hamiltonian

$$H = \sum_{i=1}^{M} H_i \tag{5.5}$$

of the system is always a sum of terms which are elements of the group G. In general the classification of the symmetry protected topological phases in such a system relies on the ground state of the closed chain. Nonetheless it might be very difficult to determine the ground state for some systems. This is where we can use the stabilizer codes. We will also use open chains and determine the phase by the action of the symmetry on the edge of the system.

In many cases (especially in the systems we consider in this thesis) the Hamiltonian terms can be written as $H_i = c \cdot g_i$ with some elements $g_i \in G$ and a global constant c for all terms. As we already observed that this constant does not affect the phase of the system, we assume $c = -1$. If the terms H_i furthermore commute and square to $\mathbb{1}$,[2] we can use the stabilizer formalism. As we know that the eigenvalues of the elements g_i and all Hamiltonian terms commute, we also know that the ground state of the system is also an eigenstate of all terms H_i with eigenvalue -1.

Now we rescale the Hamiltonian by dividing it by c. Then the ground state is the state with the highest energy M and all rescaled terms $H_i = g_i$ act on this state as identities. Here we see that the terms H_i generate a stabilizer group S and the ground states of the systems are the set PS.

Instead of writing down the state, we now have a set of Pauli matrices and say that the ground states are all states which have the eigenvalue 1 for these combined Pauli matrices. How does this help to classify the phases? We know how the symmetry operators act on the system. They are also elements of the group G. As the symmetry acts trivially on the ground state of a closed chain we expect something similar for the open chain but not on the edges.

Consider a symmetry operator U. All elements of the stabilizer group S act as $\mathbb{1}$ on the ground states $|\psi_i\rangle$, so we know that

$$U\,|\psi_i\rangle = Ug\,|\psi_i\rangle \tag{5.6}$$

for all $g \in S$. Now we simply multiply elements of the stabilizer group S (which are products of the terms H_i) onto the symmetry operator until it acts as a $\mathbb{1}$ on the bulk

[2] If that is not the case, the stabilizer method cannot be used.

of the system. This procedure does not change the action of U onto the ground states at all. In some cases we will see that the whole operator U can be transformed into a trivial $\mathbb{1}$ which then shows us that the system is in the trivial phase. In general, we will see that there will be an action of U on the edges of the system which cannot be annihilated by terms of H. These actions on the edge will help us to identify the phase of the system. This concept is based on the bulk-boundary correspondence which we already discussed in Section 3.4.

5.3. Stabilizer Formalism on the SSH Chain

Now we will show specific examples for the application of the stabilizer formalism which also are part of this thesis. We choose the symmetry group $\mathbb{Z}_2 \times \mathbb{Z}_2^T$ which we already discussed in Section 4.1. Here we know that we can realize four phases using two chains as long as we choose the symmetry representations correctly.

Consider for example two bosonic SSH chains in the fully dimerized limit which are both in the trivial phase. The Hamiltonian of this system is then given by[3]

$$H = \sum_{k=1}^{L} \left(\sigma_{4k-3}^{+} \sigma_{4k}^{-} + \sigma_{4k-2}^{+} \sigma_{4k-1}^{-} \right) + \text{h.c.}. \tag{5.7}$$

Now we use the identity $\sigma_i^+ \sigma_j^- + \sigma_j^+ \sigma_i^- = \sigma_i^x \sigma_j^x + \sigma_i^y \sigma_j^y$. This enables the following notation:

$$H = \sum_{k=1}^{L} \left(\sigma_{4k-3}^{x} \sigma_{4k}^{x} + \sigma_{4k-3}^{y} \sigma_{4k}^{y} + \sigma_{4k-2}^{x} \sigma_{4k-1}^{x} + \sigma_{4k-2}^{y} \sigma_{4k-1}^{y} \right) . \tag{5.8}$$

To make all the following calculations much easier we rewrite the Hamiltonian as

$$H = \begin{array}{cc} \scriptstyle 1 & \scriptstyle 2 \\ X & X \\ 1 & 1 \end{array} + \begin{array}{cc} \scriptstyle 1 & \scriptstyle 2 \\ Y & Y \\ 1 & 1 \end{array} + \begin{array}{cc} \scriptstyle 1 & \scriptstyle 2 \\ 1 & 1 \\ X & X \end{array} + \begin{array}{cc} \scriptstyle 1 & \scriptstyle 2 \\ 1 & 1 \\ Y & Y \end{array} + \begin{array}{cc} \scriptstyle 3 & \scriptstyle 4 \\ X & X \\ 1 & 1 \end{array} + \begin{array}{cc} \scriptstyle 3 & \scriptstyle 4 \\ Y & Y \\ 1 & 1 \end{array} + \begin{array}{cc} \scriptstyle 3 & \scriptstyle 4 \\ 1 & 1 \\ X & X \end{array} + \begin{array}{cc} \scriptstyle 3 & \scriptstyle 4 \\ 1 & 1 \\ Y & Y \end{array} + \cdots . \tag{5.9}$$

Each position on these matrices corresponds to a physical site. The letters X, Y, Z and 1 label the Pauli matrices which act on the site. Above each matrix we write down the column on the chain on witch these matrices act (If we had only one SSH chain, this would be simply the number of each site.). Now we choose the sublattice symmetry representation

$$S = \begin{array}{cccc} \scriptstyle 1 & \scriptstyle 2 & \scriptstyle \cdots & \scriptstyle 2L \\ X & X & \cdots & X \\ Y & Y & \cdots & Y \end{array} \tag{5.10}$$

and the parity symmetry representation

$$P = \begin{array}{cccc} \scriptstyle 1 & \scriptstyle 2 & \scriptstyle \cdots & \scriptstyle 2L \\ Z & Z & \cdots & Z \\ Z & Z & \cdots & Z \end{array} . \tag{5.11}$$

[3] We enumerate the sites as in Figure 2.6.

How do these symmetries act on the actual system? We can work this out by using the terms of the Hamiltonian. It is actually easy to see that all the terms in Equation (5.9) commute which makes them perfect generators for our stabilizer group. It also means that these terms act as $\mathbb{1}$ on the ground states (in general there can be more than one ground state). Now we multiply the terms together in a specific way[4]:

$$\Omega_S = \begin{array}{cc} \scriptstyle 1 & \scriptstyle 2 \\ X & X \\ 1 & 1 \end{array} \cdot \begin{array}{cc} \scriptstyle 1 & \scriptstyle 2 \\ 1 & 1 \\ Y & Y \end{array} \cdot \begin{array}{cc} \scriptstyle 3 & \scriptstyle 4 \\ X & X \\ 1 & 1 \end{array} \cdot \begin{array}{cc} \scriptstyle 3 & \scriptstyle 4 \\ 1 & 1 \\ Y & Y \end{array} \cdots = \begin{array}{c} X \cdots X \\ Y \cdots Y \end{array}. \tag{5.12}$$

This operator is still an element of our stabilizer group and therefore acts as a one onto all ground states. If we want to know how the symmetry operator S acts onto the state, we can multiply it with Ω_S without changing anything:

$$S' = S \cdot \Omega_S = \begin{array}{c} 1 \cdots 1 \\ 1 \cdots 1 \end{array} \circ K. \tag{5.13}$$

Here we can see that the sublattice symmetry actually acts trivially onto the whole chain.

We can do a similar calculation for the parity symmetry P by multiplying all terms of H

$$\Omega_P = \begin{array}{cc} \scriptstyle 1 & \scriptstyle 2 \\ X & X \\ 1 & 1 \end{array} \cdot \begin{array}{cc} \scriptstyle 1 & \scriptstyle 2 \\ Y & Y \\ 1 & 1 \end{array} \cdot \begin{array}{cc} \scriptstyle 1 & \scriptstyle 2 \\ 1 & 1 \\ X & X \end{array} \cdot \begin{array}{cc} \scriptstyle 1 & \scriptstyle 2 \\ 1 & 1 \\ Y & Y \end{array} \cdots = \begin{array}{c} Z\,Z \cdots Z \\ Z\,Z \cdots Z \end{array} \tag{5.14}$$

and modifying the symmetry operator

$$P' = P \cdot \Omega_P = \begin{array}{c} 1 \cdots 1 \\ 1 \cdots 1 \end{array}. \tag{5.15}$$

We see that the parity symmetry also acts trivially onto the chain. These calculations show us that the system is in the trivial phase.

This conclusion becomes clearer if we take a look at two stacked SSH chains in the topological state. Then their Hamiltonian is

$$H = \begin{array}{cc} \scriptstyle 2 & \scriptstyle 3 \\ X & X \\ 1 & 1 \end{array} + \begin{array}{cc} \scriptstyle 2 & \scriptstyle 3 \\ Y & Y \\ 1 & 1 \end{array} + \begin{array}{cc} \scriptstyle 2 & \scriptstyle 3 \\ 1 & 1 \\ X & X \end{array} + \begin{array}{cc} \scriptstyle 2 & \scriptstyle 3 \\ 1 & 1 \\ Y & Y \end{array} + \begin{array}{cc} \scriptstyle 4 & \scriptstyle 5 \\ X & X \\ 1 & 1 \end{array} + \begin{array}{cc} \scriptstyle 4 & \scriptstyle 5 \\ Y & Y \\ 1 & 1 \end{array} + \begin{array}{cc} \scriptstyle 4 & \scriptstyle 5 \\ 1 & 1 \\ X & X \end{array} + \begin{array}{cc} \scriptstyle 4 & \scriptstyle 5 \\ 1 & 1 \\ Y & Y \end{array} + \cdots, \tag{5.16}$$

which does not act on the first and the last sites (columns 1 and $2L$). If we do the same calculations as above, we find

$$S' = \begin{array}{c} X\,1 \cdots 1\,X \\ Y\,1 \cdots 1\,Y \end{array} \circ K \tag{5.17}$$

and

$$P' = \begin{array}{c} Z\,1 \cdots 1\,Z \\ Z\,1 \cdots 1\,Z \end{array}. \tag{5.18}$$

[4] For operators which act on the whole system, we drop the column indices.

It is obvious that the symmetries will always act on the edges of the system in a non-trivial way. In Section 4.1 we discussed the four cohomology classes for the $\mathbb{Z}_2 \times \mathbb{Z}_2^T$ symmetry and how they differ from each other. Now we see that on the edges, the symmetries act as the operators

$$S_{\text{left}} = S_{\text{right}} = \frac{X}{Y} \circ K \tag{5.19a}$$

$$P_{\text{left}} = P_{\text{right}} = \frac{Z}{Z}. \tag{5.19b}$$

These two operators commute but $S_{\text{left}}^2 = S_{\text{right}}^2 = -\mathbb{1}$. This property is associated with the cohomology class $[\chi_3]$ (see Equation (4.1c)). We found the same result in Subsection 4.4.1.

The analogue calculations can also be made for the two other configurations of the stacked chains.

5.4. Comparison of Bosonic and Fermionic Phases

We showed how the stabilizer formalism can be used to distinguish different phases in open systems. Now we want to apply it to systems with more complicated ground states.

In this thesis we discussed fermionic and bosonic phases in stacked SSH chains. Even though for both cases we can realize up to four phases (for the given symmetry), the mechanisms to create these phases are very different. Also the bosonic phases have a $\mathbb{Z}_2^2$ group algebra while the fermionic phases are simply added in a $\mathbb{Z}_4$ structure. Now we want to understand how fermionic and bosonic phases translate.

First of all, we need to understand that transforming stacked fermionic chains into bosonic chains using the Jordan–Wigner transformation is not as trivial as for single SSH chains. Consider two stacked chains of fermions. To transform them, we have to choose a Jordan–Wigner string as shown in Figure 5.1. This sketch shows two trivial chains. If we transform them into a bosonic system, we find the Hamiltonian

$$H = \sum_{k=1}^{L} \left(\sigma_{4k-3}^{+} \sigma_{4k-2}^{z} \sigma_{4k-1}^{z} \sigma_{4k}^{-} + \sigma_{4k-2}^{+} \sigma_{4k-1}^{-} \right) + \text{h.c.}. \tag{5.20}$$

This is an interacting Hamiltonian and not the Hamiltonian of two stacked bosonic SSH chains. Both subchains are coupled by these interactions. In the dimerized limit, we can in principle always find a Jordan–Wigner string which gives us a non-interacting system but this will only hold for one phase. Switching the phases on the chains will always give us an interacting system.[5]

[5] In principle we could choose the Jordan–Wigner string such that it first goes straight through the upper chain and then through the lower chain. This would always give a non-interacting Hamiltonian (besides the interactions of hard-core bosons themselves) but it would not be local any more. Therefore we do not allow these Jordan–Wigner strings.

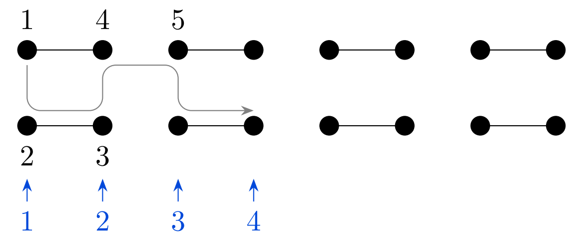

Figure 5.1.: Two fermionic SSH chains in the fully dimerized limit are stacked on top of each other. They are both in the trivial phase. We choose the Jordan–Wigner string as shown in this sketch. We also label the columns in the chain as they are used in the matrix representation of the bosonic operators (e.g. Equation (5.21)).

We will now always choose the Jordan–Wigner string shown in Figure 5.1. Other strings will give us the same qualitative results for the classificaiton. As we see, the Hamiltonian in Equation (5.20) couples the chains together. This makes it harder to write down the ground state as an MPS and classify it using Equation (3.23). This is why we introduced the stabilizer formalism. We can simply rewrite the Hamiltonian as

$$H = \begin{array}{cc} \scriptstyle 1 & \scriptstyle 2 \\ X & X \\ Z & Z \end{array} + \begin{array}{cc} \scriptstyle 1 & \scriptstyle 2 \\ Y & Y \\ Z & Z \end{array} + \begin{array}{cc} \scriptstyle 1 & \scriptstyle 2 \\ 1 & 1 \\ X & X \end{array} + \begin{array}{cc} \scriptstyle 1 & \scriptstyle 2 \\ 1 & 1 \\ Y & Y \end{array} + \cdots \tag{5.21}$$

and easily see that all terms of H commute with each other. This shows us that they generate a stabilizer group which we can now use to classify our phases.

Furthermore, we also need to choose our symmetry representations for the fermionic system and translate them into bosonic operators (using the same Jordan–Wigner string).

We represent the fermionic sublattice symmetry by

$$\hat{S}_{\mathrm{F}} = \prod_{i=1}^{L} \left[\left(\hat{c}_{4i-3} - \hat{c}^{\dagger}_{4i-3} \right) \left(\hat{c}_{4i} + \hat{c}^{\dagger}_{4i} \right) \left(\hat{c}_{4i-2} - \hat{c}^{\dagger}_{4i-2} \right) \left(\hat{c}_{4i-1} + \hat{c}^{\dagger}_{4i-1} \right) \right] \circ K. \tag{5.22}$$

It can be shown that the bosonic representation for that is

$$S = \rho_{\mathrm{JW}} \left(\hat{S}_{\mathrm{F}} \right) = \prod_{i=1}^{L} \sigma^{x}_{4i-3} \sigma^{x}_{4i} \sigma^{y}_{4i-2} \sigma^{y}_{4i-1} \circ K \tag{5.23}$$

which is the symmetry representation we already used in Figure 4.1. We will write it as

$$S = \begin{array}{c} X \cdots X \\ Y \cdots Y \end{array} \circ K. \tag{5.24}$$

To make the calculations easier we will again use the parity symmetry instead of the particle conservation symmetry. For the fermionic system this can be realized by

$$\hat{P}_{\mathrm{F}} = (-1)^{\hat{N}} = \prod_{i=1}^{4L} (-1)^{\hat{n}_i} . \tag{5.25}$$

In the bosonic picture this translates to

$$P = \rho_{\mathrm{JW}}\left(\hat{P}_{\mathrm{F}}\right) = \prod_{i=1}^{4L} \sigma_i^z \tag{5.26}$$

which we will write as

$$S = \begin{matrix} Z\cdots Z \\ Z\cdots Z \end{matrix}. \tag{5.27}$$

Now we can find a corresponding bosonic phase to the fermionic system in Figure 5.1. To do this, we multiply the following terms of the Hamiltonian:

$$\Omega_S = \begin{matrix} \scriptstyle 1 & \scriptstyle 2 \\ X & X \\ Z & Z \end{matrix} \cdot \begin{matrix} \scriptstyle 1 & \scriptstyle 2 \\ 1 & 1 \\ X & X \end{matrix} \cdot \begin{matrix} \scriptstyle 1 & \scriptstyle 2 \\ X & X \\ Z & Z \end{matrix} \cdot \begin{matrix} \scriptstyle 1 & \scriptstyle 2 \\ 1 & 1 \\ X & X \end{matrix} \cdots = \begin{matrix} X\cdots X \\ Y\cdots Y \end{matrix}. \tag{5.28}$$

As this operator does not act onto the ground state, we can multiply it to $\hat{S}$ and obtain

$$\hat{S}' = \hat{S} \cdot \hat{\Omega}_{\hat{S}} = \begin{matrix} 1\cdots 1 \\ 1\cdots 1 \end{matrix} \circ K. \tag{5.29}$$

We see that the sublattice symmetry acts trivially onto the ground state of the system.[6] For the parity symmetry, we multiply all the Hamiltonian terms together which gives

$$\Omega_P = \begin{matrix} \scriptstyle 1 & \scriptstyle 2 \\ X & X \\ Z & Z \end{matrix} \cdot \begin{matrix} \scriptstyle 1 & \scriptstyle 2 \\ Y & Y \\ Z & Z \end{matrix} \cdot \begin{matrix} \scriptstyle 1 & \scriptstyle 2 \\ 1 & 1 \\ X & X \end{matrix} \cdot \begin{matrix} \scriptstyle 1 & \scriptstyle 2 \\ 1 & 1 \\ Y & Y \end{matrix} \cdots = \begin{matrix} Z\cdots Z \\ Z\cdots Z \end{matrix}. \tag{5.30}$$

The action of the parity symmetry on the ground state is

$$P' = P \cdot \Omega_P = \begin{matrix} 1\cdots 1 \\ 1\cdots 1 \end{matrix}. \tag{5.31}$$

Both symmetries act trivially on the edges of the system which means that the system is in the trivial phase. This is the expected result as we do not have any degenerate edge modes which would allow a non-trivial symmetry representation on the edges. To classify the phases we will again use Equation (4.1a) to Equation (4.1d). For this system, the corresponding cohomology class is $[\chi_1]$.

[6] In this case we actually know that there is only one non-degenerate ground state. This is due to the fact that we can perfectly solve the fermionic system and the Jordan–Wigner transformation is an isomorphism which does not change the energy spectrum.

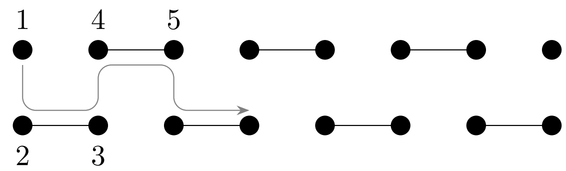

Figure 5.2.: Two fermionic SSH chains are stacked on top of each other. The upper chain is in the topological state. We choose the Jordan–Wigner string as shown in the sketch.

If we put the upper fermionic SSH chain in its topological state, this realizes the first non-trivial fermionic phase (see Subsection 2.2.1). The bosonic Hamiltonian for this system is

$$H = \overset{1\,2}{\begin{matrix}1\,1\\X\,X\end{matrix}} + \overset{1\,2}{\begin{matrix}1\,1\\Y\,Y\end{matrix}} + \overset{2\,3}{\begin{matrix}X\,X\\1\,1\end{matrix}} + \overset{2\,3}{\begin{matrix}Y\,Y\\1\,1\end{matrix}} + \cdots . \tag{5.32}$$

Again we can check that all these terms commute. Now we can combine them to

$$\Omega_S = \overset{1\,2}{\begin{matrix}1\,1\\Y\,Y\end{matrix}} \cdot \overset{2\,3}{\begin{matrix}X\,X\\1\,1\end{matrix}} \cdot \overset{3\,4}{\begin{matrix}1\,1\\Y\,Y\end{matrix}} \cdot \overset{4\,5}{\begin{matrix}X\,X\\1\,1\end{matrix}} \cdots = \begin{matrix}1\,X\cdots X\,1\\Y\,Y\cdots Y\,Y\end{matrix} \tag{5.33a}$$

$$\Omega_P = \overset{1\,2}{\begin{matrix}1\,1\\X\,X\end{matrix}} \cdot \overset{1\,2}{\begin{matrix}1\,1\\Y\,Y\end{matrix}} \cdot \overset{2\,3}{\begin{matrix}X\,X\\1\,1\end{matrix}} \cdot \overset{2\,3}{\begin{matrix}Y\,Y\\1\,1\end{matrix}} \cdots = \begin{matrix}1\,Z\cdots Z\,1\\Z\,Z\cdots Z\,Z\end{matrix}. \tag{5.33b}$$

This shows us that the actual action of the symmetries is given by

$$S' = S \cdot \Omega_S = \begin{matrix}X\,1\cdots 1\,X\\1\,1\cdots 1\,1\end{matrix} \circ K \tag{5.34a}$$

$$P' = P \cdot \Omega_P = \begin{matrix}Z\,1\cdots 1\,Z\\1\,1\cdots 1\,1\end{matrix}. \tag{5.34b}$$

This is not a trivial projective representation any more because the edges of these two operators anticommute. Therefore this system is in the bosonic phase $[\chi_2]$.

We know that the fermionic system shown in Figure 5.3 is in the same phase as the system in Figure 5.2 (see Subsection 2.2.1). As the Jordan–Wigner transformation is an isomorphism, the two corresponding bosonic systems are also in the same phase.

The Hamiltonian of the chain in Figure 5.3 is

$$H = \overset{1\,2}{\begin{matrix}X\,X\\Z\,Z\end{matrix}} + \overset{1\,2}{\begin{matrix}Y\,Y\\Z\,Z\end{matrix}} + \overset{2\,3}{\begin{matrix}Z\,Z\\X\,X\end{matrix}} + \overset{2\,3}{\begin{matrix}Z\,Z\\Y\,Y\end{matrix}} + \cdots . \tag{5.35}$$

This is now a highly interacting Hamiltonian which does not allow us to divide the chain into smaller segments. Therefore it would be very hard to classify the symmetry protected topological phase of this system using Equation (3.23). The stabilizer formalism can

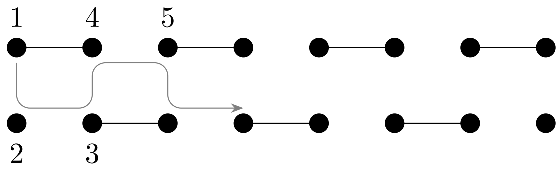

Figure 5.3.: Two fermionic SSH chains are stacked on top of each other. The lower chain is in the topological state. We choose the Jordan–Wigner string as shown in the sketch.

easily solve this problem. It can be shown that all terms in Equation (5.35) commute and therefore generate a stabilizer group. Now we can multiply them to

$$\Omega_S = \overset{1\;2}{\begin{matrix} Y\,Y \\ Z\,Z \end{matrix}} \cdot \overset{2\;3}{\begin{matrix} Z\,Z \\ X\,X \end{matrix}} \cdot \overset{3\;4}{\begin{matrix} Y\,Y \\ Z\,Z \end{matrix}} \cdot \overset{4\;5}{\begin{matrix} Z\,Z \\ X\,X \end{matrix}} \cdots = \begin{matrix} Y\,X \cdots X\,Y \\ Z\,Y \cdots Y\,Z \end{matrix} \tag{5.36a}$$

$$\Omega_P = \overset{1\;2}{\begin{matrix} X\,X \\ Z\,Z \end{matrix}} \cdot \overset{1\;2}{\begin{matrix} Y\,Y \\ Z\,Z \end{matrix}} \cdot \overset{2\;3}{\begin{matrix} Z\,Z \\ X\,X \end{matrix}} \cdot \overset{2\;3}{\begin{matrix} Z\,Z \\ Y\,Y \end{matrix}} \cdots = \begin{matrix} Z\,Z \cdots Z\,Z \\ 1\,Z \cdots Z\,1 \end{matrix}, \tag{5.36b}$$

which allows us to find the action of the symmetries on the ground states

$$S' = S \cdot \Omega_S = \begin{matrix} Z\,1 \cdots 1\,Z \\ X\,1 \cdots 1\,X \end{matrix} \circ K \tag{5.37a}$$

$$P' = P \cdot \Omega_P = \begin{matrix} 1\,1 \cdots 1\,1 \\ Z\,1 \cdots 1\,Z \end{matrix}. \tag{5.37b}$$

On the edges of the chain the symmetries act as

$$S_{\text{left}} = S_{\text{right}} = \begin{matrix} Z \\ X \end{matrix} \circ K \tag{5.38a}$$

$$P_{\text{left}} = P_{\text{right}} = \begin{matrix} 1 \\ Z \end{matrix}. \tag{5.38b}$$

Those operators anticommute and $S^2_{\text{left}} = S^2_{\text{right}} = \mathbb{1}$. This shows us, that the system is again in the bosonic phase $[\chi_2]$ as expected.

We can also consider two topological chains as shown in Figure 5.4. This system has the bosonic Hamiltonian

$$H = \overset{2\;3}{\begin{matrix} X\,X \\ Z\,Z \end{matrix}} + \overset{2\;3}{\begin{matrix} Y\,Y \\ Z\,Z \end{matrix}} + \overset{2\;3}{\begin{matrix} 1\,1 \\ X\,X \end{matrix}} + \overset{2\;3}{\begin{matrix} 1\,1 \\ Y\,Y \end{matrix}} + \cdots \tag{5.39}$$

which only consists of commuting terms. The following calculations are exactly the same as for Figure 5.1 but the first and last column of the chain are left out in the Hamiltonian.

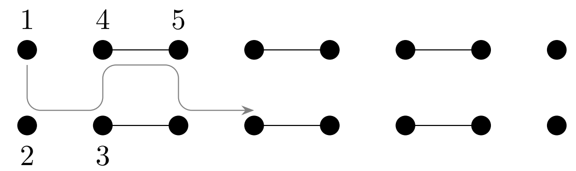

Figure 5.4.: Two fermionic SSH chains are stacked on top of each other. Both chains are in the topological state. We choose the Jordan–Wigner string as shown in the sketch.

Therefore we can directly guess the symmetry actions

$$S' = \begin{matrix} X\,1 \cdots 1\,X \\ Y\,1 \cdots 1\,Y \end{matrix} \circ K \tag{5.40a}$$

$$P' = \begin{matrix} Z\,1 \cdots 1\,Z \\ Z\,1 \cdots 1\,Z \end{matrix}. \tag{5.40b}$$

On the edges of the chain, the symmetries act as

$$S_{\text{left}} = S_{\text{right}} = \begin{matrix} X \\ Y \end{matrix} \circ K \tag{5.41a}$$

$$P_{\text{left}} = P_{\text{right}} = \begin{matrix} Z \\ Z \end{matrix}. \tag{5.41b}$$

These operators commute and $S_{\text{left}}^2 = S_{\text{right}}^2 = -\mathbb{1}$. Therefore the system in Figure 5.4 corresponds to the bosonic phase $[\chi_3]$.

Now we were able to show that two SSH chains in different configurations can be translated into bosonic systems in the phases $[\chi_1]$, $[\chi_2]$ and $[\chi_3]$.[7] This matches the observation made in Subsection 2.2.1, that two fermionic SSH chains can realize three different fermionic phases. We are not able to realize the $[\chi_4]$ phase in this fermionic system.

If we want to find all four fermionic and bosonic phases, we need three chains. We use the system and the Jordan–Wigner string shown in Figure 5.5. There are $2^3 = 8$ different possible configurations for three SSH chains. Therefore we will not write down the full calculations here.

We use the sublattice symmetry representation

$$\begin{aligned}\hat{S}_{\text{F}} = \prod_{i=1}^{L} \Big[&\left(\hat{c}_{6i-5} - \hat{c}_{6i-5}^\dagger\right) \left(\hat{c}_{6i} - \hat{c}_{6i}^\dagger\right) \left(\hat{c}_{6i-4} - \hat{c}_{6i-4}^\dagger\right) \\ &\cdot \left(\hat{c}_{6i-1} + \hat{c}_{6i-1}^\dagger\right) \left(\hat{c}_{6i-3} - \hat{c}_{6i-3}^\dagger\right) \left(\hat{c}_{6i-2} + \hat{c}_{6i-2}^\dagger\right) \Big] \circ K \end{aligned} \tag{5.42}$$

[7] This result might look different if we had chosen a different Jordan–Wigner string or a different symmetry representation $\hat{S}_{\text{F}}$ in Equation (5.22). Then we can in principle find different non-trivial bosonic phases. The qualitative result would still have been the same and we could obviously still only realize three bosonic phases.

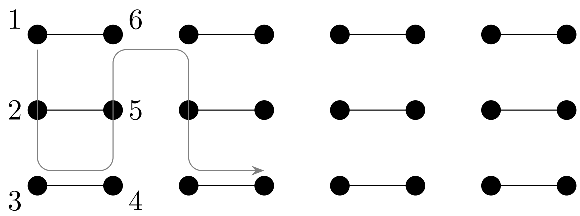

Figure 5.5.: Sketch of three fermionic SSH chains stacked on top of each other. We use the Jordan–Wigner string shown in this image to transform the system into a system of hard-core bosons.

Fermionic Phase	Corresponding Bosonic Phase
0	$[\chi_1]$
1	$[\chi_2]$
2	$[\chi_4]$
3	$[\chi_3]$

Table 5.1.: Comparison of the fermionic and corresponding bosonic phases in the system shown in Figure 5.5. The fermionic phases are simply classified by the number of topological chains in the system. The corresponding bosonic phases can easily be obtained via the stabilizer formalism.

which translates to the bosonic operator

$$S = \rho_{\mathrm{JW}}\left(\hat{S}_{\mathrm{F}}\right) = \begin{matrix} X \cdots X \\ Y \cdots Y \\ X \cdots X \end{matrix} \circ K. \tag{5.43}$$

The bosonic parity symmetry representations is as always

$$P = \begin{matrix} Z \cdots Z \\ Z \cdots Z \\ Z \cdots Z \end{matrix}. \tag{5.44}$$

Now we can again apply the stabilizer formalism.[8] The results are shown in Table 5.1. Indeed we can see that the four fermionic phases are translated to four bosonic phases. Still, we need three fermionic chains but we could realize four bosonic phases with just two bosonic SSH chains. The problem is that these bosonic chains would not translate to fermionic SSH chains (just like the fermionic SSH chains do not translate to bosonic SSH chains) but to more complicated interacting fermionic systems.

[8]It can be shown that for all configurations of chains, the terms of the Hamiltonian commute.

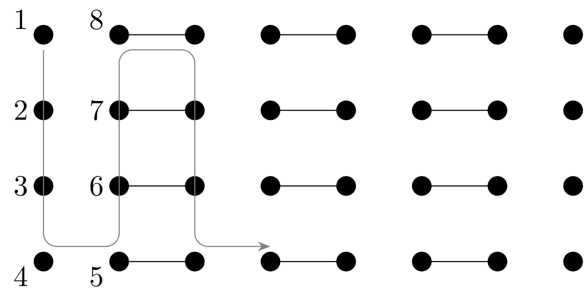

Figure 5.6.: Sketch of four fermionic SSH chains stacked on top of each other. We use the Jordan–Wigner string shown in this image to transform the system into a system of hard-core bosons.

5.5. Breakdown of Fermionic Phases with Stabilizers

In Section 2.3 we discussed the breakdown of the classification of fermionic phases to $\mathbb{Z}_4$ as we introduced interactions. Even though we already gave a proof for this, we briefly want to show a second proof using stabilizer codes.

Consider four fermionic SSH chains in the topological state (see Figure 5.6). We can now translate this system into a system of hard-core bosons. Using the stabilizer formalism we will show that the bosonic system (which always includes interactions) is in the trivial state $[\chi_1]$. Then, as we now have a better understanding of the connection between fermionic and bosonic phases, we know that also the fermionic system is in its trivial phase. We choose the symmetries as before which gives us the operators

$$S = \begin{matrix} X \cdots X \\ Y \cdots Y \\ X \cdots X \\ Y \cdots Y \end{matrix} \circ K \tag{5.45a}$$

$$P = \begin{matrix} Z \cdots Z \\ Z \cdots Z \\ Z \cdots Z \\ Z \cdots Z \end{matrix}. \tag{5.45b}$$

The Hamiltonian of the system is

$$H = \begin{matrix} {\scriptstyle 2\ 3} \\ X\,X \\ 1\ 1 \\ 1\ 1 \\ 1\ 1 \end{matrix} + \begin{matrix} {\scriptstyle 2\ 3} \\ Y\,Y \\ 1\ 1 \\ 1\ 1 \\ 1\ 1 \end{matrix} + \begin{matrix} {\scriptstyle 2\ 3} \\ Z\,Z \\ X\,X \\ 1\ 1 \\ 1\ 1 \end{matrix} + \begin{matrix} {\scriptstyle 2\ 3} \\ Z\,Z \\ Y\,Y \\ 1\ 1 \\ 1\ 1 \end{matrix} + \begin{matrix} {\scriptstyle 2\ 3} \\ Z\,Z \\ Z\,Z \\ X\,X \\ 1\ 1 \end{matrix} + \begin{matrix} {\scriptstyle 2\ 3} \\ Z\,Z \\ Z\,Z \\ Y\,Y \\ 1\ 1 \end{matrix} + \begin{matrix} {\scriptstyle 2\ 3} \\ Z\,Z \\ Z\,Z \\ Z\,Z \\ X\,X \end{matrix} + \begin{matrix} {\scriptstyle 2\ 3} \\ Z\,Z \\ Z\,Z \\ Z\,Z \\ Y\,Y \end{matrix} + \cdots \tag{5.46}$$

and consists of commuting terms. Now it is easy to show that the symmetry operators act on the ground states as

$$S' = \begin{matrix} X\,1\cdots 1\,X \\ Y\,1\cdots 1\,Y \\ X\,1\cdots 1\,X \\ Y\,1\cdots 1\,Y \end{matrix} \circ K \tag{5.47a}$$

$$P' = \begin{matrix} Z\,1\cdots 1\,Z \\ Z\,1\cdots 1\,Z \\ Z\,1\cdots 1\,Z \\ Z\,1\cdots 1\,Z \end{matrix}. \tag{5.47b}$$

These operators act on the edges as

$$S_{\text{left}} = S_{\text{right}} = \begin{matrix} X \\ Y \\ X \\ Y \end{matrix} \circ K \tag{5.48a}$$

$$P_{\text{left}} = P_{\text{right}} = \begin{matrix} Z \\ Z \\ Z \\ Z \end{matrix}. \tag{5.48b}$$

It is straightforward to see that both operators commute and the sublattice operator squares to one. This shows us that the system is in the phase $[\chi_1]$.

These calculations are in direct correspondence to the work by Kitaev in [9]. In this paper, the breakdown of fermionic phases in stacked Majorana chains to $\mathbb{Z}_8$ was discussed. With the bosonic systems corresponding to fermionic SSH chains we can prove a breakdown to $\mathbb{Z}_4$ which we already found in Section 2.3. Because of the special nature of the Majorana chains, these systems allow the existence of intermediate phases. These cannot exist in corresponding bosonic systems because they translate to non-localities. We discuss this in more detail in Appendix C.

6. Conclusion

In this thesis, we discussed different aspects of symmetry protected topological phases. Thereby we were able to establish a deeper understanding of the physical mechanisms which are the essential to the topological phases protected by abstract cohomology theory. We also used SSH chains as concrete examples. We covered fermionic phases as well as bosonic phases.

In Chapter 1, we gave an introduction to the classification of symmetry protected topological phases of non-interacting fermionic phases. We introduced symmetries and gave a special emphasis on the winding number, which is a topological invariant of the phases.

With Chapter 2 we introduced the fermionic SSH chain. We showed that with stacked SSH chains, one can realize an arbitrary number of phases. Following the work of Kitaev [9], we proved that with the introduction of interactions, the fermionic classification of phases in stacked SSH chains breaks down to $\mathbb{Z}_4$. Using stacked SSH chains, we showed how these four phases can be realized.

In Chapter 3, we introduced the Jordan–Wigner transformation to translate fermionic systems into systems of hard-core bosons. As the classification of fermionic phases via the winding number relies on non-interacting systems, this formalism cannot be applied for interacting bosons. Instead, we showed how the cohomology theory can be used to establish a classification of bosonic phases. To this end, we gave an introduction to matrix-product states.

The cohomology theory allows predictions of the maximum number of realizable phases in a system for given symmetries. In Chapter 4, we were able to show that the symmetry groups $\mathbb{Z}_2 \times \mathbb{Z}_2^T$ and $U(1) \times \mathbb{Z}_2^T$ each allow four non-equivalent projective symmetry representations with a $\mathbb{Z}_2^2$ group structure – which can directly be related to the existence of symmetry protected topological phases. For stacked SSH chains, we explicitly realized all those phases. Furthermore, we showed that using four SSH chains and the $D_2 \times \mathbb{Z}_2^T$ symmetry group, we can even realize 16 different phases with a $\mathbb{Z}_2^4$ structure.

The classification of bosonic symmetry protected topological phases in one dimension relies on the matrix-product state representation of the ground states in the system of consideration. As in some systems it can be very hard to find the explicit ground states analytically, in Chapter 5 we introduced another formalism for the classification of bosonic phases. It is based on the stabilizer formalism and the bulk-boundary correspondence. The stabilizer formalism can be used without knowledge of the ground states of a system. We applied it to compare fermionic and bosonic phases in stacked SSH chains.

Outlook

A few aspects of this thesis are not completely understood yet. Therefore, it would be interesting to do some future considerations following our work. Firstly, the stabilizer formalism is subtle when anti-unitary symmetries are involved. Further investigations on this topic could give deeper insights, especially when anti-unitarily realized symmetries are involved. Furthermore, one could do more general considerations on the comparison of fermionic and bosonic phases.

The systems we considered in this thesis are mostly very abstract and conceptual. Therefore, it would be interesting to search for actual physical realizations of the discussed systems. This includes the search for symmetries which are actually conserved in real systems and lead to the same classifications that we found in this thesis.

Appendices

A. Gapped transitions in two SSH chains

We want to show, that the path constructed in Equation (2.35) is actually gapped. To do so, we will investigate the Hamiltonians of the cells shown in Figure 2.10.

We will start with the cell of four sites. In the path this cell has the Hamiltonian

$$\begin{aligned}\hat{H}(\lambda) = &(1-\lambda)\left(\hat{c}_1^\dagger \hat{c}_4 + \hat{c}_4^\dagger \hat{c}_1 + \hat{c}_2^\dagger \hat{c}_3 + \hat{c}_3^\dagger \hat{c}_2\right) \\ &+ \lambda\left(\hat{c}_1^\dagger \hat{c}_2 + \hat{c}_2^\dagger \hat{c}_1 - \hat{c}_4^\dagger \hat{c}_3 - \hat{c}_3^\dagger \hat{c}_4\right).\end{aligned} \tag{A.1}$$

Using Pauli matrices as representations of the operators, we diagonalize this 16-dimensional Hamiltonian analytically and find the eigenvalues $\epsilon_1 = 0$ (six-fold degenerate), $\epsilon_{2,3} = \pm\sqrt{1-2\lambda+2\lambda^2}$ (three-fold degenerate) and $\epsilon_{4,5} = \pm 2\sqrt{1-2\lambda+2\lambda^2}$ (non-degenerate). The energies can be seen in Figure A.1. The band gap is the energy difference between the lowest and the second lowest energy. As can be seen, the gap is never closed.

The same holds for the eight-dimensional system of three sites in Figure 2.11, which has the Hamiltonian

$$\hat{H}(\lambda) = (1-\lambda)\left(\hat{c}_1^\dagger \hat{c}_2 + \hat{c}_2^\dagger \hat{c}_1\right) + \lambda\left(\hat{c}_2^\dagger \hat{c}_3 + \hat{c}_3^\dagger \hat{c}_2\right). \tag{A.2}$$

The eigenvalues of this Hamiltonian are $\epsilon_1 = 0$ (four-fold degenerate) and $\epsilon_{2,3} = \pm\sqrt{1-2\lambda+2\lambda^2}$ (two-fold degenerate). These energies are plotted in Figure A.2. Besides of the degeneracy of the ground state (which is due to the symmetry protected edge state of the system) the band gap remains open.

These calculations prove, that the path in Equation (2.35) is gapped.

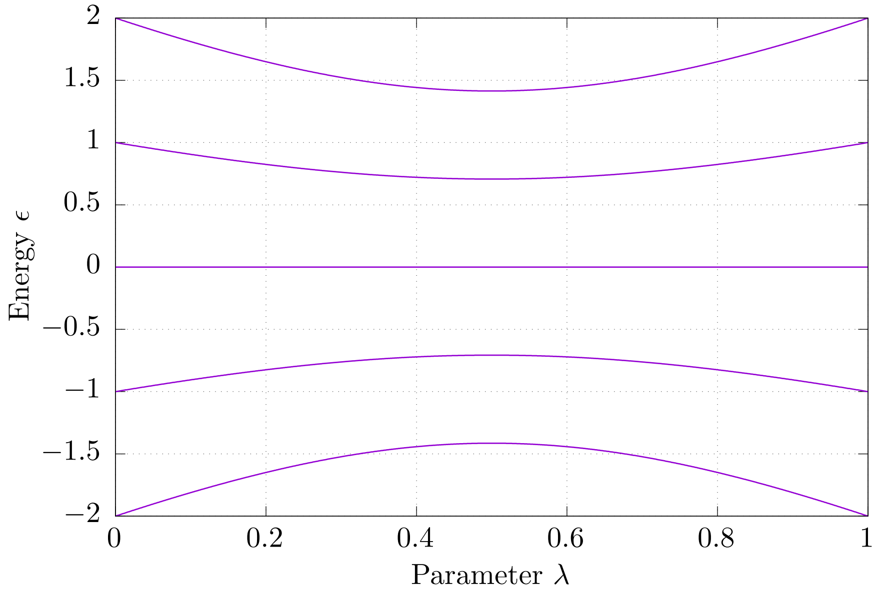

Figure A.1.: Eigenenergies of the cell of four sites for the path of Equation (A.1). As we can see, the gap stays open along this path.

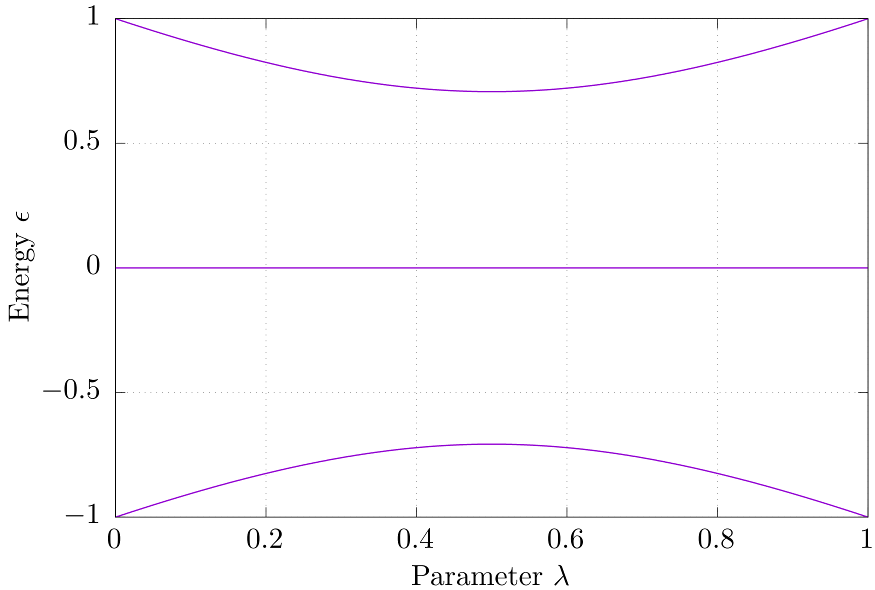

Figure A.2.: Eigenenergies of the cell of three sites for the path of Equation (A.2). As we can see, the gap stays open along this path. The ground state has a two-fold degeneracy which corresponds to the protected edge state of the system in Figure 2.10.

B. More on the Classification of Bosonic Phases

We discussed the classification of bosonic symmetry protected topological phases in Section 3.3. Here, we want to give some further incomplete insights on this classification. This mainly concerns the derivation of Equation (3.23) which is highly non-trivial. All calculations are performed in a translational invariant closed chain with periodic boundaries.

B.1. First Considerations

First of all, we want to consider Equation (3.23) and prove that it implies the ground state of the system being symmetric under our symmetry action. This does not prove this equation, but it gives a first sense of how it works.

A state $|\psi\rangle$ is symmetric under a symmetry representation $\rho(g)$ with $g \in G$ if

$$\rho(g) |\psi\rangle = \gamma(g) |\psi\rangle . \tag{B.1}$$

This means that the state does not change under the symmetry action, except for a global phase $\gamma(g)$ which itself is a one-dimensional representation of the symmetry group G. As in Equation (3.20), the symmetry ρ is represented on each site by π.

Let us now consider the left side of Equation (B.1) and transform it by inserting an MPS for $|\psi\rangle$:

$$\rho(g) |\psi\rangle = \sum_{\cdots i_j \cdots} \mathrm{Tr}\big[\cdots A_{i_j} \cdots\big] \cdots \pi(g) \cdots |\cdots i_j \cdots\rangle \tag{B.2a}$$

$$= \sum_{\cdots i_j \cdots} \mathrm{Tr}\big[\cdots A_{i_j} \cdots\big] \cdots \sum_{v} (\pi(g))_{i_j,v} \cdots |\cdots v \cdots\rangle \tag{B.2b}$$

$$= \sum_{\cdots i_j \cdots} \mathrm{Tr}\left[\cdots \sum_{v} (\pi(g))_{i_j,v} A_{i_j} \cdots\right] |\cdots v \cdots\rangle \tag{B.2c}$$

$$= \sum_{\cdots i_j \cdots} \sum_{\cdots v \cdots} \mathrm{Tr}\Big[\cdots \Big((\pi(g))_{i_j,v} A_{i_j}\Big) \cdots\Big] |\cdots v \cdots\rangle \tag{B.2d}$$

$$= \sum_{\cdots v \cdots} \mathrm{Tr}\left[\cdots \left(\sum_{i_j} (\pi(g))_{i_j,v} A_{i_j}\right) \cdots\right] |\cdots v \cdots\rangle \tag{B.2e}$$

Now we look at the right side of Equation (B.1) and write the phase $\gamma(g) = \prod_i \gamma_i(g)$. We also insert an invertible matrix $V(g)$ of size $D \times D$:

$$\gamma(g)\,|\psi\rangle = \gamma(g) \sum_{\cdots} \mathrm{Tr}\big[\cdots A_{i_j} \cdots\big]\,|\cdots i_j \cdots\rangle \tag{B.3a}$$

$$= \sum_{\cdots} \mathrm{Tr}\big[\cdots \gamma_j(g)\,A_{i_j} \cdots\big]\,|\cdots i_j \cdots\rangle \tag{B.3b}$$

$$= \sum_{\cdots} \mathrm{Tr}\big[\cdots \big(\gamma_j(g)\,V^{-1}(g) \cdot A_{i_j} \cdot V(g)\big) \cdots\big]\,|\cdots i_j \cdots\rangle\,. \tag{B.3c}$$

If we compare the traces in Equation (B.2e) and Equation (B.3c) we see that Equation (B.1) will always be fulfilled if Equation (3.23) holds.

B.2. Double Tensor of the MPS

The following remarks are based on the works [23, 21, 26, 22]. To develop a classification of bosonic symmetry protected topological phases based on the ground state $|\psi\rangle$, we first need to understand how two states in different phases differ from each other.

Let $A_{i,\alpha\beta}$ be a matrix of the MPS of $|\psi\rangle$. The virtual indices α and β are the actual indices of the matrix elements. The physical index i denotes the state of the unit cell corresponding to $A_{i,\alpha\beta}$. We define the double tensor

$$\mathbb{E}_{\alpha\gamma,\beta\chi} = \sum_i A_{i,\alpha\beta}\,(A_{i,\gamma\chi})^* \tag{B.4}$$

which uniquely determines the ground state up to a local change of basis on each unit cell [23, 25, 21, 30].

Usually we define our phases as an equivalence relation of gapped Hamiltonians. An equivalent definition is the following [23, 6, 31]: Two ground states belong to the same phase if there is a local unitary transformation connecting them, i.e. they share the same double tensor $\mathbb{E}$.

The tensor $\mathbb{E}$ has some important properties. We require the ground state of our chain to be short-range correlated. This is only fulfilled if the tensor $\mathbb{E}$ has a largest non-degenerate eigenvalue[1] [23, 25], which we can set to 1 (we discuss this in Section B.4). This requirement is equivalent to the injectivity condition mentioned in Section 3.3. It states that for a large enough number n, the set of matrices $A_{i_1} \cdots A_{i_n}$ on consecutive sites for all $i_j \in \{1, \cdots, d\}$ span the space of all $D \times D$ matrices. Every MPS that satisfies the injectivity condition is a unique gapped ground state of a local Hamiltonian [23, 25, 20, 21].

We also want to introduce the tensor

$$\mathbb{E}[O]_{\alpha\gamma,\beta\chi} = \sum_{ij} O_{ij} A_{i,\alpha\beta} A^*_{j,\gamma\chi} \tag{B.5}$$

[1] In the following, we will talk about eigenvectors which are actually matrices. We interpret them as vectors with double indices.

for any operator O. This will be useful later on.

Instead of the double tensor, we will also use the linear map

$$E(X) = \sum_i A_i X A_i^\dagger. \tag{B.6}$$

We see that this is directly related to Equation (B.4) because

$$[E(X)]_{\alpha\gamma} = \sum_{\beta\chi} \mathbb{E}_{\alpha\gamma,\beta\chi} X_{\beta\chi}. \tag{B.7}$$

Similarly we define the transfer map

$$E_O(X) = \sum_{ij} \langle i \,|\, O \,|\, j \rangle \, A_i X A_j^\dagger \tag{B.8}$$

which corresponds to Equation (B.5).

B.3. Transformation Behaviour of the MPS Matrices

We will now derive Equation (3.23)

$$\sum_i [\pi(g)]_{ij} \, A_i = \gamma(g) \, V^{-1}(g) \cdot A_j \cdot V(g) \, . \tag{B.9}$$

This will require some assumptions. We will follow the calculations in [22].

We assume:[2]

- The matrix $\mathbb{1}$ is the only eigenvector of E for the eigenvalue 1: $E(\mathbb{1}) = \mathbb{1}$. This implies $\sum_i A_i A_i^\dagger = \mathbb{1}$ (see [21]).
- There exists a diagonal, positive, invertible and unique matrix Λ, such that $\sum_i A_i^\dagger \Lambda A_i = \Lambda$ (see [21]).
- The largest non-degenerate eigenvalue of $E_\pi(X)$ is 1 for the local physical symmetry representation $\pi(g)$ on a unit cell.

Now we consider Equation (3.23). The physical symmetry representation $\pi(g)$ has a physical eigenbasis.[3] If we choose this basis for our physical indices, we find

$$\pi = \sum_j e^{\mathrm{i}\theta_j} \, |j\rangle \, \langle j| \tag{B.10a}$$

because symmetry operators are unitary and all eigenvalues take the form $\lambda_i = e^{\mathrm{i}\theta_i}$. Now Equation (3.23) takes the form

$$e^{\mathrm{i}\theta_j} A_j = \gamma V \cdot A_j \cdot V^{-1} \tag{B.11}$$

with the phase γ. In the following, we perform some isolated calculations which will be useful later.

[2] These assumptions seem to be the crux of the proof. To the best of my knowledge, at least the first two assumptions are related to the injectivity condition of the MPS.

[3] From now on, we will drop the g-dependence of the symmetry related operators.

B.3.1. Spectral Radius of the Transfer Map

The transfer map of the symmetry is

$$E_\pi(X) = \sum_j e^{i\theta_j} A_j X A_j^\dagger \tag{B.12}$$

as we use the eigenbasis of π. We will now prove that the spectral radius of this map is $\rho(E_\pi) \leq 1$.

Assume that the map $E_\pi(X)$ has an eigenvector V for the eigenvalue λ:

$$E_\pi(V) = \lambda V. \tag{B.13}$$

Then we get

$$\lambda V = \sum_j e^{i\theta_j} A_j V A_j^\dagger. \tag{B.14}$$

Multiply with $\Lambda V^\dagger$ on both sides, take the trace and then take the absolute value to get

$$\left|\lambda \operatorname{Tr}\left(V\Lambda V^\dagger\right)\right| = \left|\sum_j \operatorname{Tr}\left(e^{i\theta_j} A_j V A_j^\dagger \Lambda V^\dagger\right)\right|. \tag{B.15}$$

As we already defined Λ as an invertible diagonal matrix above, the square root $\Lambda^{1/2}$ exists and $\Lambda^{1/2} = \left(\Lambda^{1/2}\right)^\dagger$. Therefore, $\operatorname{Tr}\left(V\Lambda V^\dagger\right)$ is the squared Frobenius norm of $V\Lambda^{1/2}$ and therefore ≥ 0. This yields

$$\left|\lambda \operatorname{Tr}\left(V\Lambda V^\dagger\right)\right| = |\lambda| \operatorname{Tr}\left(V\Lambda V^\dagger\right). \tag{B.16}$$

We define

$$X_j = \Lambda^{\frac{1}{2}} A_j V^\dagger \tag{B.17a}$$

$$Y_j = e^{i\theta_j} \Lambda^{\frac{1}{2}} V^\dagger A_j \tag{B.17b}$$

to simplify Equation (B.15):

$$|\lambda| \operatorname{Tr}\left(V\Lambda V^\dagger\right) = \left|\sum_j \operatorname{Tr}\left(X_j^\dagger Y_j\right)\right|. \tag{B.18}$$

Using the Cauchy–Schwarz inequality, we can transform the right side to

$$\left|\sum_j \operatorname{Tr}\left(X_j^\dagger Y_j\right)\right| \leq \sqrt{\sum_j \operatorname{Tr}\left(X_j^\dagger X_j\right)} \cdot \sqrt{\sum_j \operatorname{Tr}\left(Y_j^\dagger Y_j\right)} \tag{B.19a}$$

$$= \sqrt{\sum_j \operatorname{Tr}\left(V A_j^\dagger \Lambda A_j V^\dagger\right)} \cdot \sqrt{\sum_j \operatorname{Tr}\left(A_j^\dagger V \Lambda V^\dagger A_j\right)} \tag{B.19b}$$

$$= \sqrt{\mathrm{Tr}\left(V\left[\sum_j A_j^\dagger \Lambda A_j\right]V^\dagger\right)} \cdot \sqrt{\mathrm{Tr}\left(\left[\sum_j A_j A_j^\dagger\right]V\Lambda V^\dagger\right)} \tag{B.19c}$$

$$= \sqrt{\mathrm{Tr}(V\Lambda V^\dagger)} \cdot \sqrt{\mathrm{Tr}(V\Lambda V^\dagger)} \tag{B.19d}$$

$$= \left|\mathrm{Tr}\left(V\Lambda V^\dagger\right)\right|. \tag{B.19e}$$

Here we used the assumptions from above. Going back to Equation (B.15), we can see that $|\lambda| \leq 1$. This proves that the spectral radius $\rho(E_\pi) \leq 1$.

We assumed that the map $E_\pi(X)$ has the largest non-degenerate eigenvalue 1. This implies that there exists an eigenvector V such that $E_\pi(V) = 1 \cdot V$ and the spectral radius is $\rho(E_\pi) = 1$. The spectral radius is one, if and only if the Cauchy–Schwarz inequality becomes an equality in Equation (B.19a). This happens if the vectors X_j and Y_j are parallel such that $Y_j = \gamma X_j$ for some factor γ.

B.3.2. More on the Proportionality Factor

The vectors X_j and Y_j are connected by the proportionality factor γ. We can insert the definitions of these vectors from Equation (B.17a) and Equation (B.17b):

$$Y_j = \gamma X_j \tag{B.20a}$$

$$e^{\mathrm{i}\theta_j}\Lambda^{\frac{1}{2}} V^\dagger A_j = \gamma \Lambda^{\frac{1}{2}} A_j V^\dagger \tag{B.20b}$$

$$e^{\mathrm{i}\theta_j} V^\dagger A_j = \gamma A_j V^\dagger. \tag{B.20c}$$

We multiply both sides with their adjoint:

$$V^\dagger A_j A_j^\dagger V = |\gamma|^2 A_j V^\dagger V A_j^\dagger. \tag{B.21}$$

Furthermore, we multiply Λ to both sides of the equation, take the sum over j and take the trace:

$$\sum_j \mathrm{Tr}\left(\Lambda V^\dagger A_j A_j^\dagger V\right) = |\gamma|^2 \sum_j \mathrm{Tr}\left(\Lambda A_j V^\dagger V A_j^\dagger\right) \tag{B.22a}$$

$$\mathrm{Tr}\left(\Lambda V^\dagger\left[\sum_j A_j A_j^\dagger\right]V\right) = |\gamma|^2 \,\mathrm{Tr}\left(\left[\sum_j A_j^\dagger \Lambda A_j\right]V^\dagger V\right) \tag{B.22b}$$

$$\mathrm{Tr}\left(\Lambda V^\dagger V\right) = |\gamma|^2 \,\mathrm{Tr}\left(\Lambda V^\dagger V\right) \tag{B.22c}$$

$$1 = |\gamma|^2. \tag{B.22d}$$

This proves that γ is a phase and $|\gamma| = 1$.

B.3.3. More on the Eigenvector

Now we prove that the eigenvector V is actually a unitary matrix. To do so, we calculate $E(VV^\dagger)$:

$$E\left(V^\dagger V\right) = \sum_i A_i V^\dagger V A_i^\dagger. \tag{B.23}$$

From Equation (B.20c), we know[4]

$$A_j V^\dagger = \gamma^{-1} e^{\mathrm{i}\theta_j} V^\dagger A_j \tag{B.24a}$$
$$V A_j^\dagger = \gamma e^{-\mathrm{i}\theta_j} A_j^\dagger V. \tag{B.24b}$$

This yields

$$E\left(V^\dagger V\right) = V^\dagger \left[\sum_i A_i A_i^\dagger\right] V = V^\dagger V. \tag{B.25}$$

The Vector $V^\dagger V$ is an eigenvector of the map E with the eigenvalue 1. Following our assumptions, $\mathbb{1}$ is the only eigenvector of E for the eigenvalue 1. Therefore $V^\dagger V = \mathbb{1}$ and V is a unitary matrix.

B.3.4. Assembling the Proof

Now we have all we need to prove Equation (3.23) under the assumptions we made above. We showed that Equation (B.20c) holds. Furthermore γ is a phase and V is a unitary matrix. Therefore we can rewrite this equation to

$$e^{\mathrm{i}\theta_j} = \gamma V A_j V^\dagger \tag{B.26}$$

which is exactly Equation (B.11) or Equation (3.23) in the eigenbasis of π.

B.4. Largest Eigenvalue of the Double Tensor

We will prove that the double tensor $\mathbb{E}_{\alpha\gamma,\beta\chi}$ has a non-degenerate largest eigenvalue which we can set to one. To do so, we will follow some calculations in [23]. We will divide the proof into smaller parts and assemble them in the end.

B.4.1. Norm of the Ground State

We calculate the norm of a ground state $|\psi\rangle$ which is represented as an MPS:

$$\sum_{i_1 \cdots i_N} \mathrm{Tr}(A_{i_1} \cdots A_{i_N}) \, |i_1 \cdots i_N\rangle \,. \tag{B.27}$$

We find

[4]For the second equation, we take the hermitean conjugate on both sides.

$$
\begin{aligned}
\langle\psi\,|\,\psi\rangle &= \sum_{i_1\cdots i_N} \langle i_1\cdots i_N|\,\mathrm{Tr}\big(A^*_{i_1}\cdots A^*_{i_N}\big) \sum_{j_1\cdots j_N} \mathrm{Tr}\big(A_{j_1}\cdots A_{j_N}\big)\,|j_1\cdots j_N\rangle && \text{(B.28a)}\\
&= \sum_{i_1\cdots i_N} \mathrm{Tr}\big(A^*_{i_1}\cdots A^*_{i_N}\big)\,\mathrm{Tr}\big(A_{i_1}\cdots A_{i_N}\big) && \text{(B.28b)}\\
&= \sum_{i_1\cdots i_N} \mathrm{Tr}\big(\big[A_{i_1}\otimes A^*_{i_1}\big]\cdots\big[A_{i_N}\otimes A^*_{i_1}\big]\big) && \text{(B.28c)}\\
&= \mathrm{Tr}\left[\sum_{i_1}\big[A_{i_1}\otimes A^*_{i_1}\big]\cdots\sum_{i_N}\big[A_{i_N}\otimes A^*_{i_1}\big]\right] && \text{(B.28d)}\\
&= \mathrm{Tr}\big[\mathbb{E}^N\big]\,. && \text{(B.28e)}
\end{aligned}
$$

This connects the norm of a state to the double tensor $\mathbb{E}$. Now we scale the double tensor such that the largest eigenvalue is 1. This will only affect the norm of the MPS.

The trace is invariant under the diagonalization of $\mathbb{E}$. Therefore $\mathrm{Tr}\big[\mathbb{E}^N\big] = \sum_i \lambda_i^N$ for the eigenvalues λ_i of the double tensor. We can see that in the thermodynamic limit ($N \to \infty$) all terms $|\lambda| < 1$ will vanish. Only the eigenvalues we set to one survive. Then the norm of the ground state becomes the number of eigenvalues which are one.

B.4.2. Operator Expectation Value

Consider a local operator O acting on any site k of our system. We calculate the expectation value of O in the ground state:

$$
\begin{aligned}
\langle O\rangle &= \frac{\langle\psi\,|\,O\,|\,\psi\rangle}{\langle\psi\,|\,\psi\rangle} && \text{(B.29a)}\\
&= \frac{\sum\limits_{i_1\cdots i_N}\sum\limits_{j_1\cdots j_N} \langle i_1\cdots i_N|\,\mathrm{Tr}\big(A^*_{i_1}\cdots A^*_{i_N}\big)\,O\,\mathrm{Tr}\big(A_{i_1}\cdots A_{i_N}\big)\,|j_1\cdots j_N\rangle}{\langle\psi\,|\,\psi\rangle} && \text{(B.29b)}\\
&= \frac{\sum\limits_{i_1\cdots i_{k-1}}\sum\limits_{i_k j_k}\sum\limits_{i_{k+1}\cdots i_N} \mathrm{Tr}\Big[\big(A_{i_1}\otimes A^*_{i_1}\big)\cdots O_{i_k j_k}\Big(A_{i_k}\otimes A^*_{j_k}\Big)\cdots\big(A_{i_N}\otimes A^*_{i_N}\big)\Big]}{\langle\psi\,|\,\psi\rangle} && \text{(B.29c)}\\
&= \frac{\mathrm{Tr}\big[\mathbb{E}^{N-1}\mathbb{E}[O]\big]}{\mathrm{Tr}[\mathbb{E}^N]}. && \text{(B.29d)}
\end{aligned}
$$

B.4.3. Correlation Function

Now consider two local operators O_1 and O_2 which act on two different sites i and $j = i+L+1$, such that there are L sites inbetween them. The correlation for these operators can be calculated by $\langle O_1 O_2\rangle - \langle O_1\rangle\langle O_2\rangle$. Analogously to the previous calculations we can express it via the double tensor:

$$
\langle O_1 O_2\rangle - \langle O_1\rangle\langle O_2\rangle = \frac{\mathrm{Tr}\big[\mathbb{E}^{N-L-2}\mathbb{E}[O_1]\,\mathbb{E}^L\mathbb{E}[O_2]\big]}{\mathrm{Tr}[\mathbb{E}^N]} - \frac{\mathrm{Tr}\big[\mathbb{E}^{N-1}\mathbb{E}[O_1]\big]\,\mathrm{Tr}\big[\mathbb{E}^{N-1}\mathbb{E}[O_2]\big]}{\mathrm{Tr}^2[\mathbb{E}^N]}. \qquad \text{(B.30)}
$$

B.4.4. Jordan Normal Form

Let A be a quadratic $D \times D$ matrix. Any matrix of that form is similar to a block diagonal matrix J which means there exists a Q such that $J = Q^{-1}AQ$. This block diagonal $D \times D$ matrix

$$J = \begin{pmatrix} J_1 & & \\ & \ddots & \\ & & J_k \end{pmatrix} \tag{B.31}$$

can be always chosen such that each block J_i has the form

$$J_i = \begin{pmatrix} \lambda_i & 1 & & \\ & \lambda_i & \ddots & \\ & & \ddots & 1 \\ & & & \lambda_i \end{pmatrix}. \tag{B.32}$$

Then J is called the Jordan normal form of A. The elements λ are the eigenvalues of the matrix A. The number of blocks for a single eigenvalue λ_i is its geometric multiplicity. The sum of all sizes of blocks corresponding to one value λ_i is the algebraic multiplicity of the eigenvalue.[5]

Now we bring the double tensor in its Jordan normal form

$$\tilde{\mathbb{E}} = \sum_\lambda \lambda P_\lambda + R_\lambda \tag{B.33}$$

with the block matrices P_λ and R_λ. The block P_λ is just the diagonal part

$$P_\lambda = \begin{pmatrix} \ddots & & & & & & \\ & 0 & & & & & \\ & & 1 & & & & \\ & & & \ddots & & & \\ & & & & 1 & & \\ & & & & & 0 & \\ & & & & & & \ddots \end{pmatrix} \tag{B.34}$$

[5] If a matrix is diagonalizable, the geometric and algebraic multiplicities of all eigenvalues are equal and all Jordan blocks have the size one.

and R_λ is the nilpotent part

$$P_\lambda = \begin{pmatrix} \ddots & & & & & & & \\ & 0 & 0 & & & & & \\ & & 0 & 1 & & & & \\ & & & \ddots & \ddots & & & \\ & & & & \ddots & 1 & & \\ & & & & & 0 & 0 & \\ & & & & & & 0 & \\ & & & & & & & \ddots \end{pmatrix} . \tag{B.35}$$

We bring $\mathbb{E}$ into the Jordan normal form by a basis transformation, but this will not change the trace.

B.4.5. Assembling the Proof

From Subsection B.4.1 we know that we can rescale the double tensor such that its largest eigenvalues live on the complex unit circle ($|\lambda| = 1$). Now we consider the expectation value of an operator in the thermodynamic limit and insert the Jordan normal form. To begin with, we assume that all eigenvalues λ_i with $|\lambda_i| = 1$ are $\lambda_i = 1$ and that these eigenvalues have the geometric multiplicity 1. Then there is only one block in the Jordan normal form which survives:[6]

$$\lim_{N\to\infty} \langle O \rangle = \lim_{N\to\infty} \frac{\mathrm{Tr}\left[\mathbb{E}^{N-1}\mathbb{E}[O]\right]}{\mathrm{Tr}[\mathbb{E}^N]} \tag{B.36a}$$

$$= \lim_{N\to\infty} \frac{\mathrm{Tr}\left[(P_1 + R_1)^{N-1}\,\tilde{\mathbb{E}}[O]\right]}{\mathrm{Tr}\left[(P_1 + R_1)^N\right]}. \tag{B.36b}$$

All Jordan blocks for smaller eigenvalues vanish in the thermodynamic limit. The denominator $\mathrm{Tr}\left[(P_1 + R_1)^N\right]$ is simply a fixed number, as all nilpotent parts vanish in the trace. This does not necessarily hold for the numerator $\mathrm{Tr}\left[(P_1 + R_1)^{N-1}\,\tilde{\mathbb{E}}[O]\right]$. If $\mathrm{Tr}\left[R_1\tilde{\mathbb{E}}[O]\right] \neq 0$, the denominator (and therefore the expectation value of O) will diverge in the thermodynamic limit.[7] The expectation value of *all* physical local operators has to be finite, therefore $R_1 = 0$ must be fulfilled and the algebraic multiplicity is one.

We can perform this calculation for more blocks (higher geometric multiplicities) with $|\lambda_i| = 1$ and will find that all those blocks have to be one-dimensional.

[6] We call $\tilde{\mathbb{E}}[O] = Q^{-1}\mathbb{E}[O]\,Q$.

[7] This is simply because $(P_1 + R_1)^{N-1} = P_1 + (N-1)R_1 + \cdots$ and $(N-1)$ diverges.

Now we consider the correlation function:

$$\begin{aligned}\langle O_1 O_2\rangle - \langle O_1\rangle\langle O_2\rangle =& \frac{\mathrm{Tr}\left[\mathbb{E}^{N-L-2}\mathbb{E}[O_1]\,\mathbb{E}^L\mathbb{E}[O_2]\right]}{\mathrm{Tr}[\mathbb{E}^N]} \\ &- \frac{\mathrm{Tr}\left[\mathbb{E}^{N-1}\mathbb{E}[O_1]\right]\mathrm{Tr}\left[\mathbb{E}^{N-1}\mathbb{E}[O_2]\right]}{\mathrm{Tr}^2[\mathbb{E}^N]} \end{aligned} \tag{B.37a}$$

$$\begin{aligned} =& \frac{\mathrm{Tr}\left[\left(\sum_\lambda \lambda P_\lambda + R_\lambda\right)^{N-L-2}\tilde{\mathbb{E}}[O_1]\left(\sum_\lambda \lambda P_\lambda + R_\lambda\right)^{L}\tilde{\mathbb{E}}[O_2]\right]}{\mathrm{Tr}[\mathbb{E}^N]} \\ &- \frac{\mathrm{Tr}\left[\left(\sum_\lambda \lambda P_\lambda + R_\lambda\right)^{N-1}\tilde{\mathbb{E}}[O_1]\right]\mathrm{Tr}\left[\left(\sum_\lambda \lambda P_\lambda + R_\lambda\right)^{N-1}\tilde{\mathbb{E}}[O_2]\right]}{\mathrm{Tr}^2[\mathbb{E}^N]}. \end{aligned} \tag{B.37b}$$

Now we assume that all eigenvalues $|\lambda_i| = 1$ are actually one ($\lambda_i = 1$) and we conclude them all in the matrices $\tilde{P}_1$ and $\tilde{R}_1$, while still $\tilde{R}_1 = 0$.[8] Then by performing the limes $N \to \infty$, we find

$$= \frac{\mathrm{Tr}\left[\tilde{P}_1\tilde{\mathbb{E}}[O_1]\left(\sum_\lambda \lambda P_\lambda + R_\lambda\right)^{L}\tilde{\mathbb{E}}[O_2]\right]}{\tilde{P}_1} - \frac{\mathrm{Tr}\left[\tilde{P}_1\tilde{\mathbb{E}}[O_1]\right]\mathrm{Tr}\left[\tilde{P}_1\tilde{\mathbb{E}}[O_2]\right]}{\mathrm{Tr}^2\left[\tilde{P}_1\right]}. \tag{B.38}$$

We can now increase the distance $L \to \infty$ in first order:

$$= \frac{\mathrm{Tr}\left[\tilde{P}_1\tilde{\mathbb{E}}[O_1]\,\tilde{P}_1\tilde{\mathbb{E}}[O_2]\right]}{\tilde{P}_1} - \frac{\mathrm{Tr}\left[\tilde{P}_1\tilde{\mathbb{E}}[O_1]\right]\mathrm{Tr}\left[\tilde{P}_1\tilde{\mathbb{E}}[O_2]\right]}{\mathrm{Tr}^2\left[\tilde{P}_1\right]}. \tag{B.39}$$

If now $\tilde{P}_1$ is only one-dimensional (has only one non-zero diagonal element), the first term decouples both operators and becomes equal to the second term, leading to

$$\lim_{L\to\infty} \langle O_1 O_2\rangle - \langle O_1\rangle\langle O_2\rangle = 0. \tag{B.40}$$

The second order decays exponentially in L.

On the other hand, if $\tilde{P}_1$ has more than one non-zero element, this argument does not apply any more and the correlation stays finite at large distances. This violates our physical requirement of the system being short-range correlated. Therefore $\tilde{P}_1$ must be one-dimensional and the largest eigenvalue 1 is unique.

As we made a few assumptions above, we will now generalize this proof. We don't immediately find a reason for all eigenvalues of $\mathbb{E}$ to be real and ≥ 0. What happens if we have complex eigenvalues?

First of all this is not an issue for all $|\lambda| < 1$, since these terms still vanish in the thermodynamic limit. For the eigenvalues $|\lambda| = 1$, this is more complicated.[9] We can

[8] This way the number of diagonal elements of $\tilde{P}_1$ is the geometrical multiplicity.

[9] Remember that the sum of all largest eigenvalues must be a positive real number such that the norm $\langle\psi\,|\,\psi\rangle > 0$ (see Equation (B.29d)).

store the phases of the largest eigenvalues in the diagonal elements of $\tilde{P}_1$. This does not change the proof for $\tilde{R}_1 = 0$, but we need to reconsider the calculation for the correlation function.

Consider the case of that P_1 being one-dimensional. Then the only largest eigenvalue has to be one (such that $\langle \psi \mid \psi \rangle > 0$) and the proof holds. In the case of a more dimensional P_1, Equation (B.39) will become more complicated but will still generally give a finite value and not vanish. Therefore the proof holds in all cases and the double tensor $\mathbb{E}$ has a non-degenerate largest eigenvalue 1.

B.4.6. Interpretation

The interesting part about this proof is that it does not require any artificial assumptions for $\mathbb{E}$. The only requirements are that the norm of the ground state is positive and all correlations vanish at large distances. Therefore the fact that the double tensor has a largest non-degenerate eigenvalue is a purely physical result and will always hold for our systems.

C. Phases in Majorana Chains

As we elaborated in Section 2.3, the classification of fermionic phases in SSH chains breaks down to $\mathbb{Z}_4$ if interactions are allowed. To find this result we used the approach of Kitaev in [9]. This paper covers the breakdown of fermionic phases in stacked Majorana chains to $\mathbb{Z}_8$. The discrepancy of $\mathbb{Z}_4$ and $\mathbb{Z}_8$ exists, because we combined two Majorana chains to one SSH chains. Single Majorana chains can realize intermediate phases which do not appear for the SSH chains. Here we want do give some additional insights for these intermediate phases using the stabilizer formalism.

C.1. Introduction of the Majorana Chain

The Majorana chain is defined in [16]. We start with a chain of L spinless fermions with ladder operators $\hat{a}_i^\dagger$ and $\hat{a}_i$. Then we define the Majorana operators

$$\hat{c}_{2i-1} = \hat{a}_i + \hat{a}_i^\dagger \tag{C.1a}$$

$$\hat{c}_{2i} = \frac{1}{\mathrm{i}}\left(\hat{a}_i - \hat{a}_i^\dagger\right). \tag{C.1b}$$

As these operators are self-adjoint, they formally correspond to quasi-particles (Majorana modes) which are their own anti-particles. The Majorana operators anticommute which makes the Majorana modes fermionic.

The Majorana chain is now defined by the Hamiltonian

$$\hat{H}_\mathrm{F} = \mathrm{i}\left(u\sum_{i=1}^{L}\hat{c}_{2i-1}\hat{c}_{2i} + v\sum_{i=1}^{L-1}\hat{c}_{2i}\hat{c}_{2i+1}\right). \tag{C.2}$$

Each unit cell of the Majorana chain contains one fermion site corresponding to two Majorana modes.[1]

As we can see, this chain has some similarities to the SSH chain. The Majorana chain is in the trivial phase for $u > v$ and in the topological phase for $u < v$. We will only consider the dimerized limit.

[1] As the SSH chain has two fermion sites per unit cell, we need two Majorana chains to construct one SSH chain.

C.2. Jordan–Wigner Transformation of the Majorana Chain

As we want to apply the stabilizer formalism, we need to perform a Jordan–Wigner transformation on the Majorana chain. The Majorana operators are translated via

$$\rho_{\mathrm{JW}}(c_{2i-1}) = \prod_{j=1}^{i-1} \sigma_j^z \cdot \sigma_i^x \tag{C.3a}$$

$$\rho_{\mathrm{JW}}(c_{2i}) = \prod_{j=1}^{i-1} \sigma_j^z \cdot \sigma_i^y. \tag{C.3b}$$

This gives us the trivial ($u = 1$, $v = 0$) bosonic Hamiltonian[2]

$$H_{\mathrm{triv}} = \overset{1}{Z} + \overset{2}{Z} + \overset{3}{Z} + \cdots \tag{C.4}$$

and the topological ($u = 0$, $v = 1$) Hamiltonian

$$H_{\mathrm{triv}} = \overset{1}{X}\overset{2}{X} + \overset{2}{X}\overset{3}{X} + \overset{3}{X}\overset{4}{X} + \cdots . \tag{C.5}$$

We can immediately see that these terms all commute and therefore can be used to generate a stabilizer group.

C.3. Symmetry of the Majorana Chain

As we defined the SSH chains out of Majorana chains, we gave them a sublattice symmetry, but originally the Majorana chain has a time-reversal symmetry[3] $\hat{T}_{\mathrm{F}}$ which fulfils the following conditions [9]:

$$\hat{T}_{\mathrm{F}} \hat{c}_{2i-1} \hat{T}_{\mathrm{F}}^{-1} = -\hat{c}_{2i-1} \tag{C.6a}$$

$$\hat{T}_{\mathrm{F}} \hat{c}_{2i} \hat{T}_{\mathrm{F}}^{-1} = \hat{c}_{2i} \tag{C.6b}$$

$$\hat{T}_{\mathrm{F}} \mathrm{i} \hat{T}_{\mathrm{F}}^{-1} = -\mathrm{i} \tag{C.6c}$$

$$\hat{T}_{\mathrm{F}}^2 = 1. \tag{C.6d}$$

These conditions are satisfied by the operator

$$\hat{T}_{\mathrm{F}} = \prod_{i=1}^{L} \hat{c}_{2i-1} \hat{c}_{2i} \circ K. \tag{C.7}$$

It can be shown, that $\hat{T}_{\mathrm{F}} \hat{H}_{\mathrm{F}} \hat{T}_{\mathrm{F}}^{-1} = \hat{H}_{\mathrm{F}}$.

In the bosonic picture the time-reversal symmetry becomes

$$T = \rho_{\mathrm{JW}}\left(\hat{T}_{\mathrm{F}}\right) = Z \cdots Z \circ K. \tag{C.8}$$

[2] As we will apply the stabilizer formalism, we ignore any prefactors of the Hamiltonian.

[3] Time-reversal symmetries are anti-unitarily realized (see Subsection 1.2.2).

C.4. Intermediate Phases in Majorana Chains

Now we can apply the stabilizer formalism on the Majorana chain. In the trivial case, we can immediately see that the time-reversal symmetry acts trivially on the whole chain.[4] The topological chain is much more interesting. Here we can see that the terms of the Hamiltonian H_{triv} cannot be used to simplify the action of the symmetry on the bulk. This means that the symmetry acts non-trivially onto the whole chain and not just on the edges. Therefore, we cannot classify this system any more using the stabilizer formalism (cf. Chapter 5).

C.5. Phases in Stacked Majorana Chains

Consider two stacked Majorana chains which are both in the topological state. The Hamiltonian is[5]

$$H = \begin{array}{cc} \scriptstyle 1 & \scriptstyle 2 \\ X & X \\ Z & 1 \end{array} + \begin{array}{cc} \scriptstyle 1 & \scriptstyle 2 \\ 1 & Z \\ X & X \end{array} + \begin{array}{cc} \scriptstyle 2 & \scriptstyle 3 \\ X & X \\ Z & 1 \end{array} + \begin{array}{cc} \scriptstyle 2 & \scriptstyle 3 \\ 1 & Z \\ X & X \end{array} + \cdots . \tag{C.9}$$

All terms of H commute with each other. The time-reversal symmetry is represented by

$$T = \begin{array}{c} Z \cdots Z \\ Z \cdots Z \end{array} \circ K. \tag{C.10}$$

Now we multiply all terms of the Hamiltonian to

$$\Omega_T = \begin{array}{cc} \scriptstyle 1 & \scriptstyle 2 \\ X & X \\ Z & 1 \end{array} \cdot \begin{array}{cc} \scriptstyle 1 & \scriptstyle 2 \\ 1 & Z \\ X & X \end{array} \cdot \begin{array}{cc} \scriptstyle 2 & \scriptstyle 3 \\ X & X \\ Z & 1 \end{array} \cdot \begin{array}{cc} \scriptstyle 2 & \scriptstyle 3 \\ 1 & Z \\ X & X \end{array} \cdots = \begin{array}{c} X\,Z \cdots Z\,Y \\ Y\,Z \cdots Z\,X \end{array}. \tag{C.11}$$

Now we can see the action of the time-reversal symmetry on the ground states:

$$T' = T \cdot \Omega_T = \begin{array}{c} Y\,1 \cdots 1\,X \\ X\,1 \cdots 1\,Y \end{array} \circ K. \tag{C.12}$$

If two Majorana chains are stacked on top of each other, we can reduce the action of the symmetry to an action on the edges of the system. These actions on the edge square to $-\mathbb{1}$ and are therefore non-trivial.

The same pattern repeats itself. Even numbers of topological Majorana chains can be classified and odd numbers of topological Majorana chains lead to an action of the symmetry on the bulk. Therefore, we called the odd phases *intermediate*. These considerations give a better understanding of the difference between the phases in SSH chains (which behave like the even phases in Majorana chains) and the odd phases of Majorana chains.

[4] Simply multiply all terms of the Hamiltonian to the symmetry operator.

[5] This Hamiltonian is obviously dependent on the Jordan–Wigner string. Other strings would yield the same results.

C.6. Additional Comments

We want to mention that the stabilizer formalism seems to yield some problems in these systems. The issues are related to anti-unitarily realized symmetries.

If we would have defined other Majorana operators, the time-reversal symmetry would have been just a complex conjugation $\hat{T}_{\mathrm{F}} = K$. Then we cannot use stabilizer formalism (at its current state) any more as a tool for the classification of topological phases because this symmetry always acts trivially on the bulk. It is still a non-trivial symmetry operation because of the complex conjugation. Therefore we believe that the stabilizer formalism is subtle if anti-unitarily realized symmetries are considered. This will require some further investigations. Nonetheless, we trust our results in Chapter 5.

Bibliography

[1] L. D. Landau. 'On the theory of phase transitions'. In: *Zh. Eksp. Teor. Fiz.* 7 (1937). [Ukr. J. Phys.53,25(2008)], pp. 19–32.

[2] K. v. Klitzing, G. Dorda and M. Pepper. 'New Method for High-Accuracy Determination of the Fine-Structure Constant Based on Quantized Hall Resistance'. In: *Phys. Rev. Lett.* 45 (6 Aug. 1980), pp. 494–497. DOI: 10.1103/PhysRevLett.45.494. URL: https://link.aps.org/doi/10.1103/PhysRevLett.45.494.

[3] D. C. Tsui, H. L. Stormer and A. C. Gossard. 'Two-Dimensional Magnetotransport in the Extreme Quantum Limit'. In: *Phys. Rev. Lett.* 48 (22 May 1982), pp. 1559–1562. DOI: 10.1103/PhysRevLett.48.1559. URL: https://link.aps.org/doi/10.1103/PhysRevLett.48.1559.

[4] Edward Witten. 'Topological quantum field theory'. In: *Communications in Mathematical Physics* 117.3 (Sept. 1988), pp. 353–386. ISSN: 1432-0916. DOI: 10.1007/BF01223371. URL: https://doi.org/10.1007/BF01223371.

[5] X. G.wen. 'Topological orders in rigid states'. In: *International Journal of Modern Physics B* 04 (Jan. 2012). DOI: 10.1142/S0217979290000139.

[6] Xie Chen, Zheng-Cheng Gu and Xiao-Gang Wen. 'Local unitary transformation, long-range quantum entanglement, wave function renormalization, and topological order'. In: *Phys. Rev. B* 82 (15 Oct. 2010), p. 155138. DOI: 10.1103/PhysRevB.82.155138. URL: https://link.aps.org/doi/10.1103/PhysRevB.82.155138.

[7] Sylvain de Léséleuc et al. 'Observation of a symmetry-protected topological phase of interacting bosons with Rydberg atoms'. In: *Science* 365.6455 (2019), pp. 775–780. ISSN: 0036-8075. DOI: 10.1126/science.aav9105. eprint: https://science.sciencemag.org/content/365/6455/775.full.pdf. URL: https://science.sciencemag.org/content/365/6455/775.

[8] Xie Chen et al. 'Symmetry protected topological orders and the group cohomology of their symmetry group'. In: *Phys. Rev. B* 87 (15 Apr. 2013), p. 155114. DOI: 10.1103/PhysRevB.87.155114. URL: https://link.aps.org/doi/10.1103/PhysRevB.87.155114.

[9] Lukasz Fidkowski and Alexei Kitaev. 'Effects of interactions on the topological classification of free fermion systems'. In: *Phys. Rev. B* 81 (13 Apr. 2010), p. 134509. DOI: 10.1103/PhysRevB.81.134509. URL: https://link.aps.org/doi/10.1103/PhysRevB.81.134509.

[10] Andreas W W Ludwig. 'Topological phases: classification of topological insulators and superconductors of non-interacting fermions, and beyond'. In: *Physica Scripta* T168 (Dec. 2015), p. 014001. DOI: 10.1088/0031-8949/2015/t168/014001. URL: https://doi.org/10.1088%2F0031-8949%2F2015%2Ft168%2F014001.

[11] J. Zak. 'Berry's phase for energy bands in solids'. In: *Phys. Rev. Lett.* 62 (23 June 1989), pp. 2747–2750. DOI: 10.1103/PhysRevLett.62.2747. URL: https://link.aps.org/doi/10.1103/PhysRevLett.62.2747.

[12] Sujit Sarkar. 'Quantization of geometric phase with integer and fractional topological characterization in a quantum Ising chain with long-range interaction'. In: *Scientific Reports* 8.1 (Apr. 2018), p. 5864. ISSN: 2045-2322. URL: https://doi.org/10.1038/s41598-018-24136-1.

[13] Maria Maffei et al. 'Topological characterization of chiral models through their long time dynamics'. In: *New Journal of Physics* 20.1 (Jan. 2018), p. 013023. DOI: 10.1088/1367-2630/aa9d4c. URL: https://doi.org/10.1088%2F1367-2630%2Faa9d4c.

[14] András Pályi János K. Asbóth László Oroszlány. 'A Short Course on Topological Insulators: Band-structure topology and edge states in one and two dimensions'. In: (Sept. 2015). DOI: 10.1007/978-3-319-25607-8. URL: https://arxiv.org/abs/1509.02295.

[15] Jun-Won Rhim, Jens H. Bardarson and Robert-Jan Slager. 'Unified bulk-boundary correspondence for band insulators'. In: *Phys. Rev. B* 97 (11 Mar. 2018), p. 115143. DOI: 10.1103/PhysRevB.97.115143. URL: https://link.aps.org/doi/10.1103/PhysRevB.97.115143.

[16] A Yu Kitaev. 'Unpaired Majorana fermions in quantum wires'. In: *Physics-Uspekhi* 44.10S (Oct. 2001), pp. 131–136. DOI: 10.1070/1063-7869/44/10s/s29. URL: https://doi.org/10.1070%2F1063-7869%2F44%2F10s%2Fs29.

[17] J. R. Schrieffer W. P. Su and A. J. Heeger. *Solitons in Polyacetylene.* June 1979. URL: http://dx.doi.org/10.1103/PhysRevLett.42.1698.

[18] Ulrich Schollwöck. 'The density-matrix renormalization group in the age of matrix product states'. In: *Annals of Physics* 326.1 (2011), pp. 96–192.

[19] Bei Zeng et al. 'Quantum information meets quantum matter'. In: *arXiv preprint arXiv:1508.02595* (2015).

[20] M. Fannes, B. Nachtergaele and R. F. Werner. 'Finitely correlated states on quantum spin chains'. In: *Communications in Mathematical Physics* 144.3 (Mar. 1992), pp. 443–490. ISSN: 1432-0916. DOI: 10.1007/BF02099178. URL: https://doi.org/10.1007/BF02099178.

[21] David Perez-Garcia et al. 'Matrix product state representations'. In: *arXiv preprint quant-ph/0608197* (2006).

[22] Kasper Duivenvoorden. 'Symmetry Protected Topological Phases of Spin Chains'. PhD thesis. Universität zu Köln, 2013.

[23] Xie Chen, Zheng-Cheng Gu and Xiao-Gang Wen. 'Classification of gapped symmetric phases in one-dimensional spin systems'. In: *Phys. Rev. B* 83 (3 Jan. 2011), p. 035107. DOI: 10.1103/PhysRevB.83.035107. URL: https://link.aps.org/doi/10.1103/PhysRevB.83.035107.

[24] Norbert Schuch, David Pérez-García and Ignacio Cirac. 'Classifying quantum phases using matrix product states and projected entangled pair states'. In: *Phys. Rev. B* 84 (16 Oct. 2011), p. 165139. DOI: 10.1103/PhysRevB.84.165139. URL: https://link.aps.org/doi/10.1103/PhysRevB.84.165139.

[25] Xie Chen, Zheng-Cheng Gu and Xiao-Gang Wen. 'Complete classification of one-dimensional gapped quantum phases in interacting spin systems'. In: *Phys. Rev. B* 84 (23 Dec. 2011), p. 235128. DOI: 10.1103/PhysRevB.84.235128. URL: https://link.aps.org/doi/10.1103/PhysRevB.84.235128.

[26] D. Pérez-García et al. 'String Order and Symmetries in Quantum Spin Lattices'. In: *Phys. Rev. Lett.* 100 (16 Apr. 2008), p. 167202. DOI: 10.1103/PhysRevLett.100.167202. URL: https://link.aps.org/doi/10.1103/PhysRevLett.100.167202.

[27] Frank Pollmann et al. 'Entanglement spectrum of a topological phase in one dimension'. In: *Phys. Rev. B* 81 (6 Feb. 2010), p. 064439. DOI: 10.1103/PhysRevB.81.064439. URL: https://link.aps.org/doi/10.1103/PhysRevB.81.064439.

[28] Nicolasi Lang. 'One-Dimensional Topological States op Synthetic Quantum Matter'. PhD thesis. Univartität Stuttgart, 2019.

[29] Daniel Gottesman. 'Class of quantum error-correcting codes saturating the quantum Hamming bound'. In: *Phys. Rev. A* 54 (3 Sept. 1996), pp. 1862–1868. DOI: 10.1103/PhysRevA.54.1862. URL: https://link.aps.org/doi/10.1103/PhysRevA.54.1862.

[30] Michael A. Nielsen and Isaac L. Chuang. *Quantum Computation and Quantum Information: 10th Anniversary Edition*. 10th. New York, NY, USA: Cambridge University Press, 2011. ISBN: 1107002176, 9781107002173.

[31] F. Verstraete et al. 'Renormalization-Group Transformations on Quantum States'. In: *Phys. Rev. Lett.* 94 (14 Apr. 2005), p. 140601. DOI: 10.1103/PhysRevLett.94.140601. URL: https://link.aps.org/doi/10.1103/PhysRevLett.94.140601.

Acknowledgements

This thesis could not have come together without the help and support of many others. Therefore, I would like to take this opportunity to thank those people who made all this possible.

First of all, I want to thank Prof. Büchler for giving me the opportunity to work at the ITP3. He has invested a lot of time in me and our discussions were always helpful and encouraging.

Furthermore, I would also like to thank my secondary supervisor Prof. Lutz for our useful discussions.

It is not self-evident to have a mentor, who always has an open door for all questions and does not hesitate to spend countless hours in discussing them. Therefore, I want to express my deep gratitude to Nicolai Lang. Our many useful discussions helped me a lot and without him, this thesis would not have come together.

I also want to thank the whole institute for the great working atmosphere, which made me enjoy the last year very much. This includes Oliver Nagel, Sebastian Weber, Jan Kumlin, Tobias Ilg, Kevin Kleinbeck, Luka Jibuti, Rukmani Bai and Joseph Eix. Special thanks goes to my fellow musician Christoph Pitzal, who helped me proofreading this thesis and found many splelling errors. Working with this group has been an immense pleasure and even improved my volleyball skills.

As this thesis also marks the end of five years of study, I want to thank all those who made this time go by so fast. This includes Tobias Reinsch, Luca Blessing, Benedikt Herkommer, Elias Arnold, Christian Hölzl, Fabian Munkes, Jakob Haag and many more. I especially want to thank Michael Scharwaechter for being a great fellow student and roommate. My biggest thank goes to Annika Belz. Without her I would not even have survived the first semester. Also, she helped me to write this section...

Finally, I thank my family for their great support during the last years and my girlfriend Nina for being the strongest person I have ever known.